BIOCATALYST AND BIOREACTOR DESIGN FOR THE PRODUCTION OF GREEN-NOTE VOLATILES: CHARACTERIZATION OF THEIR INVOLVEMENT IN PLANT-PATHOGEN DEFENSE AND SENESCENCE

by

Frank Schade

A thesis

presented to the University of Waterloo

in fulfilment of the

thesis requirement for the degree of

Doctor of Philosophy

in

Biology

Waterloo, Ontario, Canada, 2000

© Frank Schade, 2000

National Library of Canada
Acquisitions and Bibliographic Services
395 Wellington Street
Ottawa ON K1A 0N4
Canada

Bibliothèque nationale du Canada
Acquisitions et services bibliographiques
395, rue Wellington
Ottawa ON K1A 0N4
Canada

Your file Votre référence

Our file Notre référence

The author has granted a non-exclusive licence allowing the National Library of Canada to reproduce, loan, distribute or sell copies of this thesis in microform, paper or electronic formats.

L'auteur a accordé une licence non exclusive permettant à la Bibliothèque nationale du Canada de reproduire, prêter, distribuer ou vendre des copies de cette thèse sous la forme de microfiche/film, de reproduction sur papier ou sur format électronique.

The author retains ownership of the copyright in this thesis. Neither the thesis nor substantial extracts from it may be printed or otherwise reproduced without the author's permission.

L'auteur conserve la propriété du droit d'auteur qui protège cette thèse. Ni la thèse ni des extraits substantiels de celle-ci ne doivent être imprimés ou autrement reproduits sans son autorisation.

0-612-53512-6

Canada

The University of Waterloo requires the signatures of all persons using or photocopying this thesis. Please sign below, and give address and date.

Abstract

The international market for fragrances and food flavours is worth several billion U.S.-dollars annually. The volatiles, hexanal and *(3Z)*-hexenal, which are key organoleptic elements of green-note, are important components of both fragrance and flavour, and find widespread consumer acceptance if naturally derived. Therefore, the industry is intensifying its efforts to produce green-note volatiles through extraction from naturally enriched plant sources.

In this dissertation, novel, alternative processes for the natural production of hexanal and *(3Z)*-hexenal are presented. Enzyme templates, known to be responsible for the synthesis of hexanal from linoleic acid (18:2), were isolated from naturally enriched tissues. These templates were immobilized in a natural alginate matrix and used as a biocatalyst within a packed-bed bioreactor. Product recovery was achieved on-line using a hollow-fiber ultrafiltration unit. Key parameters - namely pH, reaction temperature, and substrate and catalyst concentrations - affecting hexanal generation were identified and optimized. Utilizing these optimized conditions, hexanal production in the bioreactor over a 30 minute period proved to be 112-fold higher than endogenous steady-state levels of the volatile in a corresponding amount of tissue. In addition, due to the anti-microbial properties of hexanal, bacterial contamination in the bioreactor was not observed. However, bioreactor-based generation and recovery of *(3Z)*-hexenal from linolenic acid (18:3) was not achieved due to the high reactivity of *(3Z)*-hexenal. Therefore, *Arabidopsis thaliana* was genetically modified by up-regulating hydroperoxide lyase, one of the key enzymes involved in the *in vivo* formation of *(3Z)*-hexenal. Over-expression of

hydroperoxide lyase cDNA in transgenic *Arabidopsis* plants resulted in increased levels of *(3Z)*-hexenal of up to 29-fold by comparison with wild-type plants, whereas hexanal levels remained unaltered. Thus, these transformed plants are suitable bioreactors for *(3Z)*-hexenal production in themselves.

Transgenic *Arabidopsis thaliana* plants with up-regulated *(3Z)*-hexenal levels were tested for increased resistance against virulent bacteria and for enhanced systemic required resistance. *In planta* bacterial counts revealed increased resistance against virulent *Pseudomonas syringae* by a factor of 6 and a 15-fold enhancement of systemic acquired resistance for the transgenic lines in comparison to wild-type plants. Thus, overall resistance against bacterial infection was increased by 90-fold in the transgenic plants.

The transgenic *Arabidopsis thaliana* plants were also more resistant than wild-type plants to the effect of anoxic stress induced by flooding. Water-flooding of the soil resulted in impaired leaf growth in wild-type plants, whereas leaf development in the transgenic plants was unaffected. In addition, levels of peroxidized lipid in membranes of the transgenic plants were reduced by ~ 1/3 in comparison to wild-type plants. These observations collectively indicate that hydroperoxide lyase plays an important role in membrane turnover. It is also apparent that up-regulation of hydroperoxide lyase reduces the effects of anoxic stress, presumably by converting membrane-bilayer destabilizing peroxides into green-note volatiles which readily diffuse out of the membranes.

Acknowledgements

I would like to express my sincere appreciation to Dr. John E. Thompson and Dr. Raymond L. Legge for their invaluable supervision, support and encouragement throughout the course of this study, and for their assistance in the preparation of this dissertation.

I would also like to thank the members of my supervisory committee, Dr. C. Moresoli, Dr. B. R. Glick and Dr. O. P. Ward, for their valuable assistance and continued interest in my work.

Thanks also to the staff and my fellow graduate students in the Departments of Biology and Chemical Engineering, and particular thanks to Li Wang, Lynn Hoyles, Maisie K.Y. Lo and Catherine A. Taylor for their technical assistance.

I am indebted to Dr. R. K. Cameron for collaboration in respect of plant-pathogen studies and to Dr. C. D. Froese and Angela R. Whitham for proof-reading this manuscript.

A special thank you to my family for their constant encouragement and manifold support.

This work was supported through a NSERC grant to J.E. Thompson and through scholarships and teaching assistantships provided by the Ontario Government and the University of Waterloo.

Table of Contents

Abstract iv

Acknowledgements vi

List of Tables xi

List of Figures xii

List of Abbreviations and Symbols xv

Introduction 1

1. Green-Note Volatiles 1
   1.1. The Lipoxygenase Pathway 2

2. Plant Responses to Stress and Senescence 8
   2.1. Abiotic Stress-Flooding 11
   2.2. Biotic Stress-Ingression 13

3. Bioreactors 16
   3.1. Enzyme Immobilization 17
   3.2. Packed-bed Bioreactor 20
   3.3. Product Purification and Retrieval 21
   3.4. Bioreactor and Product Optimization Using Two-Level Factorial Designs 22

Materials and Methods 28

1. Chemicals 28

2. Preparation of a Biocatalyst for Continuous Production of C_6-Aldehydes ---- 28
2.1. Plant Material and Growth Conditions ---- 28
2.1.1. Carnation Flowers ---- 28
2.1.2. Strawberry Plants ---- 29
2.1.3. Tomato Plants ---- 29
2.2. Tissue Homogenization ---- 30
2.3. Subcellular Fractionation ---- 30
2.4. Volatile Analysis ---- 31
2.5. Enzyme Entrapment ---- 32
2.6. Measurements of Bead Size and Geometry ---- 32

3. Bioreactor Design and Operation ---- 35
3.1. Substrate Preparation ---- 35
3.2. Membrane Selection for the Ultrafiltration Unit ---- 35
3.3. Bioreactor Design ---- 36
3.4. Operation of the Bioreactor ---- 39
3.5. Reactor Regeneration ---- 39
3.6. Factorial Reactor Design ---- 40

4. Preparation of Transgenic *Arabidopsis thaliana* Plants ---- 40
4.1. Plant Material and Growth Conditions ---- 41
4.2. Hydroperoxide Lyase Transgene Construct and Plant Transformation ---- 41
4.3. Screening of T_3 Transgenic Lines and Volatile Analysis ---- 46
4.4. Northern Blot Analysis ---- 47

5. Root-Flooding of Transgenic and Wild-type *Arabidopsis thaliana* Plants ---- 49

6. Infection of Transgenic and Wild-type *Arabidopsis thaliana* Plants with *Pseudomonas syringae* ---- 49

7. Protein Analysis ---- 52

8. Measurement of Chlorophyll ---- 52

9. Measurement of Peroxidized Lipids in Total Membranes ---- 53

10. Plant Weight Determination ---- 54

11. Lipid Extraction and Quantitation ---- 54

Results ---- 55

1. Biocatalyst and Bioreactor Design ---- 55
   - 1.1. Immobilization of Total Membranes and Tissue Homogenates in a Calcium-alginate Matrix ---- 57
   - 1.2. Substrate Considerations ---- 59
   - 1.3. Membrane Selection for the Hollow-Fibre Recovery Unit ---- 60

2. Bioreactor Operation ---- 61
   - 2.1. Minimum Substrate Requirement and Selection of the Biocatalyst ---- 61
   - 2.2. Effect of pH and Temperature on Hexanal Generation ---- 63
   - 2.3. Effect of Substrate and Catalyst Concentrations on Hexanal Formation ---- 71

3. Characterization of the Involvement of C_6-aldehydes in Plant-Pathogen Defence ---- 82

3.1. Transformation of *Arabidopsis thaliana* with Hydroperoxide Lyase and Determination of Endogenous C_6-aldehyde Levels ---- 83

3.2. *In planta* Bacterial Growth in Wild-type and Transgenic *Arabidopsis thaliana* Infected with *Pseudomonas syringae* ---- 89

4. Up-regulation of Hydroperoxide Lyase and its Impact on Stress-Induced Senescence ---- 99

Discussion ---- 123

Literature Cited ---- 141

List of Tables

1	2^2-Design. Data-set for a typical experiment	26
2	2^2-Design. Possible regression models	27
3	Levels of hexanal in tissue homogenates	56
4	Size distribution of alginate beads containing entrapped membrane biocatalyst	58
5	Determination of the minimum concentration of linoleic acid required for bioreactor-based production of hexanal	62
6	Bioreactor-based production of hexanal	64
7	Effect of varying the reactor temperature on the bioreactor-based production of hexanal	68
8	2^2-Experimental design for the bioreactor-based production of hexanal	73
9	ANOVA of the 2^2-factorial design regression	74
10	Treatment combinations for inoculation of *Arabidopsis* plants with *Pseudomonas syringae*	92

List of Figures

1 The lipoxygenase pathway ——— 4

2 The aldehyde pathway ——— 6

3 Schematic diagram of the bead-making device ——— 34

4 Schematic diagram of the bioreactor and ultrafiltration unit ——— 38

5 Nucleotide and deduced amino acid sequence for full-length *Arabidopsis thaliana* cDNA encoding hydroperoxide lyase ——— 43

6 pKYLX-HPL construct ——— 45

7 Effect of reactor temperature on permeate flux ——— 67

8 Time course for bioreactor-generated hexanal levels as a function of varying reactor temperature ——— 70

9 Plot of the residuals, ε, of the regression model ——— 76

10 Coded response surface plot of hexanal yield based on the first-order model with interactions ——— 78

11 Time course of retentate flux and permeate flux for the four factorial design points ——— 81

12 Analysis of hexanal, *(3Z)*-hexenal and *(2E)*-hexenal in leaves of wild-type *Arabidopsis* plants and in leaves of T_3 transgenic lines ——— 86

13 Mass spectrometric identification of *(3Z)*-hexenal from leaves of transgenic *Arabidopsis thaliana* ——— 88

14 Northern blot analysis of total RNA isolated from leaves of wild-type *Arabidopsis thaliana* plants and transgenic lines ——— 91

15 Illustration of first and second inoculations of *Arabidopsis* plants with *Pseudomonas syringae* ——— 95

16 *In planta* bacterial growth in challenged leaves of wild-type and transgenic *Arabidopsis* plants ——— 97

17 Changes in bolt number of over-watered wild-type and transgenic *Arabidopsis* plants during development and senescence ——— 101

18 Changes in bolt length of over-watered wild-type and transgenic *Arabidopsis* plants during development and senescence ——— 104

19 Changes in fresh weight of the rosette leaf aggregate for over-watered wild-type and transgenic *Arabidopsis* plants during development and senescence ——— 106

20 Digital pictures of over-watered wild-type and transgenic *Arabidopsis* plants 23 and 25 days after planting ——— 108

21 Digital pictures of control (normal watering) *Arabidopsis* plants 29 days after planting ——— 110

22 Digital pictures of over-watered *Arabidopsis* plants 29 days after planting ——— 112

23 Changes in dry weight of the aggregate of rosette leaves of over-watered wild-type and transgenic *Arabidopsis* plants during development and senescence ——— 115

24 Changes in leaf chlorophyll levels of over-watered wild-type and transgenic *Arabidopsis* plants ——— 117

25 Digital pictures of over-watered *Arabidopsis* plants 46 days after planting ——— 119

26 Changes in levels of peroxized lipids in total membrane preparations from leaves of over-watered wild-type and transgenic *Arabidopsis* plants ——— 122

List of Abbreviations and Symbols

Acronyms

18:2	linoleic acid
18:3	linolenic acid
ACC	1-amino-cyclopropane-1-carboxylic acid
ANOVA	analysis of variance
BH	benzamadine hydrochloride
cfu	colony forming unit
C_6	six-carbon
CSTR	continuously-stirred tank reactor
DEPC	diethyl pyrocarbonate
EDTA	ethylenediaminetetraacetic acid
EGTA	ethylene glycol-bis-(β-aminoethyl ether)N,N,N',N'-tetraacetic acid
EPPS	N-(2-hydroxyethyl)piperizine-N'3-propanesulfonic acid
FID	flame ionization detector
GC	gas chromatograph
GIT	guanidine isothionite
g f w	gram fresh weight
HPL	hydroperoxide lyase
kDA	kilo Dalton
LOX	lipoxygenase
MS	mass spectrometer
MW	molecular weight
MWCO	molecular weight cut-off
m/z	mass to charge ratio
OD	optical density

PFTR	plug-flow tank reactor
PMSF	phenylmethylsulfonyl fluoride
ppb	parts per billion
PR	pathogenesis-related gene
Pst	*Pseudomonas syringae* pv. tomato
RSM	response surface model
SA	salicylic acid
SAG	senescence-associated gene
SAM	S-adenosylmethionine
SAR	systemic acquired resistance
SDS	sodium dodecyl sulfate
SSC	sodium chloride and sodium citrate
TMP	transmembrane pressure
TRIS	tri(hydroxymethyl)-aminomethane
Tween 20	polyoxyethylenesorbitan monolaurate

Symbols

(1), a, b or ab	symbols representing sums of replicates
a_i, b_i, c_i, or d_i	i^{th} replicate of experiment a, b, c or d
A	avirulent infection
β_i	i^{th} parameter of regression model
c	chlorophyll concentration in microgram per milliliter
d	bead diameter in millimeter
M	mock inoculation
n	number of replicates
Δp	pressure drop along packing of a packed-bed

σ^2	variance
t	reaction time in minutes
T_i	i^{th} transgenic generation
u	flow rate in centimeter per second
v	volume
V	virulent infection
w	weight
x_i	coded or uncoded predictor factor i
X_i	average effect of factor x_i
X_0	grand average of 4 n observations
X_{ij}	average effect of interacting factors x_i and x_j
y	experimental hexanal production (response variable)
Y	hexanal yield predicted via regression model

Introduction

1. Green-Note Volatiles.

The C_6 - aldehydes, hexanal, (*2E*)-hexenal and (*3Z*)-hexenal, are important constituents of the complement of green-note volatiles (Gardner, 1995). These volatiles are chemicals utilized in food and fragrance applications because of their fresh organoleptic note, and they find widespread consumer acceptance if derived naturally (Rouhi, 1999; Bate *et al.*, 1998). Their freshness can be perceived at very low concentrations. Specifically, hexanal, (*2E*)-hexenal and (*3Z*)-hexenal can be detected by the human sensory system at concentrations as low as 5, 17 and 0.25 ppb, respectively (Ohloff, 1994).

In plants, C_6-aldehydes are common elements of floral and leaf scent. They are part of the plant's composite of volatile chemicals and are reported to have anti-fungal, anti-microbial and anti-insect properties (Farmer *et al.*, 1998; Nitrampemba, 1998; Gardner, 1995; Kondo *et al.*, 1995; Croft *et al.*, 1993; Knudsen *et al.*, 1993). Farmer *et al.* (1998) and Croft *et al.* (1993) not only reported the anti-microbial nature of hexanal and (*2E*)-hexenal, but also demonstrated that high concentrations of *(2E)*-hexenal cause necrosis and that the production of both volatiles increases during the hypersensitive resistance response. This suggests that C_6-aldehydes play an important role in plant defense against pathogen ingression. However, it may only be the unsaturated C_6-aldehydes that play a key role in the response to pathogen ingression (Croft *et al.*, 1993). Localized hypersensitive response is currently believed to be correlated with, but not essential for, systemic acquired resistance (Cameron *et al.*, 1994).

1.1. The Lipoxygenase Pathway.

The C_6 - aldehydes are formed through the lipoxygenase pathway (Fig. 1), a complex multi-branching pathway common to animals and plants (Gardner, 1995). One branch, which leads to the production of green-note volatiles and is referred to as the aldehyde pathway (Fig. 2), is only present in plants and is particularly well characterized for leaves (Bate *et al.*, 1998; Grechkin, 1998). In the first enzymatic step of the lipoxygenase pathway, a lipase hydrolytically deesterifies membrane glyceride lipids resulting in the release of free fatty acids, specifically linoleic acid (18:2) and linolenic acid (18:3) (Fig. 1). It has been reported that this lipase is expressed at the onset of senescence, the terminal phase of plant development (Hong *et al.*, 2000).

Activation of this pathway occurs not only during senescence, but also in the event of abiotic and biotic stresses such as flooding, wounding or pathogen attack (Matsui *et al.*, 1999; Gardner, 1995). Furthermore, linoleic and linolenic acids are direct substrates for the aldehyde pathway (Fig. 2) and are converted in a two-step enzymatic reaction involving the enzymes lipoxygenase (LOX) and hydroperoxide lyase (HPL) into C_6-aldehydes (Gardner, 1995). Specifically, linoleic and linolenic acids are converted to their respective 13-hydroperoxides by lipoxygenase. These in turn are hydrolysed by hydroperoxide lyase forming hexanal and *(3Z)*-hexenal, respectively (Fig.2). *(3Z)*-Hexenal is chemically labile and can be isomerized

Figure 1. The lipoxygenase pathway. Adapted from Gardner (1995).

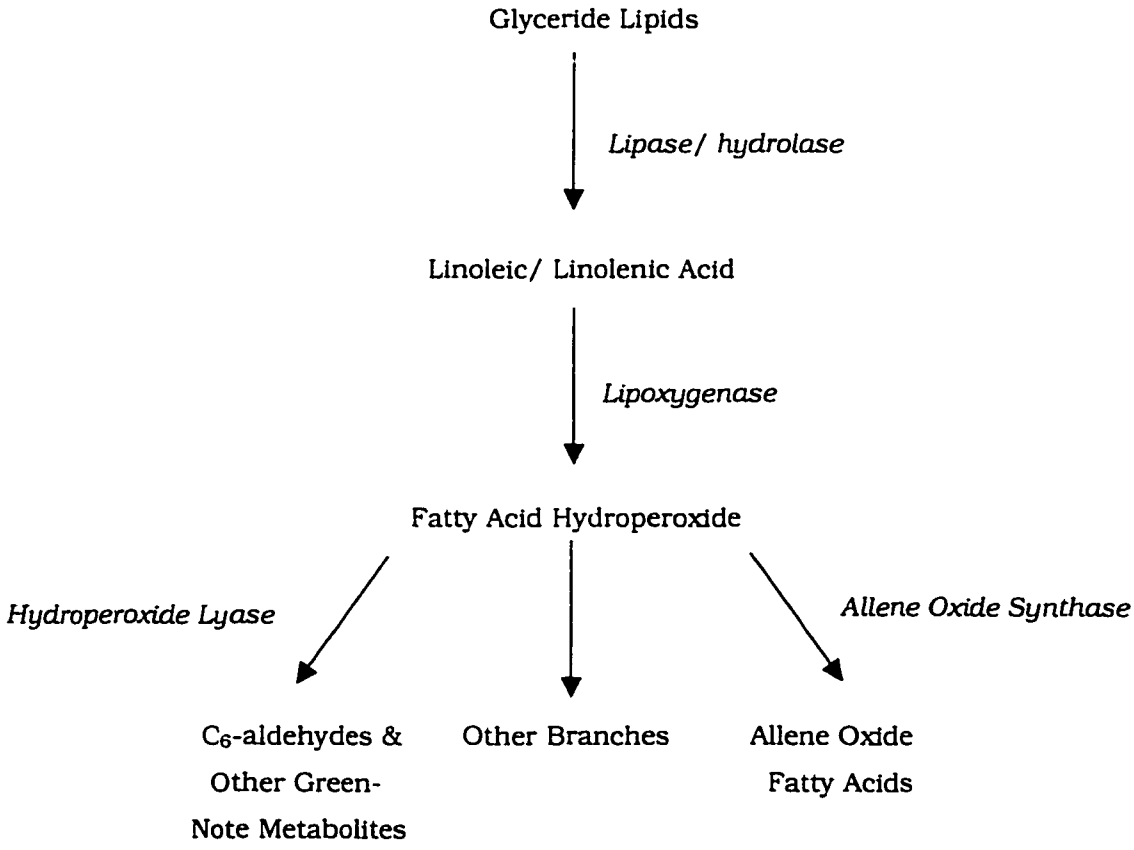
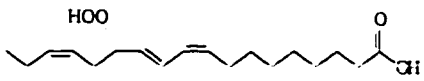

Glyceride Lipids
Lipase/ hydrolase
Linoleic/ Linolenic Acid
Lipoxygenase
Fatty Acid Hydroperoxide
Hydroperoxide Lyase
Allene Oxide Synthase
C6-aldehydes & Other Green-Note Metabolites
Other Branches
Allene Oxide Fatty Acids

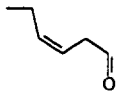
Figure 2. The aldehyde pathway. Adapted from Gardner (1995).

α-Linolenic Acid

↓ *13-Hydroperoxide Lipoxygenase*

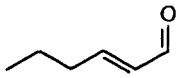


↓ *Hydroperoxide Lyase* ↓

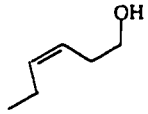


(3Z)-Hexenal

↓ *Alkenal Isomerase* ↓ *Alcohol Dehydrogenase*

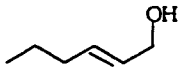


(2E)-Hexenal



(3Z)-Hexenol

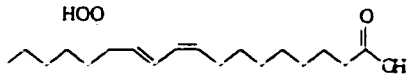
↓ *Alcohol Dehydrogenase*



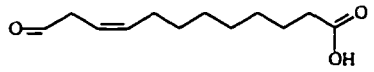
(3Z)-Hexenol

α-Linoleic Acid

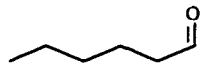
↓



↓ *Hydroperoxide Lyase* ↓

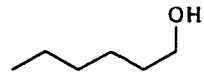


Oxo Acid



Hexanal

Alcohol Dehydrogenase ↓



Hexanol

to *(2E)*-hexenal (Ohloff, 1984). In addition, all of the C_6-aldehydes can be reduced to their corresponding alcohols by alcohol dehydrogenase (Fig. 2).

Lipoxygenases are non-heme, iron-containing enzymes (Kausch and Handa, 1997; Droillard *et al.*, 1993; Rouet-Mayer *et al.*, 1992; Todd *et al.*, 1990). Multiple isoforms of lipoxygenases exist, both in soluble and membrane-bound forms, and several membrane-associated lipoxygenase isoforms have been thoroughly characterized. They have molecular weights between 92 and 100 kDa, and they show maximum activity within a pH range of 4.5 to 8 (Kausch and Handa, 1997; Blée and Joyard, 1996; Rouet-Mayer *et al.*, 1992).

Two isoforms of hydroperoxide lyase are known to exist, one catalyzing the formation of *(3Z)*-hexenal from linolenic acid hydroperoxide and the other catalyzing the formation of hexanal from linoleic acid hydroperoxide (Matsui *et al.*, 1999; Noordermeer *et al.*, 1999; Matsui *et al.*, 1996; Gardner, 1995; Matsui *et al.*, 1989). The two hydroperoxide lyase isoforms are reported to be 200 to 250 kDa in size, and they are thought to be tetramers (Itoh and Vick, 1999; Grechkin, 1998). They have maximum activity within a pH range of 6 to 8 (Suurmeijer *et al.*, 2000, Riley *et al.*, 1996). Recent evidence indicates that hydroperoxide lyase is associated with plastid envelope membranes in leaves (Blée and Joyard, 1996). Hydroperoxide lyase is also associated with microsomal membrane preparations from ripening strawberry (Perez *et al.*, 1999), which would contain vesicles of plastid envelope membrane. Subcellular fractionation studies with carnation flower petals have indicated that green-note volatiles also originate from membranes within this tissue (Schade *et al.*, 2000; Hudak and Thompson, 1997). Furthermore, Matsui *et al.* (1997) reported

that homogenization of bell pepper fruit resulted in the formation of mainly monounsaturated C_6-components. Linoleic acid gives rise to saturated C_6-aldehydes, whereas use of linolenic acid as substrate results in the formation of monounsaturated aldehydes. Thus, the results of Matsui *et al.* (1997) indicate that linolenic acid, which is in high abundance in chloroplast thylakoid membranes, is the preferred substrate for hydroperoxide lyase *in vitro*. Although most of the evidence to date indicates that hydroperoxide lyase is membrane-bound, there is one report of a soluble hydroperoxide lyase in watermelon (Grechkin, 1998).

2. Plant Responses to Stress and Senescence.

Membrane deterioration is a common feature of both senescence and the response of plant tissues to stress. This distinction may not be altogether clear-cut, as acute stress of various types, such as extreme temperatures, poor light, flooding and pathogen ingression, result in premature induction of senescence (Noodén and Leopold, 1988). Root-flooding, for example, triggers senescence-like symptoms in plants (Noodén and Leopold, 1988). In general, stress phenomena are diverse and can be classified by their cause as abiotic, for example flooding, or biotic, for example bacterial infections. Both types of stress can result in senescence of the tissue or the whole plant if they are of sufficient intensity and duration (Agrios, 1996).

Perhaps the clearest manifestation of membrane deterioration in the event of senescence or episodes of environmental stress is the onset of membrane leakiness. This is commonly measured as an increase in tissue

diffusate conductivity and has been observed for senescing tissues and for tissues exposed to drought stress, temperature stress and various types of chemical stress (Thompson *et al.*, 1997). There is growing evidence to indicate that this leakiness is attributable to lipid phase separations in membrane bilayers (Senaratra *et al.*, 1987; Leshem *et al.*, 1984). Normally, membrane bilayers are exclusively liquid-crystalline reflecting the fact that the fatty acid side chains exhibit rotational motion (Lodish *et al.*, 1995). However, at the onset of senescence or following exposure to environmental stress coexisting domains of gel phase lipid and liquid-crystalline phase lipid are discernable in membrane bilayers, and this causes the membranes to become leaky because of packing imperfections at the phase boundaries (Thompson *et al.*, 1998; Thompson *et al.*, 1997).

The domains of gel phase lipid in senescing membranes are comprised mainly of fatty acids (Senaratra *et al.*, 1987; Platt-Aloia and Thomson, 1985; Leshem *et al.*, 1984). Indeed, a decline in membrane phospholipid is also a characteristic feature of senescence, and it reflects deesterification of fatty acids from both the sn-1 and sn-2 position of the phospholipid (Thompson *et al.*, 1997). This selective depletion of fatty acids from senescing membranes results in an increase in the sterol: fatty acid ratio and a corresponding decrease in bulk lipid fluidity (Thompson *et al.*, 1998; Thompson *et al.*, 1997). Recently, the gene for a senescence-induced lipase has been isolated from carnation. The expression of this gene is up-regulated in carnation flowers coincident with the onset of senescence, and its expression is also ethylene-induced (Hong *et al.*, 2000). Moreover, the recombinant protein produced when cDNA encoding the gene is over-expressed in *E. coli* is capable of deesterifying fatty acids from both the sn-1 and sn-2 positions of phospholipid (Hong *et al.*, 2000). It would appear,

therefore that the lipase encoded by this gene deesterifies fatty acids in senescing membranes, thereby inducing the lipid phase separations that cause the membrane to become leaky. This leakiness in turn results in loss of ion and metabolite gradients that are essential for cell function (Siedow, 1991; Hildebrand, 1989).

There is also an accumulation of peroxidized lipids in membranes during senescence that is attributable in part to the action of lipoxygenase (Thompson *et al.*, 1997). Moreover, this has been correlated temporally with deesterification of free fatty acid substrate for lipoxygenase, namely free linoleic acid and free linolenic acid, from membrane phospholipids (Lynch and Thompson 1984). Once lipid peroxidation has been initiated, it continues autocatalytically (Thompson *et al.*, 1997; Kappus, 1985). There are reports that the lipoxygenase itself generates superoxide (O_2^{-} •), which can in turn readily be converted to the hydroxyl radical (OH•) through the Weiss reaction (Kappus, 1985). Alkoxy radicals (RO•) are also formed during lipid peroxidation (Kappus, 1985).

This increased titre of activated oxygen species in senescing tissues promotes lipid peroxidation (Thompson *et al.*, 1997). However, there is also evidence that membrane proteins become damaged during senescence. This arises in part because of the decrease in bulk lipid fluidity in senescing membranes. Specifically, membrane proteins are vertically displaced towards the membrane surface as a consequence of decreasing membrane fluidity, and hence regions of the protein, which are normally in a hydrophobic environment, are displaced into a hydrophilic melieu (Shinitzky, 1984). This in turn causes changes in the conformation of the displaced proteins, which renders them prone to proteolysis (Duxbury *et al.*, 1991). There is also evidence for free radical reactions with membrane

proteins in senescing tissue. In particular, reactions of activated oxygen with amino acid residues result in alterations in protein conformation and ensuing proteolysis (Duxbury *et al.*, 1991).

A number of genes apart from lipase, including those encoding enzymes participating in the lipoxygenase pathway, are expressed at the onset of senescence (Buchanan-Wollaston, 1997). These are referred to as senescence-associated genes (SAGs) and are expressed in senescing but not mature tissue. Senescence-associated genes also include genes encoding pathogenesis-related proteins (PR), which accumulate after pathogen attack and, among other functions, promote the release of phytoalexins (Sticher *et al.*, 1997; Buchanan-Wollaston, 1997).

2.1. Abiotic Stress – Flooding.

Saturation of soil with water influences several factors in the rhizosphere of the plant. In particular, it results in low oxygen content in the soil. At the point of water-saturation, the rate of O_2 diffusion from the atmosphere into the soil is reduced by a factor of 10^4 due to increased diffusional resistance of O_2 in water compared with air. Furthermore, the solubility of O_2 in water is particularly low (Perry, 1999; Bailey and Ollis, 1986). Prolonged low oxygen partial pressure (< 50 mmol m^{-3}) causes hypoxia, and in extreme cases in which oxygen is no longer available, anoxia. In both cases, the soil becomes depleted of aerobic bacteria. There is an ensuing growth of anaerobic bacteria with accompanying changes in the chemical composition of the soil and availability of important nutrients to the plant.

In addition, low O_2 levels have direct deleterious effects on plant growth and development (Nilson and Orcutt, 1996). The most immediate effects of anaerobic soil conditions are engendered by the switch from aerobic to anaerobic respiration. This is manifested in reduced stomatal conductance, a rapid decrease in photosynthesis, a dramatic decline in the synthesis of most proteins and expression of senescence-associated genes (Nilson and Orcutt, 1996; Drew 1992). Stomatal conductance in response to low O_2 levels is not caused by low leaf water levels. Rather, it appears to be induced by a combination of reduced cytokinin levels and increased transport of abscisic acid from the roots, which is accompanied by an increased synthesis of ethylene (Zhang and Davis, 1987; Raskin and Kende, 1984).

Ethylene is synthesized from S-adenosylmethionine (SAM) in a two-step enzymatic reaction. Specifically, SAM is converted to 1-amino-cyclopropane-1-carboxylic acid (ACC) by ACC synthase, and ACC is then oxidized by ACC oxidase to form ethylene (Shah *et al.*, 1998). Under anoxic conditions, the stele of the roots becomes anoxic before the peripheral cortex because radial diffusion of O_2 is inhibited (Nilson and Orcutt, 1996). Several ACC synthase genes exist, and Zarambinski and Theologis (1993) have demonstrated that at least one is transcribed specifically under anoxic conditions. Thus, ACC is synthesized in increasing amounts in the anoxic core and then diffuses to the outer hypoxic root cells where ACC oxidase catalysis ethylene formation (Armstrong, 1994). The increase in ethylene synthesis results in elevated ethylene diffusion from roots to leaves and other plant organs. In addition, aerenchyma are formed, which are gas-filled, highly porous passages extending throughout the plant, and these facilitate accelerated intercellular ethylene transport to other plant organs

(Pennel and Lamb, 1997; Brailsford *et al.*, 1993; Wiedenroth, 1992). Over time, the outer root cells also become anoxic, and ethylene synthesis in the roots is inhibited. This occurs because the last step in the ethylene biosynthetic pathway, which is mediated by ACC oxidase, requires O_2. Thus ACC accumulates. However, ACC can be transported to aerated parts of the plant, primarily leaves, where the availability of O_2 allows ACC to be oxidized to ethylene. Furthermore, ethylene is less soluble in water than in air, and this leads to enhancement of its diffusion from the roots to aerial portions of the plant (Nilson and Orcutt, 1996). Consequently, upon flooding ethylene levels increase in roots, leaves and other plant organs.

2.2. Biotic Stress - Ingression.

Plants have a wide-ranging array of mechanisms for defense against pathogens. Some of the defense mechanisms are constitutive including, for example, pre-existing structural and chemical defenses, whereas others are inducible upon pathogen attack (Agrios, 1996). As well, defense mechanisms comprise an integrated response that provides protection to the plant both locally at the site of the ingression and systemically throughout the plant (Agrios, 1996). Induced resistance, for example, can be invoked locally and systemically. Both require recognition of the pathogen and subsequent signal transduction leading to activation of defense responses (Mauch-Mani and Métraux, 1998). For example, it has been demonstrated that localized immunization of *Arabidopsis thaliana* leaves with avirulent *Pseudomonas syringae* pv. tomato *(Pst)* has two distinct effects. First, it results in reduced *in planta* bacterial counts upon

subsequent infection with a virulent *Pst* strain at the site of primary inoculation and in adjacent tissue. Second, it confers systemic resistance two days after inoculation in tissues remote from the initial site of infection (Cameron *et al.*, 1994; Whalen *et al.*, 1991). In general, the recognition of an avirulent gene product by a plant resistance gene product leads to induction of local or systemic defense responses to subsequent (virulent) pathogen attacks and is referred to as the gene-for-gene concept (Dong *et al.*, 1991).

The general mechanism leading to a systemic response is known as systemic acquired resistance (SAR). SAR promotes long-lasting protection against secondary infection by a wide range of pathogens, not merely the original infecting pathogen (Maleck and Lawton, 1998). The effects of SAR are comparable to immunization in animals, although the underlying mechanisms differ since plants lack a circulatory system and antibodies (Sticher *et al.*, 1997). SAR is not only induced by pathogens, but can also be invoked by treatment with several chemical compounds. These include salicylic acid (SA) and synthetic inducers like benzoic acid derivatives and 2,6-dichloroisonicotinic acid (Hammerschmidt, 1999; Uknes *et al.*, 1992), which are chemical agents that do not possess anti-microbial activity *in vitro* or *in planta*. In addition, Cohen *et al.* (1991) have reported that linoleic and linolenic acids induce SAR against *P. infestans* in potato. Interestingly, SAR cannot be induced after the onset of flowering (Kessmann *et al.*, 1994).

SAR is inducible in monocots and dicots. It has been shown to be effective against fungal, viral and bacterial pathogens (Sticher *et al.*, 1997; Hammerschmidt and Kuc, 1995; Kuc, 1982; Ross, 1966). The induction of resistance in parts of the plant remote from the initial site of attack, which is the essential feature of SAR, is postulated to result from the translocation of an unknown systemic signal produced at the site of primary attack. This

signal is believed to prime protection against further pathogen attack by triggering a complex array of defense mechanisms (Hammerschmidt, 1999; Dong, 1998; Mauch-Mani and Métraux, 1998). One of these defense mechanisms is the induced synthesis of pathogenesis-related proteins. They accumulate at the site of infection and at remote, non-inoculated locations (Sticher *et al.*, 1998; Bate and Rothstein, 1998).

Some of the PR-genes can be induced by ethylene, and enhanced ethylene production can be observed at early stages of plant-pathogen interactions. Indeed, ethylene appears to control both the development and amplitude of pathogen ingression symptoms, especially after inoculation with virulent pathogens. Nevertheless, it is unlikely that ethylene is the unknown systemic signal, as SAR-gene expression in ethylene-insensitive mutants of *Arabidopsis thaliana* is unimpaired when compared to that in wild-type plants (Knoester *et al.*, 1998; Reymond and Farmer, 1998; Sticher *et al.*, 1997). Although SAR is characterized by suppressed bacterial growth of one to three orders of magnitude, little is known about the sequence of events between the inducing stimulus and the onset of resistance (Hammerschmidt, 1999). Characterization of SAR in a variety of plant species has indicated that it is invoked by a complex signaling network involving enhanced synthesis of ethylene as well as of jasmonic and salicylic acids, which are possible signal transduction molecules (Farmer *et al.*, 1998). The amount of time needed to establish SAR also varies depending upon the plant species and the inducing agent (Sticher *et al.*, 1997).

Although the parameters that are critical for the induction of SAR are not well understood, common features of most inducing treatments appear to be salicylic acid accumulation, local development of necrosis and, often, activation of the lipoxygenase pathway (Mauch-Mani and Métraux,

1998; Gardner, 1995; Goodman and Novacky, 1994; Melan *et al.*, 1993). Melan *et al.* (1993) have reported up-regulation of lipoxygenase in *Arabidopsis thaliana* leaves upon infection with strains of *Pseudomonas syringae*, and Goodman and Novacky (1994) suggested that increased levels of salicylic acid give rise to salicylic acid free radicals, which initiate lipid peroxidation. It has also been reported that high concentrations of *(2E)*-hexenal cause necrosis, which is a manifestation of the hypersensitive resistance response (Croft *et al.*, 1993). As well, Bate *et al.* (1998) have demonstrated that treatment of *Arabidopsis thaliana* with *(2E)*-hexenal results in up-regulation of genes encoding enzymes of the lipoxygenase pathway.

3. Bioreactors.

Linoleic and linolenic acids are immediate substrates for the aldehyde pathway (Fig. 2). They are converted to their corresponding fatty acid hydroperoxides by lipoxygenase in a two-step enzymatic reaction, and thence to C_6-aldehydes by hydroperoxide lyase. Linoleic and linolenic acids are also available commercially for use in a bioreactor. However, if the enzymes mediating their conversion to C_6-aldehydes were simply purified and used directly in a bioreactor to produce green-note volatiles, they would be subjected to reactor operation-induced denaturation and possible degradation by contaminating proteases, which would result in loss of enzyme activity (Bryjak and Kolarz, 1997; Bailey and Ollis, 1986). Moreover, hydroperoxide lyase and lipoxygenase are both membrane-associated enzymes and when removed from their membrane environment

are unlikely to be active. However, loss of enzyme activity can be minimized by immobilizing the membrane fraction containing such enzymes in an appropriate matrix in combination with highly effective protease inhibitors (ICN, 1997; Bailey and Ollis, 1986; Gray, 1982). Thus, protease-protected, purified membrane fractions challenged with exogenous linoleic and linolenic acids as substrates can be used as a basis for developing an immobilized bioreactor system for *in vitro* production of C_6-aldehydes.

3.1. Enzyme Immobilization.

The immobilization of enzymes in a bioreactor refers to their confinement and localization for continuous use. As such, they constitute a biocatalyst, and a number of processes for utilizing biocatalysts on a large-scale are well established (Buchholz and Klein, 1987; Bailey and Ollis, 1986). Immobilization within a biocatalyst provides a non-leaking matrix. Thus, no undesirable impurities leak into the product stream because there is separation of the products and the catalyst(s). Furthermore, immobilization provides a high catalytic density, high operational and storage stability, as well as the possibility of co-immobilization of enzymes participating in catalytic sequence in a biochemical pathway (Rehm, 1995; Luther *et al.*, 1992; Bailey and Ollis, 1986).

Over the last fifteen years, several immobilization techniques for whole cells and enzymes have been developed (Hsu et al., 1997; Smidsroed and Sjak-Braek, 1990; Mattiasson, 1983). The two most common enzyme entrapment techniques are immobilization within a continuously operated hollow-fiber ultrafiltration system and immobilization within insoluble gel-

matrices (Luther *et al.*, 1992). Although a semi-permeable hollow-fiber membrane allows removal of the products from the complete reaction mixtures in a single reactor unit, flow-induced enzyme denaturation and a low mass transfer rate limit the efficiency of this immobilization system (Luther *et al.*, 1992).

Among gel-matrices, Ca-alginate has proven to be a superior immobilization system for biocatalysts (Hsu *et al.*, 1997; Mattiason, 1983; Haumont *et al*, 1991). For example, Hsu *et al.* (1997) successfully immobilized lipoxygenase in a modified alginate matrix, and demonstrated the superiority of this method in comparison to adsorption or covalent linkage to different matrices (Pinto and Macias, 1996; Cuperus *et al.*, 1995; Battu *et al.*, 1994). Alginates, which are derived from *Laminaria hyperborea*, are glycuronans consisting of linear chains of β-(1,4)-linked residues of β-D-mannuronic acid and α-L-guluronic acid, arranged as a block-polymer in different sequences and compositions (Amsden and Turner, 1999; Martinsen *et al.*, 1992). The droplet-generating procedure of Klein *et al.* (1983) allows alginate, cross-linked with divalent Ca^{2+}-ions, to mechanically entrap enzymes, subcellular fractions or cells in a three-dimensional, thermostable (0-100°C), spherical macroporous matrix. The time required for complete polymerization can be estimated at 25°C according to Skjak-Braek *et al.* (1989) as:

$$t = 7.44\ d^2 \qquad \text{with } [t] = \text{min}, [d] = \text{mm} \qquad (1).$$

Small beads not only reduce the polymerization time, but also the pore length of the beads. Shorter pores would be expected to facilitate diffusion and, consequently, increase the reaction yield (Perry, 1999).

However, Haumont *et al.* (1991) demonstrated that yield of product by microsomes immobilized in alginate beads did not change significantly for bead-sizes ranging from 0.74 to 2.2 mm in diameter. This finding is of particular importance if a packed-bed bioreactor design is chosen, as the pressure drop (Δp) along the packing will increase with decreasing bead-size (Perry, 1999).

Alginates of high guluronic acid content give rise to flexible matrices with increased mechanical stability, porosity and tolerance to salts and chelating agents (Wang, 1996; Martinsen *et al.*, 1992). Mechanical stability of the immobilized biocatalyst is of particular importance if a packed-bed reactor configuration with a pressure-driven filtration product-retrieval unit is used. Specifically, this reactor configuration will engender a pressure-drop because of bed-compression at a given flow rate (u) along a packing of defined geometry, which could, if it is large, preclude effective operation of the pressure-driven recovery unit. Bed-compression is not linear because Δp versus u is non-linear, and may result in a high Δp that could block flow. Thus, mechanical stability against pressure, which is a key feature of alginates, represents a critical parameter for biocatalyst design (Perry, 1999; Buchholz and Klein, 1987).

Alginate matrices also provide high loading capacities, high affinity for water, mild entrapment conditions and low diffusional resistance (Martinsen *et al.*, 1992; Smidsroed and Sjak-Braek, 1990; Tanaka *et al.*, 1984; Bucke, 1983). Tanaka *et al.* (1984) demonstrated that solutes with a molecular weight $< 2 \cdot 10^4$ g/mol flow in and out of an alginate matrix by pore diffusion and show no reduction in diffusion coefficient in comparison with their corresponding free diffusion coefficients in water. One disadvantage of alginates is that the high porosity of the matrix can lead to

leakage of the immobilized fractions over time (Dainty *et al.*, 1986; Nillson and Mosbach, 1980). However, Kierstan and Bucke (1977) reported elimination of such leakage by cross-linking the alginate matrix with Ca^{2+}. They demonstrated that inulase, an enzyme with a molecular weight > 100 000 Da, was totally retained at alginate and Ca^{2+} concentrations of 2 % and 0.5 M, respectively. At the same time, the substrate and the product, both with a molecular weight < 5000 g/mol, were not subjected to any additional diffusional resistance (Tanaka *et al.*, 1984). Hydroperoxide lyase has also been successfully immobilized, although not in an alginate matrix. Nunez *et al.* (1997) demonstrated high activity and storage stability of partially purified hydroperoxide lyase immobilized in various types of affinity gels at pH 6.5.

3.2. Packed-bed Bioreactor.

In industrial applications of immobilized enzymatic reactions, the packed-bed bioreactor is most often used as a continuous operating system because it is easily automated and controlled, and its operating costs are low (Perry, 1999; Bodalo-Santoya *et al.*, 1999; Levenspiel, 1989). For example, packed-bed bioreactors have been used for glucose isomerization, for selective penicillin hydrolysis and for separating racemic mixtures (Bailey and Ollis, 1986). Notable features of packed-bed reactors are continuous use of the biocatalyst and maintenance of a constant physical and chemical environment for the immobilized enzymes. Confinement of the catalyst in the bed prevents contamination of the product and loss of biocatalyst (Bodalo-Santoya *et al.*, 1999). This latter feature is of particular

importance if the enzymes (enzyme preparation) are expensive. Furthermore, mechanical stirring is not necessary, and thus the immobilized enzymes are not damaged by impact with the impeller (Bodalo-Santoya *et al.*, 1999).

A packed-bed reactor consists of a cylindrical tube filled with catalytic pellets. It can be modelled in the first approximation as a plug-flow tank reactor (PFTR) without dispersion provided the substrate conversion per pass is greater than 1%. If the substrate conversion is smaller than 1%, the bioreactor can be modelled as a constant stirred tank reactor (CSTR) (Levenspiel, 1989; Bailey and Ollis, 1986). Basic and advanced performance equations, as well as their integrated counterparts under defined conditions, are well established in the literature (Perry, 1997; Levenspiel, 1989; Webb *et al.*, 1986).

3.3. Product Purification and Retrieval.

Pressure-driven ultrafiltration can be used for on-line retrieval of the products generated in a bioreactor. This continuous removal lowers the concentration of the product in the solvent stream, and enhances its partitioning out of the immobilization matrix. Consequently, the possibility of product-inhibition of the reaction can be minimized (Belfort, 1994; Bailey and Ollis, 1986). Polymeric, isotropic semi-permeable membranes are normally used in these applications of pressure-driven ultrafiltration (Bunch, 1988). Ideally, under constant pressure across the membrane, known as the transmembrane pressure (TMP), small dissolved solutes pass through the membrane (permeate) while solutes of high molecular weight

including proteins are rejected (retentate) (Grund *et al.*, 1992). Thus, in theory increasing permeate flux should result in a corresponding linear increase in the removal of small solutes. However, in practice the filtration process is complex, and changes in permeate flux over time attributable to build-up of a concentration-polarization boundary layer and gel-layers on the membrane with ensuing pore occlusion inevitably occur (Cass *et al.*, 1998, Grund *et al.*, 1992). This is referred to as fouling and has been studied extensively (Nilsson, 1990). Fouling decreases the permeate flux under constant transmembrane pressure until a lower, constant flux is reached (Grund *et al.*, 1992). Tangential recirculation of the feed stream over the membrane surface, known as cross-flow, reduces on-stream fouling by exerting increased shear on the concentration-polarization boundary layer (Robinson *et al.*, 1993). Other important factors influencing the flux and, consequently, yield of product are temperature and pH of the retentate stream (A/G Technology Corporation, 1997). Hollow fibre modules are often the first choice for the filtration unit as they provide a high membrane surface to volume ratio and low liquid hold-up, and they are also characterized by low energy consumption (Luther *et al.*, 1992).

3.4. Bioreactor and Product Optimization Using Two-Level Factorial Designs.

Optimization of processes and correct analysis of data are important challenges encountered in engineering and science. Achieving this is particularly important for a biochemical process consisting of a sequence of steps. For example, independent optimizations of a bioreactor core and the

associated separation unit will result in sub-optimal performance of the overall process (Groep *et al.*, 2000).

Any response variable y can be expressed as a function of a set of predictor factors $x_1, x_2, \ldots, x_k$. If the underlying scientific and technical principles are known, a precise, mechanistic model of the form $y = g(x_1, x_2, \ldots, x_k)$ can be derived. However, in most situations, these principles are not fully elucidated due to the complexity of the interactions among the factors and lack of manifold data. Thus, the response variable y must be fitted with an appropriate empirical model of the form

$$y = f(x_1, x_2, \ldots, x_k) + \varepsilon \qquad (2).$$

Such models, referred to as response surface models (RSMs), are widely used in designing and developing processes or in optimizing existing designs (Ergun and Mutlu, 2000; Takamizawa *et al*, 1996; Myers and Montgomery, 1995). Specifically, 2^2-factorial designs leading to first-order response surface models allow screening of two factors by identifying their importance and their possible joint-effects on the response variable. 2^2-Factorial designs require minimal experimentation, yet maximum information can be obtained (Ergun and Mutlu, 2000). Furthermore, their factor-effect estimates can be used for model optimization or as building blocks for more elaborate response surface models, such as central composite designs and Box-Wilson designs (Myers and Montgomery, 1995; Horitsu *et al.*, 1992).

Within a 2^2-factorial design, f [equation (2)] represents a true, but unknown, response function and can be modelled as

$$f(x_1, x_2) = Y = \beta_0 + \beta_1 x_1 + \beta_2 x_2 + \beta_{12} x_1 x_2 \quad (3)$$

provided there is minimal curvature of the true response surface. ε [equation (2)] characterizes variability not accounted for in f, such as measurement errors, and can be considered as a statistical error with normal distribution with mean zero and variance σ^2 (Myers and Montgomery, 1995). Equation (3) demonstrates that only four experiments are required in which the two factors, x_1 and x_2, each have to be run at two levels in order to determine the parameters of the model (β_i's).

Granted the assumptions of coded factors at levels arbitrarily called +1 and -1 and that each data point is replicated n times (Table 1), the parameters can be calculated according to Myers and Montgomery (1995) as:

$$\beta_0 = X_0 \quad (4)$$

$$\beta_1 = X_1/2 \quad (5)$$

$$\beta_2 = X_2/2 \quad (6)$$

$$\beta_{12} = X_{12}/2 \quad (7)$$

where X_0 is the grand average of all $4n$ observations with,

$$X_0 = 1/(4n)\,(ab + a + b + (1)) \quad (8)$$

and X_i represents the average effect on response of factor x_i produced by a change in the level of x_i averaged over changes in level of the other factor with,

$$X_1 = 1/(2n)\ (ab + a - b - (1)) \quad (9)$$

$$X_2 = 1/(2n)\ (ab + b - a - (1)) \quad (10)$$

and X_{12} represents the average effect on response of the interacting factors x_1, x_2 with

$$X_{12} = 1/(2n)\ (ab + (1) - a - b) \quad (11).$$

Once the parameters of the model are determined, a complete analysis of variance (ANOVA) can be used to assess whether the two main effects and the interaction effect are statistically significant. Each effect that is not statistically significant can be omitted, which simplifies the regression model (Devore and Peck, 1992). Consequently, four possible regression models can be obtained resulting in different response surfaces (Table 2). The validity of the model can be tested by determining its regression coefficient and a residual analysis (Myers and Montgomery, 1995).

Table 1. 2^2 -Design. Data-set for a typical experiment.

Factor Level Combinations	Replicates	Symbols Representing Sum of Replicates
$x_1 = -1, x_2 = -1$	$a_1, a_2, \ldots, a_n$	$(1) = \sum a_i$
$x_1 = +1, x_2 = -1$	$b_1, b_2, \ldots, b_n$	$a = \sum b_i$
$x_1 = -1, x_2 = +1$	$c_1, c_2, \ldots, c_n$	$b = \sum c_i$
$x_1 = +1, x_2 = +1$	$d_1, d_2, \ldots, d_n$	$ab = \sum d_i$

Table 2. 2^2-Design. Possible regression models.

Type	Mathematical Model
First-order with Interactions	$\beta_0 + \beta_1 x_1 + \beta_2 x_2 + \beta_{12} x_1 x_2$
First-order without Interactions and two Main Effects	$\beta_0 + \beta_1 x_1 + \beta_2 x_2$
First-order without Interactions and one Main Effect	$\beta_0 + \beta_1 x_1$, or $\beta_0 + \beta_2 x_2$
Constant Model	β_0

Materials and Methods

1. Chemicals.

Chemicals were obtained from Sigma Chemical Co. (Mississauga, ON) unless otherwise stated.

2. Preparation of a Biocatalyst for Continuous Production of C_6-Aldehydes.

2.1. Plant Material and Growth Conditions.

2.1.1. Carnation Flowers.

Carnation flowers (*Dianthus caryophyllus* L. cv. Improved White Sim, California Florida Plant, Salinas, CA) were grown under greenhouse conditions as described (Hudak and Thompson, 1997). Rooted cuttings were placed in 26-cm pots filled with Premier Pro-Mix HP medium (Premier Horticulture, Riviere-du-Loup, QC) and fertilized with 28-14-14 (Plant Products, Brampton, ON). Temperature settings were 25°C and 18°C for daylight and darkness, respectively, and lighting was supplemented with high pressure sodium lamps (400 W, 210 μmol/ m^2 s). Flowers were cut at stage I of development (flower bud partially closed) and allowed to open and senesce in deionized water at 25°C under constant illumination.

2.1.2. Strawberry Plants.

Strawberry cuttings (*Fragaria ananassa* L. cv. Totem, Ken M. Spooner Farms, Inc., East Puyallup, WA) were grown in a greenhouse under the same conditions that were used for carnation flowers. Rooted cuttings were placed in 26-cm pots filled with Premier Pro-Mix HP medium (Premier Horticulture, Riviere-du-Loup, QC) and fertilized with 28-14-14 (Plant Products, Brampton, ON). Temperature settings were 25°C and 18°C for daylight and darkness, respectively, and lighting was supplemented with high pressure sodium lamps (400 W, 210 µmol/ m^2 s). Leaves from mature plants were harvested for experiments.

2.1.3. Tomato Plants.

Tomato seeds (*Lycopersicon esculentum* L. cv. Match W42, Canadianhydrogarden, Ancaster, ON) were germinated in a greenhouse in 26-cm pots filled with Premier Pro-Mix HP medium (Premier Horticulture, Riviere-du-Loup, QC). The growing plants were fertilized with 28-14-14 (Plant Products, Brampton, ON). Temperature settings were 25°C and 18°C for day light and darkness, respectively, and lighting was supplemented with high pressure sodium lamps (400 W, 210 µmol/ m^2 s). Leaves from mature plants were harvested for experiments.

2.2. Tissue Homogenization.

Tissue homogenization was achieved by blending 1.5 grams fresh weight (g f w) of carnation petals, tomato leaves or strawberry leaves in 50 mL of homogenate buffer (50 mM EPPS pH 7.4, 250 mM sorbitol, 1 mM phenylmethylsulfonylfluoride (PMSF), 1 mM benzamadine hydrochloride (BH), 5 mM amino-n-caproic acid and 4% (w/v) polyvinylpolypyrrolidone) at 4°C in a Sorvall Omnimixer (Mandel Scientific Co. Ltd., Guelph, ON) at a setting of 5 for 45 s. This was followed by an additional blending with a Polytron homogenizer (Polytron Devices, Inc., Paterson, NJ) at a setting of 6 for 60 s at 4°C. The resulting slurry was filtered through four layers of cheesecloth (Veratec, Walpole, MA).

2.3. Subcellular Fractionation.

Filtrates from the cheesecloth were centrifuged at 2°C for 2 h at 250 000 x *g* in a Beckman 60 Ti rotor (Beckman, Palo Alto, CA) to obtain total membranes (the pellet) and cytosol (the supernatant). The membranous fraction was washed by resuspending the pellet in 5 volumes of resuspension buffer (50 mM EPPS pH 7.4, 250 mM sorbitol, 1 mM PMSF, 1 mM BH, 5 mM amino-n-caproic acid) and centrifuging at 2°C for 1 h at 250 000 x *g*. The resulting pellet of washed membranes was resuspended in 10 mL of homogenate buffer.

2.4. Volatile Analysis.

The C_6-volatiles, hexanal, *(3Z)*-hexenal and *(2E)*-hexenal, were identified and analyzed by GC/MS (Bate *et al.*, 1998). For this purpose, 2.5 mL of isolated membranes, cytosol, homogenate, or bioreactor permeate were added to 2.5 mL of saturated $CaCl_2$ solution and placed on ice to quench any further possible reaction and to contain the volatiles in solution. 100 µL of Antifoam 204 (Sigma Chemical Co., Missisauga, ON) was added to each sample to prevent foaming. Samples were then purged, and the released volatiles were trapped and directly desorbed into a gas chromatograph coupled with a mass spectrometer. The samples were purged and trapped using a Tekmar 3300 Purge & Trap Concentrator (ATS, Oakville, ON) fitted with a Vocarb 3000 trap (Supelco, Oakville, ON). This entailed placing the samples in the purge vessel and purging with helium for 11 min at a flow rate of 40 mL/min at 25 °C. The trapped volatiles were desorbed for 4 min at 225°C directly into a gas chromatograph coupled with a mass spectrophotometer (GC/MS) (HP-5890 series II GC and HP-5970 MS). The GC was fitted with a DB Wax column, 30m x 0.25 mm ID, 0.25 µm film (J & W Scientific, Brockville, ON). The oven temperature was held at 35°C for 2 min and then increased to 65°C at 8°C/min, stepped to 250°C at 30°C/min and held for 5 min. The carrier gas was helium, flowing at 39 cm/s. The MS detector was operated at a scan range of 35-150 m/z at 0.16 s/scan. The separated peaks were identified using the internal mass spectra library of the detector (NIST) and by spiking the samples with an authentic standard prior to analysis (hexanal and *(2E)*-hexenal only, as an authentic standard for *(3Z)*-hexenal is not available commercially).

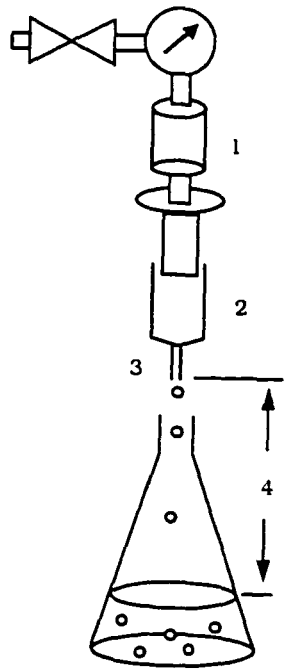
2.5. Enzyme Entrapment.

Resuspended membranes (10 mL) were combined with 10 mL of resuspension buffer and 6% (w/v) sodium alginate (BDH, Toronto, ON) at 4°C. Droplets of this well-mixed solution were extruded through a blunt sterile syringe-needle and collected in an Erlenmeyer flask containing 1 L of 0.02 M calcium chloride solution with constant stirring. Figure 3 illustrates a schematic diagram of the bead-making device. The resulting beads were of 3% alginate concentration. The hold-up volume of the syringe was 10 mL, and it was fitted with a PrecisionGlide 22 G 1.5 needle (Becton Dickinson and Company, Franklin Lakes, NJ). To obtain spherical beads of uniform size at 25°C, the droplet falling distance was set at 23 cm, the needle tip was flattened with a grinder and a constant pressure of 10 psi was applied using a pneumatic cylinder. The time required for complete polymerisation (curing) was calculated according to equation (1). Curing was carried out at 25°C. Beads were washed once with resuspension buffer prior to being used in the bioreactor. This method produced beads which averaged 2.5 mm in diameter.

2.6. Measurements of Bead Size and Geometry.

Beads were shaken for 5 min in a portable Ro-Tap Test Sieve Shaker (W.S. Tyler Company of Canada, St. Catharines, ON) to determine bead diameter distribution. In addition, beads were measured with a ruler, and their geometry was determined by optical inspection.

Figure 3. Schematic diagram of the bead-making device. 1= pneumatic cylinder powered by compressed air at 10 psi; 2 = disposable 10 mL syringe; 3 = needle (blunt-end); 4 = falling distance, measured from needle tip to liquid surface; 5 = stirred $CaCl_2$ solution.


1
2
3
4
5

3. Bioreactor Design and Operation.

3.1. Substrate Preparation.

A stock solution of 96.3 mM (9% v/v) linoleic acid containing 3% (v/v) polyoxyethylenesorbitan monolaurate (Tween 20) was prepared in 70.5 mL of boric acid buffer (0.2 mM boric acid, pH 9). This stock solution was diluted with boric acid buffer to the desired final linoleic acid concentrations. For one set of experiments, a 32.1 mM solution of linolenic containing 1% (v/v) Tween 20 was prepared in 73.52 mL of boric acid buffer.

3.2. Membrane Selection for the Ultrafiltration Unit.

Lipoxygenase and hydroperoxide lyase have molecular weights of 92-100 kDa and 200-250 kDa, respectively. Therefore, flat polysulfone membrane sheets with molecular weight cut-offs (MWCO) of 100 and 300 kDa mounted in a Minitan acrylic ultrafiltration system (Milipore, Bedford, MA) were tested for their ability to retain these enzymes from tomato fruit homogenate in order to determine the optimum MWCO of the ultrafiltration unit for the bioreactor. The tomato fruit homogenate was prepared using 500 g of tomato fruit at the red-ripe stage of development. The tomatoes were cut open, the seeds were removed, and the remaining pericap was cubed into 2-cm pieces. The tissue was homogenized in a blender (T-fal, Rumilly, France) in 250 mL homogenate buffer (50 mM EPPS pH 7.4, 250 mM sorbitol, 1 mM phenylmethylsulfonylfluoride (PMSF), 1 mM

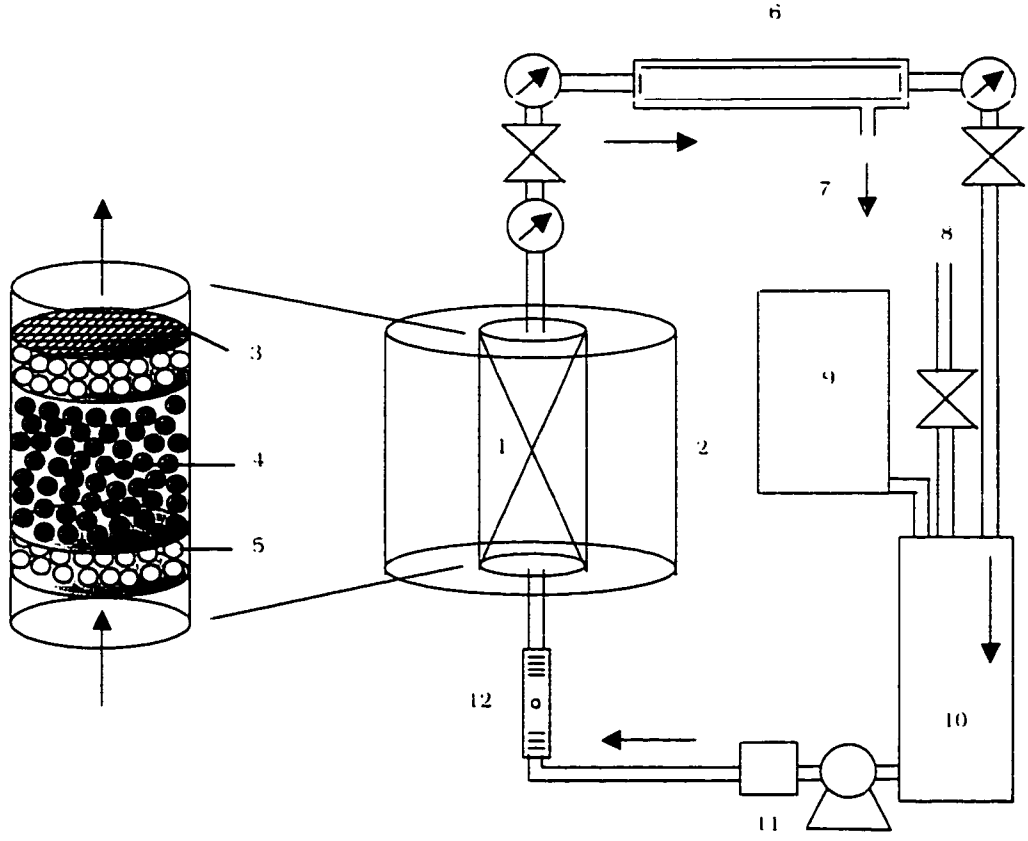
benzamadine hydrochloride (BH), 5 mM amino-n-caproic acid and 4% (w/v) polyvinylpolypyrrolidone). The homogenate was filtered through four layers of cheesecloth (Veratec, Walpole, MA), and then passed through the membrane sheets at a flow rate of 480 mL/min delivered with a peristaltic pump (Cole-Parmer, Niles, IL) at a transmembrane pressure of 12 psi.

3.3. Bioreactor Design.

A schematic drawing of the complete bioreactor is illustrated in Figure 4. The core unit is a packed-bed reactor, and a XAMPLER UFP-E-4A ultrafiltration unit was incorporated as the separation component. The packed-bed reactor was constructed using a cylindrical tube of Plexiglas™, 3.8 cm in diameter and 12.7 cm in length, and was surrounded with a heating jacket. The XAMPLER UFP-E-4A hollow-fibre ultrafiltration unit was obtained from A/G Technology Corporation (Needham, MA). The cartridge consisted of 50 polysulfone membrane fibres with a molecular weight cut-off of 100 kDa and a total membrane area of 0.042 m^2. The lumen volume was 12 mL, and the shell volume was 30 mL.

The biocatalyst was retained in the core by two layers of glass beads (2.5 mm diameter) held between stainless steel meshwork screens (Fig. 4). Tygon was used for fluid conducting elements, and a peristaltic pump (Watson Marlow, Wilmington, MA) fitted with a Cole-Parmer pulsator (Cole-Parmer, Niles, IL) was used to circulate the reaction mixture. In order to allow diafiltration, a constant retentate volume was maintained by continuously adding reactor buffer. The liquid hold-up volume of the loaded reactor was 225 mL.

Figure 4. Schematic diagram of the bioreactor and ultrafiltration unit. 1= reactor core; 2 = heating jacket; 3 = stainless steel meshwork retainers; 4 = biocatalyst; 5 = glass beads; 6 = ultrafiltration unit; 7 = product withdrawal port; 8 = substrate inlet; 9 = buffer reservoir; 10 = mixing chamber; 11 = peristaltic pump & pulsator; 12 = flowmeter. The arrows indicate direction of flow.


6
7
8
9
1
2
3
4
5
12
10
11

3.4. Operation of the Bioreactor.

Prior to operating the reactor, it was regenerated as described in Section 3.5., and all of the units except the core and mixing chamber were filled with reactor buffer (50 mM EPPS pH 7.4, 250 mM sorbitol, 1 mM PMSF, 1 mM BH, 5 mM amino-n-caproic acid). For operating, the core was loaded with the biocatalyst and set at a constant temperature, and 75 mL of substrate solution, preheated to core temperature, was added to the mixing chamber. The bioreactor was run for 1 min in total recycle mode, and then the transmembrane pressure was elevated from ambient pressure to 5psi, and the permeate flux was measured constantly. Permeate was sampled from the shell side in triplicates after 5, 10, 15 and 30 min, and analysed for volatile content.

3.5. Reactor Regeneration.

Regeneration of the reactor was required after each experiment due to membrane fouling. The biocatalyst (beads) was discarded, and the residual feed was flushed from the reactor with 2.5 L deionized water at 50°C. Terg-A-Zyme® (0.2% (v/v), 50°C) was circulated through the reactor for 2 h, and the reactor was then rinsed by circulating 2.5 L clean water (50°C). This cleaning procedure was repeated until regeneration was complete, which was indicated by a base flux for deionized water of 60-63 mL/min at 25°C and transmembrane pressure of 5 psi according to the operation manual (A/G Technology Corporation, Needham, MA).

3.6. Factorial Reactor Design.

A 2^2-factorial design with three replicates of each data point was carried out using substrate concentration and catalyst loading as independent process factors. Four replicates at the centre point were measured in order to verify the curvature of the response surface. The centre point was arbitrarily set at [substrate] = 21.5 mM, [catalyst] = membrane equivalent of 3 g f w. Substrate concentration (mM) and catalyst loading (g f w) were coded as x_1 and x_2, respectively, according to the following equations:

$$x_1 = ([\text{substrate}] - 21.5\ \text{mM})/\ 10.7\ \text{mM} \qquad (12)$$

$$x_2 = ([\text{catalyst}] - 3\ \text{g f w})/\ 1.5\ \text{g f w} \qquad (13)$$

Levels for each coded factor were +1 and −1. The response factor Y (hexanal yield) was also coded by means of relative peak area where 100 units equal 79 µg hexanal (14).

4. Preparation of Transgenic *Arabidopsis thaliana* Plants.

In an effort to increase levels of the green-note volatile, *(3Z)*-hexenal, in plant tissue, the gene for hydroperoxide lyase was up-regulated in transgenic *Arabidopsis thaliana* plants. Hydroperoxide lyase catalyzes the formation of C_6-aldehydes from linoleic and linolenic acid hydroperoxides.

4.1. Plant Material and Growth Conditions.

Arabidopsis thaliana, ecotype Columbia, seeds were sown in soil (Premier Pro-Mix BX, Premier Horticulture, Riviere-du-Loup, QC), cold-treated at 4°C in the dark overnight, and germinated in a growth chamber at 23°C under 150 μmol/(m^2s) photosynthetically active radiation in 16h light/8h dark photoperiods. Seedlings were grown to maturity under the same conditions.

4.2. Hydroperoxide Lyase Transgene Construct and Plant Transformation.

Preparation of the hydroperoxide lyase transgene construct and transformation of *Arabidopsis* with this construct were carried out by Li Wang, a technician in Dr. Thompson's laboratory, and briefly entailed the following steps. The *Arabidopsis* EST clone, 94J16, was used as the source of hydroperoxide lyase cDNA for preparation of the hydroperoxide lyase transgene construct. This 1.6 kb hydroperoxide lyase cDNA includes a small portion of the 5'-untranslated region, specifically 6 bp upstream of the ATG start codon, the entire coding sequence, and all of the 3'-untranslated region following the TAA stop codon (Fig. 5). The hydroperoxide lyase cDNA was subcloned into the *XbaI* site of pBluescript KS (Stratagene, La Jolla, CA). The resulting plasmid was digested with *XbaI* (Boehringer, Laval, QC), and the cDNA fragment was cloned into the *XbaI* site of the binary vector pKYLX71-35S^2 (Schardl *et al.*, 1987) (Fig. 6). The pKYLX-HPL construct, which contains hydroperoxide lyase cDNA in the sense orientation under

Figure 5. Nucleotide and deduced amino acid sequence for full-length *Arabidopsis thaliana* cDNA encoding hydroperoxide lyase.

M L L R T M

1 CGATAGAAAT AGAAGGCGAA GAGATAATTT CCAAAAACAA GAAAAACCTC TAAGCTCAAA AGATGTTGTT GAGAACGATG

A A T S P R P P P S T S L T S Q Q P P S P P S Q L P L

81 GCGGCGACTT CCCCGCGGCC ACCACCGTCA ACATCCCTAA CATCTCAGCA GCCACCATCA CCCCCCTCAC AGCTTCCCCT

R T M P G S Y G W P L V G P L S D R L D Y F W F Q G

161 CCGTACAATG CCGGGATCGT ACGGCTGGCC GTTGGTTGGA CCATTATCGG ACCGTTTAGA TTACTTCTGG TTCCAAGGAC

P D K F F R T R A E K Y K S T V F R T N I P P T F P F

241 CCGATAAGTT TTTCCGGACA AGAGCTGAGA AGTATAAGAC CACTGTGTTC CGTACAAATA TTCCTCCGAC GTTTCCTTTC

F G N V N P N I V A V L D V K S F S H L F D M D L V D

321 TTCGGCAACG TTAACCCTAA CATCGTCGCC GTTCTTGACG TCAAGTCTTT TAGCCATCTT TTTGACATGG ATCTAGTTGA

K R D V L I G D F R P S L G F Y G G V C V G V N L D

401 TAAAAGAGAT GTTCTCATCG GAGACTTCCG GCCTAGCCTT GGGTTCTACG GCGGCGTTTG TGTGGGAGTT AATCTGGACA

T T E P K H A K I K G F A M E T L K R S S K V W L Q E

481 CTACTGAGCC AAAGCACGCC AAGATAAAAG GTTTCGCTAT GGAAACACTA AAACGAAGCT CAAAAGTATG CTACAAGAG

L R S N L N I F W G T I E S E I S K N G A A S Y I F P

561 CTTCGTTCAA ACCTAAACAT TTTCTGGGGA ACAATCGAAT CGAAAATCTC CAAAAACGGT GCCGCTTCAT ATATCTTCCC

L Q R C I F S F L C A S L A G V D A S V S P D I A E

641 TCTCCAACGT TGCATCTTCA GTTTCCTCTG CGCCTCTCTC GCCGGCGTTG ACGCTTCCGT ATCGCCGGAC ATCGCTGAGA

N G W K T I N T W L A L Q V I P T A K L G V V P Q P L

721 ACGGTTGGAA AACAATCAAT ACTTGGCTTG CGTTGCAAGT TATTCCCACT GCTAAACTTG GCGTAGTTCC TCAGCCTCTT

E E I L L H T W P Y P S L L I A G N Y K K L Y N F I D

801 GAAGAGATTT TACTTCATAC TTGGCCTTAT CCTTCTCTCT TAATCGCCGG AAATTACAAA AAGCTTTACA ATTTCATCGA

E N A G D C L R L G Q E F F R L T R D E A I Q N L L

881 CGAGAACGCC GGAGATTGTC TCCGGTTAGG TCAAGAAGAA TTCCGGTTGA CCCGAGATGA GGCTATTCAA AATCTTCTCT

F V L G F N A Y G G F S V F L P S L I G R I T G D N S

961 TTGTTTTAGG TTTTAATGCC TACGGGGGCT TTTCCGTCTT CTTACCTTCT TTGATCGGGA GAATAACCGG CGACAATTCC

G L Q E R I R T E V R R V C G S G S D L N F K T V N E

1041 GGTTTACAGG AGAGGATTAG AACCGAAGTC AGGAGAGTTT GCGGATCCGG GTCGGATCTT AATTTCAAGA CGGTTAACGA

M E L V K S V V Y E T L R F N P P V P L Q F A R A R

1121 AATGGAGCTG GTTAAATCCG TGGTTTACGA AACGCTGCGT TTTAATCCTC CGGTTCCGCT GCAATTCGCA CGTGCGAGGA

K D F Q I S S H A D V F E V K K G E L L C G Y Q P L V

1201 AAGATTTTCA GATAAGTTCA CACGATGCTG TTTTTGAGGT CAAGAAAGGT GAGCTTCTTT GTGGTTATCA GCCGCTTGTG

M R D A N V F D E P E E F K P D R Y V G E T G S E L L

1281 ATGAGAGACG CTAATGTTTT TGACGAACCG GAGGAATTTA AACCGGACCG GTATGTTGGT GAGACCGGGT CTGAATTGCT

N Y L Y W S N G P Q T G T P S A S N K Q C A A K D I

1361 GAATTATCTC TACTGGTCTA ACGGTCCACA AACCGGTACC CCGAGCGCGT CTAACAAACA GTGTGCAGCT AAGGACATTG

V T L T A S L L V A D L F L R Y D T I T G D S G S I K

1441 TCACTCTCAC GGCTTCCTTG CTCGTTGCCG ATTTATTTCT CCGGTATGAT ACGATTACTG GTGACTCCGG TTCAATTAAA

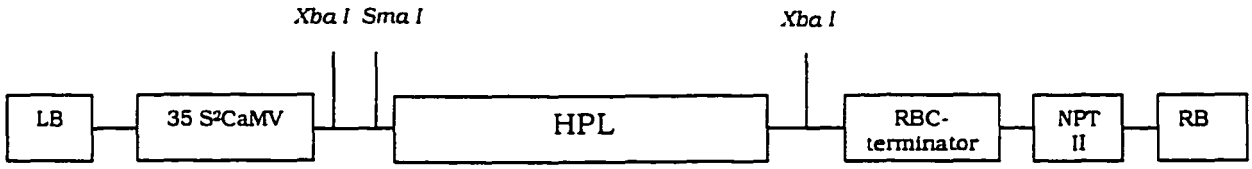
A V V K A K

1521 GCTGTTGTTA AAGCTAAATA AGTTAAAGAT TGATTAGTGT TTAATGTTAT GTAATCAATC TTCAACGGTT TCATTTGTTC

1601 GGAGTGTATA AATTATATGT AAACTAAAAT AATCCGAATT GAAACTCAAA TTGTTATGTT AGATGGTGTT GCTATGTTAG

1681 AGAGATTTTA ACTAAAAAAA AAAAAAAAAA A

Figure 6. pKYLX-HPL construct. The construct contains full-length *Arabidopsis thaliana* cDNA encoding hydroperoxide lyase in the sense orientation under the regulation of the cauliflower mosaic virus double 35S promoter. The cDNA fragment was cloned into the *XbaI* site of the binary vector pKYLX71-35S^2 according to Schardl *et al.* (1987). LB, left border; 35S^{2}CaMV, cauliflower mosaic virus double 35S promoter; HPL, cDNA encoding hydroperoxide lyase; RBC-terminator, transcription terminator; NPT II, plant selectable marker; RB, right border.


Xba I Sma I
Xba I
LB
35 S²CaMV
HPL
RBC-
terminator
NPT
II
RB

the control of the cauliflower mosaic virus double 35S promoter (Fig. 6), was introduced into *Agrobacterium tumefaciens* C58 by electroporation and transferred to *Arabidopsis thaliana* leaves by vacuum infiltration (Bechtold *et al.*, 1998). The primary transformants T_0 were allowed to mature and set seed in the growth chamber. T_1 seedlings were selected on Murashige and Skoog medium containing 50 mg/L kanamycin, 50 mg/L carbenicillin, 0.8% agar and 1% sucrose. The kanamycin-resistant seedlings were planted in soil and grown to maturity. T_2 and T_3 seedlings were similarly selected. Seedlings from T_3 lines that were kanamycin-resistant were considered to be homozygous and were used for subsequent analysis.

4.3. Screening of T_3 Transgenic Lines and Volatile Analysis.

Leaf tissue (100 mg) was collected from 4-week-old *Arabidopsis thaliana* transgenic and wild-type plants and ground to a fine powder in liquid nitrogen. The frozen tissue powder was immediately mixed with 2.5 mL of a buffer consisting of 50 mM EPPS pH 7.4, 250 mM sorbitol, 5 mM amino n-caproic acid, 4% (w/w) polyvinylpolypyrollidone, 10 mM EDTA, 2 mM EGTA, 1 mM BH, 1 mM PMSF, 2.5 mL saturated $CaCl_2$ solution and 100 µL of Antifoam 204. Transgenic plants were screened by GC/MS analysis of volatile levels in these suspensions as described in Section 1.3.

4.4. Northern Blot Analysis.

Total RNA was extracted from leaves of *Arabidopsis thaliana* transgenic and wild-type plants as described by Chirgwin *et al.* (1979) and modified by Ohan and Heikkila (1995): The aerial portions (1.5 g f w equivalent) of frozen wild-type and transgenic *Arabidopsis thaliana* plants were ground into a fine powder in liquid nitrogen using a mortar and pestle. 10 mL of guanidine isothiocyanate buffer was added (4 M guanidine isothionite (GIT) enzyme grade, BRL# 5535 U, 25 mM sodium acetate pH 6, 120 mM β-mercaptoethanol, in 0.1% (v/v) diethyl pyrocarbonate (DEPC)-treated water), and the samples were vortexed. The samples were then centrifuged at 7700 x g for 10 min using a Sorvall SS34 rotor (Mandel Scientific Co. Ltd., Guelph, ON). Afterwards, the supernatant was carefully layered onto 3.3 mL of filter-sterilized cesium chloride buffer (5.7 M CsCl optical grade, BRL# 55074A, 25 mM sodium acetate pH 6, in 0.1 % (v/v) DEPC-treated water) in Ultra-clear® ultracentrifuge tubes (14x89 mm, Beckmann, Palo Alto, CA). To pellet the RNA, samples were centrifuged at 111 000 x g for 23h at 20°C in a Beckmann L8-70 ultracentrifuge using a SW-41 Ti rotor (Beckman, Palo Alto, CA). The buffer was gently removed, and the tube was inverted to drain any residual buffer. The resulting RNA pellet was rinsed with ice cold 70% (v/v) ethanol and inverted to drain for 10 min. The pellet was then resuspended in 360 µL TES buffer (10 mM Tris HCl pH 7.4, 5 mM EDTA, 1% (w/v) SDS [sodium dodecyl sulfate]) and incubated on ice for 10 min. This RNA suspension was transferred to a 1.5 mL Eppendorf tube and ethanol-precipitated by adding 100% ice-cold ethanol for 30 min at -80°C. The precipitated RNA was collected by centrifugation at maximum speed in an Eppendorf microfuge (Brinkmann

Instruments Inc., Mississauga, ON) for 10 min at 4°C. The supernatant was removed, and the pellet was resuspended in 360 µL 0.1% (v/v) DEPC-treated water and ethanol-precipitated once more. The RNA pellet was then left to dry at room temperature by inverting the Eppendorf tube for 15 min. The dried pellet was resuspended in 76 µL 0.1% (v/v) DEPC-treated water.

The resuspended RNA was fractionated by denaturing 1% formaldehyde-agarose gel (1% agarose, 5 mL 10x MOPS [0.2 M MOPS, 50 mM sodium acetate·$3H_2O$, pH 7, 10 mM EDTA], 36 mL DEPC treated water) electrophoresis. 10 µg of RNA per sample was mixed with 20 µL denaturing solution (50% (v/v) formamide, 16% (v/v) formaldehyde, 10% (v/v) 10x MOPS, 6.7% (v/v) DEPC-treated water, 5% (v/v) bromophenol blue [1%]). Ethidium bromide (0.01%) was included (0.5 µL per sample) to verify equal loading of RNA, and electrophoresis was performed at 75 volts for 2 h (running buffer: 1x MOPS). The fractionated RNA was then transferred onto a Hybond™-N nylon membrane (Amersham, Pharmacia Biotech Inc., Piscataway, NJ). After transfer, the membranes were incubated with ^{32}P-labeled *Arabidopsis* hydroperoxide lyase cDNA (Feinberg and Vogelstein, 1983) in 50% formamide, 5x SSC (0.75 M NaCl, 0.075 M sodium citrate), 1x Denhart's solution, 0.1% (w/v) SDS and 100 µg/ mL of denatured salmon sperm DNA at 42°C. Membranes were washed for 20 min at 60°C with 2x SSC and 0.1% SDS, and then for a further 15 min at 60°C with 0.5x SSC and 0.1% SDS. The washed membranes were exposed to X-Omat-AR films (Eastman Kodak, Rochester, NJ) at –80°C for 6 days.

5. Root-Flooding of Transgenic and Wild-type *Arabidopsis thaliana* Plants.

In order to determine the impact of up-regulating hydroperoxide lyase on the response of plants to stress, the effects of reduced oxygen stress on transgenic and wild-type *Arabidopsis* plants were compared. Reduced-oxygen stress was induced by subjecting growing plants to root-flooding. To vary O_2 availability, the soil was either periodically moistened every second day with 10 mL of water per plant (control) or continuously flooded. Continuous flooding was achieved by placing the potted plants in trays constantly filled with water, and by additional watering of the soil from the top with 15 mL of water per plant on a daily schedule.

6. Infection of Transgenic and Wild-type *Arabidopsis thaliana* Plants with *Pseudomonas syringae* pv. tomato (*Pst*).

C_6-aldehydes and C_6-alcohols are known to act as anti-bacterial agents (Croft *et al.*, 1993). Accordingly, the effects of infection with the bacterial pathogen *P. syringae* pv. tomato were compared for transgenic and wild-type *Arabidopsis thaliana*. Seeds of transgenic and wild-type plants were agitated for 2 min in 1 mL of 70% ethanol. After discarding the ethanol, 1 mL of seed sterilizing solution (15 mL bleach (6%), 0.05 mL Tween 20, and 40 mL sterile water) was added, and the seeds were left for 10 min in an Eppendorf tube with occasional agitation. After discarding the sterilizing solution, the seeds were rinsed 5 times with sterile water, and then suspended in 0.5–1 mL phytagar (0.1%) and left overnight at 4°C.

These seeds were grown on MS plates (4.3 g Murashige & Skoog salt mixture, 20 g sucrose, 8 g phytagar, 1 mL 1000 x MS vitamins, 1 L sterile water and 100 mg kanamycin) in a growth chamber at 22°C under 150 μmol/(m^2s) photosynthetically active radiation with 14h light and 10h dark cycles. After three days, the plants were transplanted to soil (Premier Pro-Mix, 1g/L 20-20-20 fertilizer) and allowed to continue growing in the same chamber.

Infection of transgenic and wild-type *Arabidopsis thaliana* was carried out according to Cameron *et al.* (1994) and Whalen *et al.* (1991) with the following bacterial strains:

Pst strain DC3000 (pVSP 61) - virulent bacterium (rifampicin and kanamycin resistant)

Pst strain DC3000 (pV288, avrRpt2) - avirulent bacterium (rifampicin and kanamycin resistant)

The bacterial stock cultures were diluted in 10 mM $MgCl_2$ to 10^6 colony forming units (cfu)/mL inoculum for infection (0.1 OD_{600} = 1 x 10^8 colony forming units/mL) in a total volume of 5 mL. Well-watered plants were exposed to increased light-levels for several minutes to ensure that the stomata were open, and then 1 mL of bacterial suspension was pressure-infiltrated into the underside of the leaf using an 1 mL syringe. Each treatment consisted of a primary inoculation of one leaf per plant and a second inoculation two days later of four other leaves per plant. The following treatments were carried out:

(M,M): primary and secondary inoculation with 1 mL of 10 mM $MgCl_2$ (mock control)

(M,A): primary inoculation with 1 mL of 10 mM $MgCl_2$, secondary inoculation with 1 mL of avirulent bacteria at a dose of 10^6 colony forming units (cfu)/mL

(M,V): primary inoculation with 1 mL of 10 mM $MgCl_2$, secondary inoculation with 1mL of virulent bacteria at a dose of 10^6 cfu/mL

(A,V): primary inoculation with 1 mL of avirulent bacteria at a dose of 10^6 cfu/mL, secondary inoculation with 1 mL of virulent bacteria at a dose of to 10^6 cfu/mL

Plants were placed back in the growth chamber (14h light/10h dark cycle, 22°C) for 3 days. The plants were then checked for symptoms, and *in planta* bacterial counts were also made.

To isolate and quantify bacteria from the infected plants, leaves were surface-sterilized in 50% ethanol, followed by two rinses of sterile water. Two leaf discs were taken from the center of each infected leaf using a cork borer (d=4 mm) and placed in an Eppendorf tube. These leaf disks were homogenized in 500 µL 10 mM $MgCl_2$ with a hobby drilling machine and drill (Canadian Tire, Toronto, ON) and then diluted 10^{-2}, 10^{-4} and 10^{-6} in 10mL of 10mM $MgCl_2$ solution. A 0.1 mL sample of each dilution was distributed evenly on a King's B rifampicin/kanamycin plate. (Preparation of 1L King's B rifampicin/kanamycin medium: 20 g protease peptone, 10 mL glycerol, 1.5 g K_2HPO_4, 15 g bacteriological agar and 1 L Milli-Q-water were autoclaved for 20 min and allowed to cool. 6 mL $MgSO_4$, 10 mL kanamycin (5 mg/mL) and 5 mL rifampicin (10 mg/mL) were added before the plates

were poured). The plates were kept in the dark at 25°C, and colony forming units were determined for each plate.

7. Protein Analysis.

Protein levels were determined spectrophotometrically using the BCA Protein Assay Reagent according to Pierce (Rockford, IL). A standard or unknown protein sample (0.1 mL) was mixed with working reagent (2 mL, Pierce, Rockford, IL). After 2h incubation at room temperature, the absorbance of the sample was read at 562 nm with a Beckman DU-64 spectrophotometer (Beckman, Palo Alto, CA) and compared to bovine serum albumin (BSA) standards.

8. Measurement of Chlorophyll.

To measure chlorophyll, an aliquot of 0.1 mL of homogenate was added to 9.9 mL acetone (80%), vortexed and centrifuged at 8200 x g for 1 min using an Eppendorf microfuge (Brinkmann Instruments Inc., Mississauga, ON). The pellet was discarded, and the absorbance of the supernatant was read at 645 and 663 nm with a Beckman DU-64 spectrophotometer (Beckman, Palo Alto, CA). The total chlorophyll concentration (c) was determined according to Edelman *et al.* (1982) as:

$$c = 10 \cdot (20.2 \cdot A_{645} + 8.02 \cdot A_{663}) \qquad (15) \qquad \text{with } [c] = \mu g/mL.$$

9. Measurement of Peroxidized Lipids in Total Membranes.

Tissue homogenization for the purpose of isolating total membranes was achieved by blending 1.5 grams fresh weight (g f w) of *Arabidopsis thaliana* leaves in 50 mL of homogenate buffer (50 mM EPPS pH 7.4, 250 mM sorbitol, 1 mM phenylmethylsulfonylfluoride (PMSF), 1 mM benzamadine hydrochloride (BH), 5 mM amino-n-caproic acid and 4% (w/v) polyvinylpolypyrrolidone) at 4°C in a Sorvall Omnimixer (Mandel Scientific Co. Ltd., Guelph, ON) at a setting of 5 for 45s. This was followed by an additional blending with a Polytron homogenizer (Polytron Devices, Inc., Paterson, NJ) at a setting of 6 for 60s at 4°C. The resulting slurry was filtered through four layers of cheesecloth (Veratec, Walpole, MA). Filtrates were centrifuged at 2°C for 2 h at 250 000 x *g* in a Beckman 60 Ti rotor (Beckman, Palo Alto, CA) to obtain total membranes (the pellet) and cytosol (the supernatant). The membranous fraction was washed by resuspending the pellet in 5 volumes of resuspension buffer (50 mM EPPS pH 7.4, 250 mM sorbitol, 1 mM PMSF, 1 mM benzamadine hydrochloride (BH), 5 mM amino-n-caproic acid) and centrifuging at 2°C for 1 h at 250 000 x *g*. The resulting pellet of washed membranes was resuspended in 10 mL of homogenate buffer. Resuspended membranes were centrifuged at 8200 x g for 1 min using an Eppendorf microfuge (Brinkmann Instruments Inc., Mississauga, ON), and the supernatant was used for peroxidized lipid determination. This was achieved by measuring the absorbance at 234 nm with a Beckman DU-64 spectrophotometer (Beckman, Palo Alto, CA) according to Gutteridge and Halliwell (1990).

10. Plant Weight Determination.

Rosette leaves of *Arabidopsis thaliana* were harvested, and any attached soil was removed. The leaves were weighed immediately and then dried for 72 h at 60°C and weighed again in order to determine fresh and dry weights, respectively.

11. Lipid Extraction and Quantitation.

Lipids were extracted according to Hudak (1995). One volume of sample and three volumes of methanol: chloroform (2:1 v/v) were vortexed, and 0.8 volumes of 0.73% NaCl (w/v) and one volume of chloroform were then added. The resulting mixture was vortexed again, and allowed to phase separate. The lower phase was drawn off and dried under inert gas, and 1 mL of 14% boron trifluoride was added. This mixture was heated in sealed tubes to 90°C for 1h and then allowed to cool. After the addition of 0.5 mL water, the methylated fatty acids were extracted with 1mL of hexane and analyzed by gas chromatography. The gas chromatograph (HP-5890 series II) was equipped with a 0.75 mm inlet liner, set at 250°C and 25 kPa at a split ratio of 100:1, and fitted with a DB Wax column, 30m x 0.25 mm ID, 0.25 μm film (J & W Scientific, Brockville, ON) and a FID set at 275°C. The oven temperature was held at 180°C for 8 min, and the carrier gas was helium, flowing at 39 cm/s. The methyl esters were identified using authentic standards, and quantified by using heptadecanoic acid as an internal standard, added prior to lipid extraction.

Results

1. Biocatalyst and Bioreactor Design.

Hexanal is one of the key green-note volatiles (Gardner, 1995). Steady-state levels of hexanal were quantified by gas chromatography and mass spectroscopy (GC/MS) for crude homogenates of mature strawberry leaves, mature tomato leaves and carnation flower petals at stage II of development in order to determine whether these tissues could be utilized as biocatalysts for bioreactor-based production of hexanal. Stage II carnation flowers were selected for this purpose because levels of green-note volatiles in the petals are highest at this stage of post-harvest flower development (Schade *et al.*, 2000).

Hexanal was present in crude homogenates of tomato leaves, strawberry leaves and carnation petals at levels of 1.50, 0.68 and 0.28 μg/ g fresh weight of tissue, respectively (Table 3). Although tomato leaves are the richest source for hexanal, the concentrations in all three tissues were of a similar order of magnitude. Thus, all three tissues were further investigated as potential experimental systems.

Preparations of total membrane from these tissues were used as biocatalysts since several lines of evidence indicate that membranes are the predominant subcellular sites of hexanal generation. In particular, recent studies have indicated that the gene encoding hydroperoxide lyase has a plastid envelope targeting sequence (Blée and Joyard, 1996). In addition, subcellular fractionation studies of carnation petals have demonstrated that isolated membranes are capable of synthesizing hexanal from linoleic acid (Schade *et al.*, 2000). As hexanal is formed from linoleic acid through the

Table 3. Levels of hexanal in tissue homogenates expressed as µg per g fresh weight of plant material. Values are means ± SE for n = 3.

Plant System	Hexanal (µg/g f w)
Strage II Carnation Petals*	0.28 ± 0.02
Strawberry Leaves	0.68 ± 0.03
Tomato Leaves	1.50 ± 0.24

*Carnation petals displayed highest values at stage II (petals fully expanded and flowers fully open with yellow-tinted centres) of post-harvest flower development (Schade *et al.*, 2000).

lipoxygenase pathway (Figs. 1 and 2), preparations of total membrane entrapped in a natural alginate matrix within a packed-bed reactor were challenged with exogenous linoleic acid.

1.1. Immobilization of Total Membranes and Tissue Homogenate in a Calcium-alginate Matrix.

Immobilization of membranes in alginate was accomplished by combining equal volumes of 6% alginate solution and membrane suspension, and extruding the mixture through a needle-syringe (Fig. 3). In some experiments, tissue homogenates rather than membrane preparations were entrapped. The droplets were collected and cured in a stirred $CaCl_2$ - solution. These droplets had an alginate concentration of 3%, and although higher alginate concentrations would have resulted in increased mechanical bead strength, they were found to be too viscous for the bead-making device. Indeed, alginate concentrations exceeding 3% resulted in needle-clogging despite powering the device with a pneumatic cylinder.

To obtain uniform reaction conditions in the packed-bed of the reactor, uniform spherical beads were produced by adjusting the droplet falling distance to 23 cm, and flattening the tip of the 22 G 1.5 needle. Size distribution of the beads was determined by sieve analysis and manual measurements of their diameter with a ruler. Based on sieve analysis, the beads were mainly of two sizes. One fraction, comprising 32% of the total bead population, ranged from 2 to 2.35 mm in diameter, and the second, accounting for 67% of the bead population, ranged from 2.36 to 3 mm in diameter (Table 4). Manual measurements identified mainly one fraction

Table 4. Size distribution of alginate beads containing entrapped membrane biocatalyst determined by sieve-shaker analysis (n = 4627) and manual measurement with a ruler (n = 100). Values are from a single experiment.

Method	Diameter (mm)	Relative Bead Number
Sieve-Analysis	[1-2]	1%
	[2-2.35]	32%
	[2.35-3]	67%
Manual Measurement	[1-2]	5%
	[2-3]	92%
	[3-4]	3%

comprising 92% of the bead population with a size range of 2 to 3 mm in diameter (Table 4). Both types of measurements indicated that the average bead diameter was 2.5 mm.

The enzymes of the lipoxygenase pathway are sensitive to Ca^{2+}-concentrations (Riley *et al.*, 1996), and Ghandi and Robinson have determined that the enzymes involved in hexanal formation function optimally at a Ca^{2+}-concentration of 0.02 M (unpublished data). Consequently, the beads were cured in 0.02 M $CaCl_2$ for 46.5 min, as the curing time (t) required for complete polymerization of the calcium-alginate was determined to be 46.5 min according to equation (1).

High alginate concentrations not only increase mechanical strength, but also reduce the diameter and length of pores in the beads (Martinsen *et al.*, 1992). Consequently, low alginate concentrations may result in leakage of entrapped enzymes from the beads due to larger pore sizes. Accordingly, beads containing immobilized tomato leaf homogenate were tested for protein leakage by submerging them at 25°C in a solution that resembles the reactor retentate at optimum operating conditions, removing them after 30 min, and measuring the protein content of the solution. Leakage of protein from crude tomato leaf homogenate entrapped within the beads was less than 2.5%, and this presumably represented proteins washed from the surfaces of the beads.

1.2. Substrate Considerations.

In order to maximize the availability of linoleic acid, the substrate for the biocatalyst, to the entrapped enzymes, Tween 20 was added to the

linoleic acid suspension. This improves the solubility of linoleic acid by forming mixed micelles. However, interactions between Tween 20 and linoleic acid are of a complex nature (Lichtenberg, 1985; Lichtenberg *et al.*, 1983). Hence, the optimum amount of Tween 20 was determined empirically by adding it dropwise until complete clearing of the substrate solution was achieved. In this manner, it was established that 0.75 mL of Tween 20 were required to clear 75 mL of 32.1 mM linoleic acid.

1.3. Membrane Selection for the Hollow-Fibre Recovery Unit.

Measurements of resistances using polysulfone flat membrane sheets in the Minitan system yielded values of 20.6 Pa s/m and 15 Pa s/m for the 100 and 300 kDa molecular weight cut-off membranes, respectively. Thus, resistances were of a comparable order of magnitude irrespective of which of these molecular weight cut-off membranes was used. Challenging either permeate with exogenous linoleic acid (32.1 mM) did not result in hexanal production, indicating that lipoxygenase and hydroperoxide lyase, the two enzymes required for the reaction, were both retained by either membrane. Consequently, even if the small amounts of protein leaking from the beads in the bioreactor do contain enzymes of the lipoxygenase pathway, they will be retained within the retentate by either of these membranes. Measurements of linoleic acid fluxes across the membranes revealed that it was all retained in the retentate with the 100 kDa cut-off membrane, whereas 11.6% of the substrate passed through the 300 kDa membrane. Based on these findings, the 100 kDa molecular weight cut-off membrane was chosen for the hollow fibre product recovery unit.

2. Bioreactor Operation.

The initial phase of designing any bioreactor system consists of establishing operating parameters that will maintain stability of the biocatalyst and allow for efficient recovery of the product. To this end, the effects of varying the substrate concentration (linoleic acid), catalyst loading, temperature and pH were analyzed for bioreactor-based hexanal formation. A constant transmembrane pressure (TMP) of 5 psi was applied to conserve buffer. Hexanal production was evaluated by sampling the permeate after 5, 10, 15 and 30 minutes of reactor operation, and analysing hexanal levels by gas chromatography/mass spectroscopy (GC/MS). Measurements of the permeate and retentate flux were also taken at these time points.

2.1. Minimum Substrate Requirement and Selection of the Biocatalyst.

The production of hexanal from immobilized total membranes of tomato leaves was examined at 25°C at several substrate concentrations (Table 5). Of particular interest is the finding that hexanal was not detectable in the permeate at a linoleic acid concentration of 2.7 mM, whereas trace amounts were detectable at a substrate concentration of 6.7 mM and clearly measurable amounts of hexanal were formed at a substrate concentration of 10.7 mM (Table 5). These measurements not only allowed determination of a minimum substrate requirement of 10.7 mM, but also indirectly demonstrated that the bioreactor does produce hexanal. Specifically, hexanal levels in the permeate did not reflect endogenous

Table 5. Determination of the minimum concentration of linoleic acid required for bioreactor-based production of hexanal. Values are means ± SE for n = 3 measurements at pH = 7.4; T = 25°C; transmembrane pressure = 5psi; catalyst loading = membrane equivalent of 1.5 g f w tomato leaves.

Linoleic Acid Concentration in the Reactor (mM)	Hexanal (μg/g f w)/ 30 min
2.7	Not Detectable
6.7	Trace Amount
10.7	80.2 ± 7.10

hexanal levels of the biocatalyst, as hexanal was not detectable at low substrate concentrations. Furthermore, challenging the permeate with 10.7 mM linoleic acid did not result in any further increase in hexanal.

Tomato leaves appear to be the best-suited tissue of those tested for the bioreactor-based generation of hexanal based on the finding that they have highest steady-state hexanal levels (Table 3). This contention was also supported by experiments in which biocatalysts comprising total membrane equivalents of 1.5 g f w of stage II carnation petals, strawberry leaves and tomato leaves were challenged with linoleic acid substrate at a concentration of 10.7 mM in the bioreactor (Table 6). Membranes from tomato leaves produced ~ 4-fold and ~ 13-fold higher levels of hexanal than membranes of strawberry leaves and carnation petals, respectively (Table 6). Based on these results, only membranes from tomato leaves were utilized in further bioreactor experiments.

2.2. Effect of pH and Temperature on Hexanal Generation.

The bioreactor experiments were routinely carried out at pH 7.4, which is physiological. However, lipoxygenase and hydroperoxide lyase have been reported to be most active within pH ranges of 4.5 to 8 and 6 to 8, respectively (Suurmeijer *et al.*, 2000; Kausch and Handa, 1997; Blée and Joyard, 1996; Riley *et al.*, 1996; Rouet-Mayer *et al.*, 1992). Accordingly, in one set of experiments hexanal production was determined at pH 6, the lowest pH for optimum lipoxygenase and hydroperoxide lyase activity. In these experiments, EPPS in the homogenate, resuspension and reactor buffers was replaced with sodium acetate (0.2M) adjusted to pH 6. At the

Table 6. Bioreactor-based production of hexanal. Values are means ± SE for n=3 measurements at pH = 7.4; T = 25°C; transmembrane pressure = 5 psi; [linoleic acid] = 10.7 mM; catalyst loading = membrane equivalent of 1.5 g f w of according tissue.

Source of Membrane for the Biocatalyst	Hexanal (µg/g f w) / 30 min
Stage II Carnation Petals*	6.4 ± 1.03
Strawberry Leaves	22.4 ± 2.27
Tomato Leaves	80.2 ± 7.10

*Carnation petals display highest values at stage II (petals fully expanded and flowers fully open with yellow-tinted centres) of post-harvest flower development (Schade *et al.*, 2000).

lower pH, hexanal formation was 152.4 µg/ g f w at 25°C compared to 80.2 µg/ g f w at pH 7.4. However, the calcium alginate beads containing the biocatalyst started to dissolve after 15 min of reactor operation at pH 6. After 120 min at the lower pH, more than 50% of the beads had completely dissolved resulting in malfunction of the ultrafiltration unit due to clogging. Therefore, subsequent experiments were only conducted at pH 7.4.

The possibility that an increase in reactor temperature might enhance hexanal yield by increasing permeate flux and accelerating reaction rates was assessed by operating the reactor at 25, 35 and 45°C. Permeate fluxes after 30 min of operation were 1.25- and 1.3-fold higher at 35°C and 45°C, respectively, than at 25°C (Fig. 7). Interestingly, according to the Arrhenius equation reaction rates should double with each 10°C increase in temperature. Thus, overall hexanal generation should have increased 2.5 (1.25 x 2)-fold and 5.2 (1.3 x 4)-fold by increasing the temperature from 25°C to 35°C and from 25°C to 45°C, respectively. However, this was not the case. Rather, hexanal yield increased 2.1-fold, from 80.2 to 168.4 µg/ g f w, when the operating temperature of the bioreactor was increased from 25°C to 35°C (Table 7). Moreover, it decreased by a factor of 1.5, from 80.2 to 54.5 µg/ g f w, when the bioreactor was operated at 45°C instead of 25°C (Table 7).

The finding that the actual hexanal production values are considerably lower than the theoretical values suggests that the effects of temperature-enhanced permeate flux and reaction rates are tempered by progressive thermal enzyme deactivation once a specific temperature is surpassed. Further evidence to support this contention was obtained from a detailed examination of relative hexanal production rates (yield per 5 min) over a 30 min time period at different temperatures (Fig. 8). Within 10 min,

Figure 7. Effect of reactor temperature on permeate flux (◆ 25 C, □ 35 C, ▲ 45 C). Values are means for n = 3 measurements at pH = 7.4; transmembrane pressure = 5 psi; [linoleic acid] = 10.7 mM; catalyst loading = membrane equivalent of 1.5 g f.w. of tomato leaves. Standard errors are < 13.6 % and are omitted for clarity of the figure.

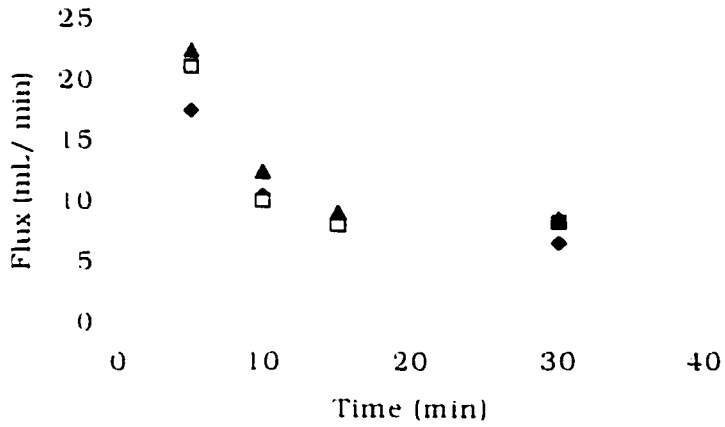
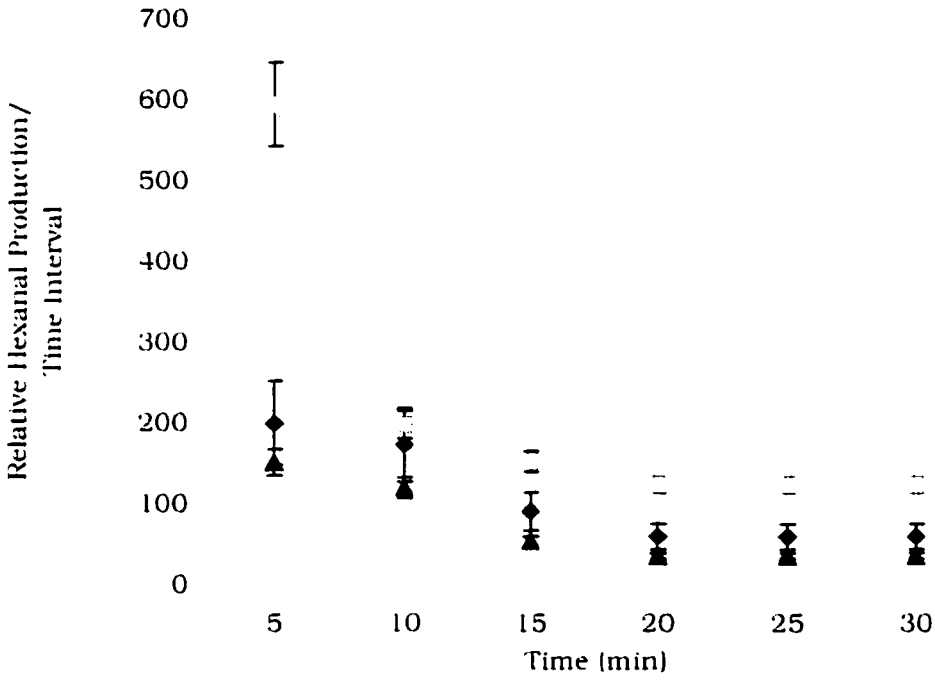

25
20
15
10
5
0
Flux (mL/ min)
0
10
20
30
40
Time (min)

Table 7. Effect of varying the reactor temperature on the bioreactor-based production of hexanal by tomato membrane biocatalyst equivalent to 1.5 g f w of tomato leaves. Values are means ± SE for n = 3 measurements at pH = 7.4; transmembrane pressure = 5 psi; [linoleic acid] = 10.7 mM.

Reactor Temperature (°C)	Hexanal (µg/g f w) / 30 min
25	80.2 ± 7.10
35	168.4 ± 18.52
45	54.5 ± 10.36

Figure 8. Time course for bioreactor-generated hexanal levels as a function of varying reactor temperature (◆ 25 C, ■ 35 C, ▲ 45 C) expressed as hexanal production per 5 minutes. Values are means ± SE for n=3 measurements at pH = 7.4; transmembrane pressure = 5psi; [linoleic acid] = 10.7 mM; catalyst loading = membrane equivalent of 1.5 g f w of tomato leaves.


Relative Hexanal Production/
Time Interval
700
600
500
400
300
200
100
0
5
10
15
20
25
30
Time (min)

the rates of hexanal production decreased as a function of temperature as follows: $r_{hexanal}(35°C) > r_{hexanal}(25°C) > r_{hexanal}(45°C)$. Within 20 min, the rates of production had reached steady-state levels, and these were correlated with temperature (Fig. 8). Thus, any initial increase resulting from increased permeate flux and accelerated reaction rate is dampened by enzyme denaturation.

2.3. Effect of Substrate and Catalyst Concentrations on Hexanal Formation.

The engineering and biochemical principles relating to substrate and catalyst concentration in a bioreactor are complex. For example, in the bioreactor for hexanal production increased substrate concentration in the retentate might yield higher hexanal levels due to increased reaction rates. On the other hand, an increase in substrate concentration will simultaneously increase the surfactant concentration, causing increased fouling of the hollow-fibre unit. This would result in decreased permeate flux, and consequently decreased hexanal generation. Thus, changing the substrate concentration may cause contradictory effects in different parts of the reactor. Furthermore, the catalyst load might affect the levels of substrate concentration at the site of reaction. Granted the assumption that entrapped total membranes exceed a molecular weight of $2 \cdot 10^4$ g/ mol, diffusion properties of the substrate will change as a function of catalyst load (Tanaka *et al.*, 1984).

A 2^2 factorial design was selected to elucidate the importance of these two factors on hexanal production in the bioreactor. Experiments were carried out at 35°C and pH 7.4. Values for linoleic acid concentrations of 10.7 and 32.1 mM, and catalyst loads of membrane equivalents of 1.5 and 4.5 g f w of tomato leaves, were coded according to equations (12) and (13). The experimental results for each data point are summarized in Table 8. Computer-assisted analysis of variance (ANOVA) for hexanal production revealed not only that both factors, substrate concentration and catalyst loading, were significant for α values of 0.05 (F_{crit} = 5.3) and 0.01 (F_{crit} = 11.3) (Devore and Peck, 1993), but their joint-effect on hexanal production was also significant (Table 9). Consequently, a coded, first-order regression model with interactions was calculated according to equations (3)–(11) for n = 3:

$$Y = 219.8 - 75.9\, x_1 - 50.8\, x_2 - 26.8\, x_1 x_2 \qquad (16)$$

The squared regression coefficient, R^2, for the model was 0.986, and analysis of the residuals (ε) confirmed good fit for the model. Residuals (ε) were calculated by subtracting the predicted values (Y) from the experimental values, (y), for all three repeats at the four points in the design, and were plotted versus Y (Fig. 9). This plot not only illustrates low scattering of ε, but also indicates the lack of any statistical scatter pattern among ε. Furthermore, repeated measurements at the centre point (x_1 = 0, x_2 = 0), with y = 204.3 ± 28.5, indicates a good fit against the calculated response (Y = 219.8) of the model.

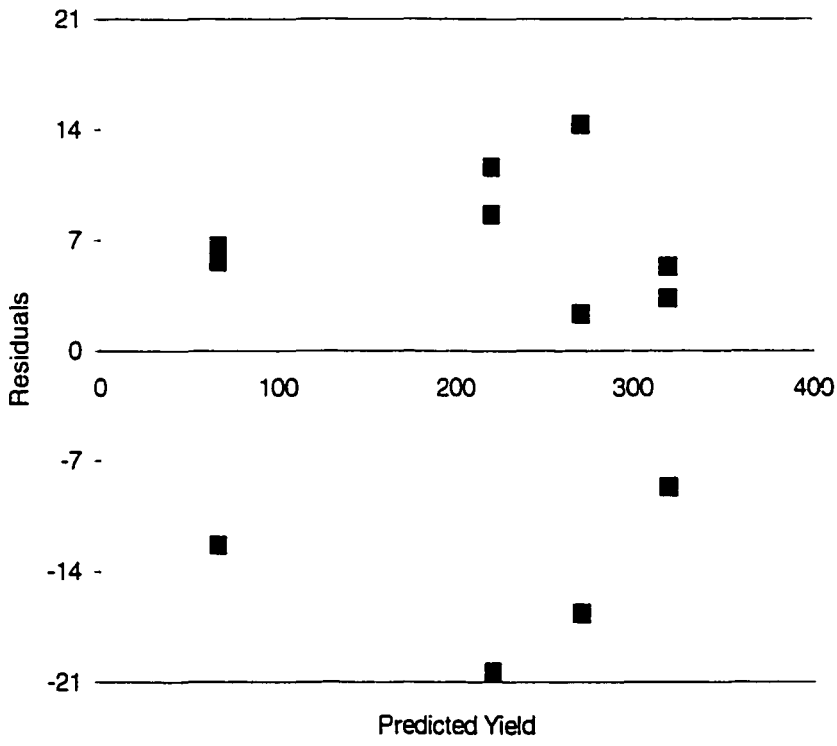
Table 8. 2^2-experimental design for the bioreactor-based production of hexanal as a function of substrate concentration (x_1) and tomato biocatalyst loading (x_2). Reactants and product were coded according to equations (11)-(13). Each experiment was replicated three times at pH = 7.4; T = 35°C; transmembrane pressure = 5 psi.

Factor Level Combinations	Hexanal Production Replicates			Sum of Replicates
	I	II	III	
$x_1 = -1, x_2 = -1$	323,	325,	311	(1) = 959
$x_1 = +1, x_2 = -1$	230,	233,	201	a = 664
$x_1 = -1, x_2 = +1$	255,	274,	286	b = 815
$x_1 = +1, x_2 = +1$	72,	73,	54	ab = 199

Table 9. ANOVA of the 2^2-factorial design regression according to Devore and Peck (1992).

Source of Variation	Sum of Squares	Freedom	Mean Square	F_0
X_1	69129.7	1	69129.7	371.9
X_2	30906.8	1	30906.8	166.3
X_{12}	8586.8	1	8586.8	46.2
error	1487	8	185.9	
total	110110.3	11		

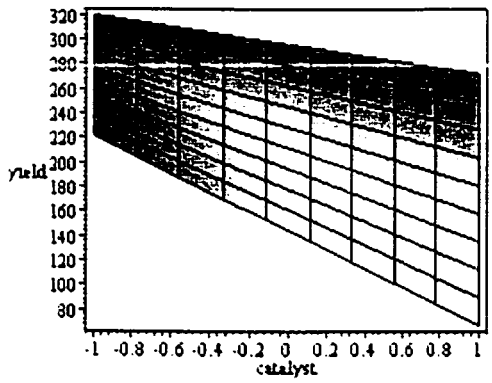
Figure 9. Plot of residuals, ε, of the regression model. The residuals were calculated by solving equation (2) for ε for all factors and replicates.


21
14
7
0
-7
-14
-21
Residuals
0
100
200
300
400
Predicted Yield

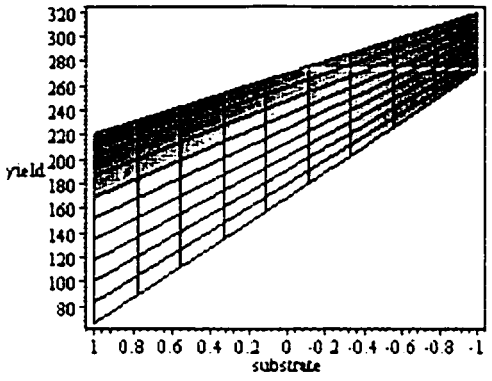
A response surface was computed according to equation (16) and plotted from three different angles in order to illustrate its curvature (Figs. 10A-C). Equation (16) and Figures 10A-C both show maximum hexanal yield, Y_{max}, at lower factor combinations, $x_1 = -1$ and $x_2 = -1$. Using these values in combination in equation (16), Y_{max} was determined to be 319.7, which corresponds according to relation (14) to 252.6 µg hexanal, or 168.4 µg / g f w. Decoding of $x_1 = -1$ and $x_2 = -1$ according to equations (12) and (13) revealed an optimum substrate concentration [18:2] of 10.7 mM and an optimum catalyst concentration equal to the membrane equivalents from 1.5 g f w tomato leaves. Examination of the response surfaces (Figs. 10 A-C) showed that hexanal yield decreases as the substrate concentration is increased from 10.7 to 32.1 mM, and the yield of hexanal also decreases as the catalyst load is increased from membrane equivalents of 1.5 to 4.5 g f w of tomato leaves.

In addition, an attempt was made to elucidate the effect of substrate and catalyst interactions upon hexanal formation in the bioreactor by measuring retentate and permeate flux for all four points of the factorial design (Figs. 11A and B). The retentate flux remained fairly constant for all design points, whereas the permeate flux decreased independently of catalyst load by up to 2-fold at design points characterized by high substrate levels ($x_1 = +1$) in comparison to low substrate levels ($x_1 = -1$) (Figs. 11A and B). A flux independent of catalyst load is consistent with the observation that beads do not leak significant amounts of protein (Section 1.1.). However, hexanal yields decreased by ~ 1.4- and ~ 4-fold for constant x_2, with $x_2 = -1$ and $x_2 = +1$, respectively, when the substrate concentration was increased from $x_1 = -1$ to $x_1 = +1$ (Table 8). Thus, a decrease in hexanal yield is not only attributable to a substrate-induced decrease in permeate

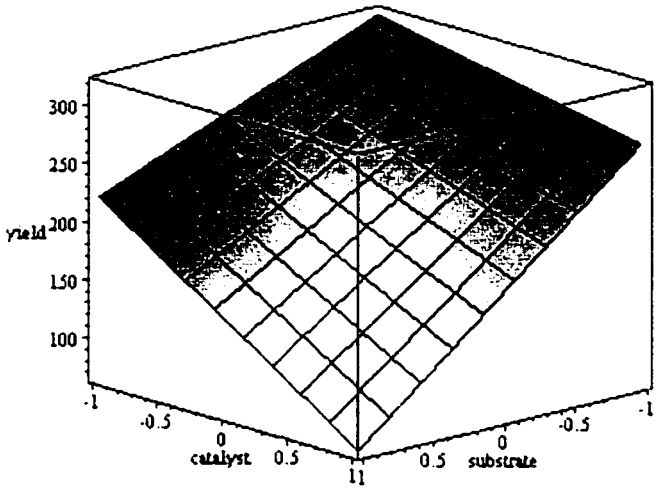
Figures 10. Coded response surface plot of hexanal yield based on the first-order model with interactions according to equation (16). Substrate concentration and tomato leaf biocatalyst loading were used as regressors. The response surface is shown from different angles (A-C) to illustrate the surface curvature.


yield
320
300
280
260
240
220
200
180
160
140
120
100
80
-1 -0.8 -0.6 -0.4 -0.2 0 0.2 0.4 0.6 0.8 1
catalyst

A.

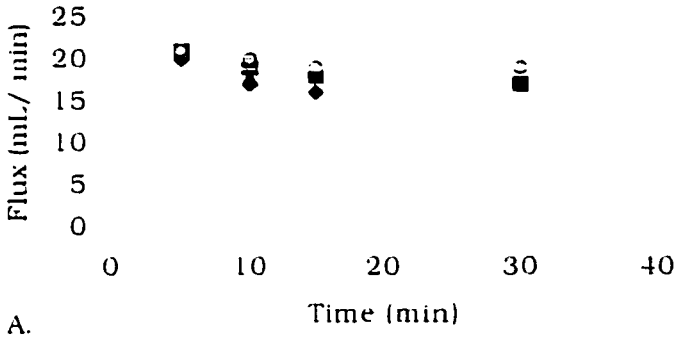

yield
320
300
280
260
240
220
200
180
160
140
120
100
80
1 0.8 0.6 0.4 0.2 0 -0.2 -0.4 -0.6 -0.8 -1
substrate

B.

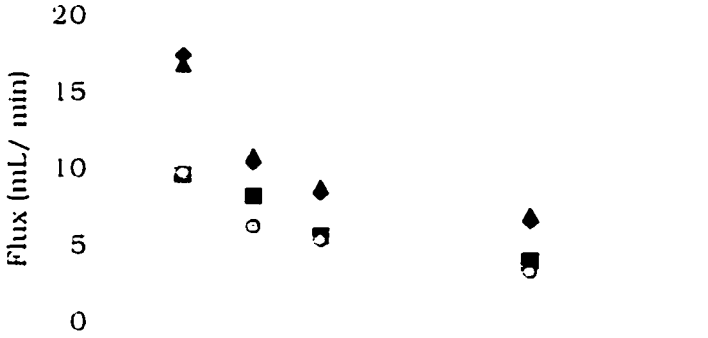

yield
300
250
200
150
100
-1
-0.5
0
0.5
1
catalyst
-1
-0.5
0
0.5
1
substrate

C.

Figures 11. Time course of (A) retentate flux, and (B) permeate flux for the four factorial design points using a tomato leaf membrane biocatalyst in the reactor (◆ factor combination (-1,-1); ■ factor combination (+1,-1); ▲ factor combination (-1,+1); ● factor combination (+1,+1)). Values are means for n=3 replicates at pH = 7.4; T = 35 C; transmembrane pressure = 5 psi. Standard errors are < 13.6 % and are omitted for clarity of the figure.


Flux (mL/ min)
25
20
15
10
5
0
0
10
20
30
40
Time (min)

A.


Flux (mL/ min)
20
15
10
5
0
0
10
20
30
40
Time (min)

B.

flux, but also to interaction of substrate and catalyst in the beads. Thus, these findings provide indirect, non-statistical evidence for the validity of equation (16).

3. Characterization of the Involvement of C_6-aldehydes in Plant-Pathogen Defence.

Normally, microbial contamination of bioreactors is a serious problem that has to be addressed. However, microbial contamination was not evident during operation of the bioreactor for production of hexanal for extended periods of time. This presumably reflects the fact that green-note volatiles are known to possess anti-microbial properties (Croft *et al.*, 1993). Consequently, the anti-microbial properties of green-note volatiles were further investigated. To this end, a specific isoform of hydroperoxide lyase was up-regulated in *Arabidopsis thaliana* in order to obtain transgenic plants with enhanced *(3Z)*-hexenal levels. This strategy was chosen since Croft *et al.* (1993) have established that the unsaturated C_6-aldehydes exhibit stronger anti-microbial activity than the saturated aldehydes. The transgenic *Arabidopsis thaliana* plants were tested for increased resistance against bacterial infection and also for enhanced systemic acquired resistance (SAR).

3.1. Transformation of *Arabidopsis thaliana* with Hydroperoxide Lyase and Determination of Endogenous C_6-aldehyde Levels.

The *Arabidopsis* hydroperoxide lyase cDNA that was used as the transgene was obtained as an *Arabidopsis* EST clone (94J16). The cDNA of this clone is 1.6 kb in length, including the 5'-untranslated region, the entire coding sequence and the complete 3'-untranslated region after the TAA stop codon. The nucleotide and deduced amino acid sequence are illustrated in Figure 5.

The binary vector, pKYLX71, containing the hydroperoxide lyase cDNA in sense orientation under the regulation of a double 35S constitutive cauliflower mosaic virus promoter (Fig. 6), was electroporated into *Agrobacterium tumefaciens* C58, and flowering *Arabidopsis thaliana* plants were transformed with *Agrobacterium* by vacuum infiltration (Bechtold *et al.*, 1998). The primary transformants T_0 were allowed to mature and set seed in a growth chamber. T_1 seedlings were selected by growth on kanamycin-containing medium and grown to maturity. T_2 and T_3 seedlings were similarly selected on kanamycin-containing media and grown to maturity. Seeds from T_3 plants that gave rise to 100% kanamycin-resistant seedlings were considered to be homozygous.

Leaves of homozygous T_3 plants were analysed for C_6 – aldehydes by gas chromatography and mass spectroscopy (GC/ MS). This analysis not only provided additional confirmation of the presence of the transgene within the different plant lines in an effective way, but also allowed identification of the lines, in which hydroperoxide lyase expression had been most strongly up-regulated. Indeed, the lines designated A, B and C have significantly increased levels of the volatile *(3Z)*-hexenal, one of two

immediate products of the aldehyde pathway (Fig. 2), in comparison with wild-type plants (Fig. 12). Line A proved to have the highest levels of *(3Z)*-hexenal, with a 29-fold increase by comparison with wild-type plants (Fig. 12). Furthermore, Figure 12 indicates that levels of hexanal remain essentially unaltered in the transgenic plants in comparison with wild-type plants for all three transgenic lines. This supports the contention that the hydroperoxide lyase transgene is a specific isoform encoding an enzyme that metabolizes linolenic acid hydroperoxide and not linoleic acid hydroperoxide. If the protein encoded by the transgene had been able to metabolize linolenic acid hydroperoxide and linoleic acid hydroperoxide, elevated levels of both hexanal and *(3Z)*-hexenal would have been observed in the transgenic plants. In addition, levels of *(2E)*-hexenal change only when *(3Z)*-hexenal levels reach high abundance (Fig. 12), which is consistent with the fact that *(2E)*-hexenal is derived from *(3Z)*-hexenal. This was only evident for line A (Fig. 12).

The identity of *(3Z)*-hexenal was confirmed by mass spectrometry (Fig. 13). This confirmation was necessary as *(3Z)*-hexenal is not commercially available as a standard. As shown in Figure 13, the observed mass/ charge fragmentation pattern is nearly identical with the theoretical fragmentation pattern for *(3Z)*-hexenal provided by the computer library. Therefore, due to the accordance of both mass/ charge fragmentation patterns, the identity of *(3Z)*-hexenal was confirmed.

That hydroperoxide lyase was up-regulated in the transgenic plants was also evident from Northern blots. Total RNA isolated from leaves of T_3 seedlings of the transgenic lines A, B and C and from wild-type plants was used for Northern blot analysis. Blots probed with full-length *Arabidopsis* hydroperoxide lyase cDNA indicated that levels of hydroperoxide lyase

Figure 12. Analysis of hexanal (■), (*3Z*)-hexenal (□), and (*2E*)-hexenal (■) in leaves of wild-type *Arabidopsis* plants and in leaves of the T_3 transgenic lines A, B and C. Volatile levels are expressed in terms of relative abundance per g fresh weight of plant leaf material. Standard errors of means are indicated for n = 3. WT, wild-type; A-C, different transgenic lines.

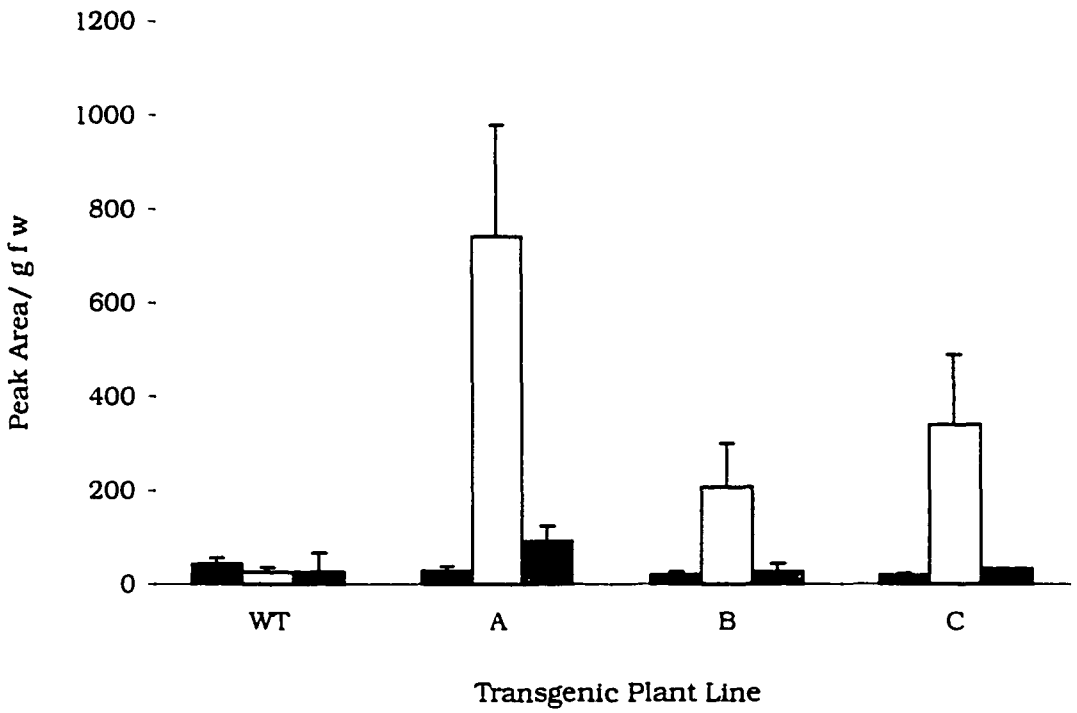
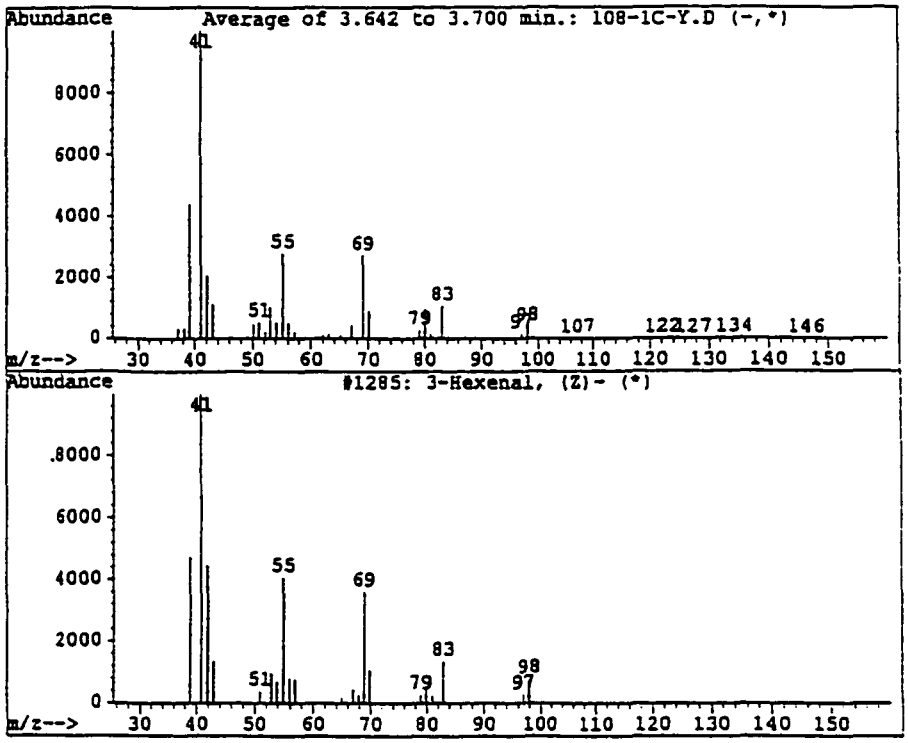

1200
1000
800
600
400
200
0
Peak Area/ g f w
WT
A
B
C
Transgenic Plant Line

Figure 13. Mass spectrometric identification of *(3Z)*-hexenal from leaves of transgenic *Arabidopsis thaliana* line A. The upper panel shows the actual mass fragmentation pattern; the lower panel shows the theoretical mass fragmentation pattern provided by the computer library (NIST).

ID : 3-Hexenal, (Z)-



mRNA were significantly higher in the transgenic lines in comparison to wild-type plants (Fig. 14). However, the results do not correlate quantitatively with measured levels of *(3Z)*-hexenal. Specifically, the band intensities reflecting mRNA levels were comparable for lines A and B (Fig. 14), yet levels of *(3Z)*-hexenal in line A were 3.6–fold higher than corresponding levels in line B (Fig. 12). Similarly, hydroperoxide transcript levels were higher for line B than for line C (Fig. 14), but steady-state levels of *(3Z)*-hexenal were higher in line C (Fig. 12). These discrepancies may reflect higher levels of other enzymes that utilize linolenic acid hydroperoxide as substrate in line B than in lines A and C.

Line A, which exhibited the highest steady-state *(3Z)*-hexenal level (Fig. 12), was used for all subsequent experiments.

3.2. *In planta* Bacterial Growth in Wild-type and Transgenic *Arabidopsis thaliana* infected with *Pseudomonas syringae*.

To evaluate the anti-microbial properties of *(3Z)*-hexenal and the effect of increased *(3Z)*-hexenal levels on systemic acquired resistance, wild-type and transgenic *Arabidopsis* plants were subjected to different combinations of primary and secondary inoculations with *Pseudomonas syringae* (Table 10). Control plants were given mock (M) inoculations with 10 mM $MgCl_2$. Plants given an avirulent (A) inoculation were treated with the avirulent strain (10^6 cfu (colony forming units)/ mL avirulent *Pst* strain DC 3000 (avrRpt2)). Plants given a virulent (V) inoculation were treated with

Figure 14. Northern blot analysis of total RNA isolated from the leaves of wild-type *Arabidopsis thaliana* plants and transgenic lines A, B, C and D.

(I) Ethidium bromide-stained gel. Each lane contained 10 µg RNA. Sizes in kb are indicated on the left side of the ethidium bromide-stained gel.

(II) Corresponding Northern blot probed with full-length *Arabidopsis* hydroperoxide lyase cDNA. WT, wild-type; A-D, different transgenic lines.

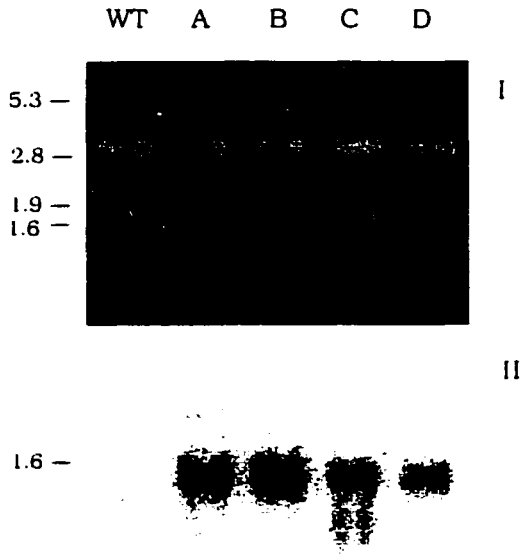

WT
A
B
C
D
5.3
2.8
1.9
1.6
I
II
1.6

Table 10. Treatment combinations for inoculation of *Arabidopsis* plants with *Pseudomonas syringae*. M, mock inoculation; A, inoculation with the avirulent strain; V, inoculation with the virulent strain. Four treatment combinations, (M,M), (M,A), (M,V) and (A,V), were used. The first letter identifies the primary inoculation on one leaf per plant, and the second letter describes the secondary inoculation two days later on four leaves per plant. Eight plants were used for each treatment combination.

	Day	(M,M) Mock	(M,A) Avirulent	(M,V) Virulent	(A,V) SAR
Primary Inoculation	0	Mock	Mock	Mock	Avirulent
Secondary Inoculation	2	Mock	Avirulent	Virulent	Virulent

the virulent strain (10^6 cfu / mL virulent *Pst* strain DC 3000). Eight plants were used for each treatment combination (Table 10).

Initially, one leaf on each of 24 plants was given a mock inoculation (M plants), and one on each of eight plants was given an avirulent inoculation (A plants) (Fig. 15A, B, C and D). Two days later, eight of the M plants were given a second mock inoculation on each of four additional leaves giving rise to eight (M,M) plants (Fig. 15A). As well, eight of the M plants were given an avirulent inoculation on each of four additional leaves, giving rise to eight (M,A) plants (Fig. 15B), and eight of the M plants were given a virulent inoculation on each of four additional leaves giving rise to eight (M,V) plants (Fig. 15C). At the same time, eight A plants were given a virulent inoculation on each of four additional leaves giving rise to eight (A,V) plants (Fig. 15D). Thus, for each of wild-type and transgenic plants there were four treatment combinations: (M,M), (M,A), (M,V) and (A,V) (Fig. 15).

Wild-type plants are susceptible to infection by the virulent *Pst* strain DC 3000, but are resistant to infection by the avirulent *Pst* strain DC 3000 (avrRpt2) (Cameron *et al.*, 1994). Consequently, *in planta* bacterial counts should be comparable for (M,M) and (M,A) treatments, and the (M,M) and (M,A) bacterial counts should both be substantially lower than those obtained for (M,V) treatments. Indeed, 110 and 155 cfu/ leaf disk were obtained for wild-type plants subjected to (M,M) and (M,A) treatments, respectively, whereas 38 000 cfu/ leaf disk were obtained for the (M,V) treatment (Fig. 16). *In planta* counts for (M,M) reflect the presence of endogenous non-pathogenic bacteria.

Figure 15. Illustration of first and second inoculations of *Arabidopsis* plants with *Pseudomonas syringae*. A. (M,M) treatment; B. (M,A) treatment; C. (M,V) treatment; D. (A,V) treatment.

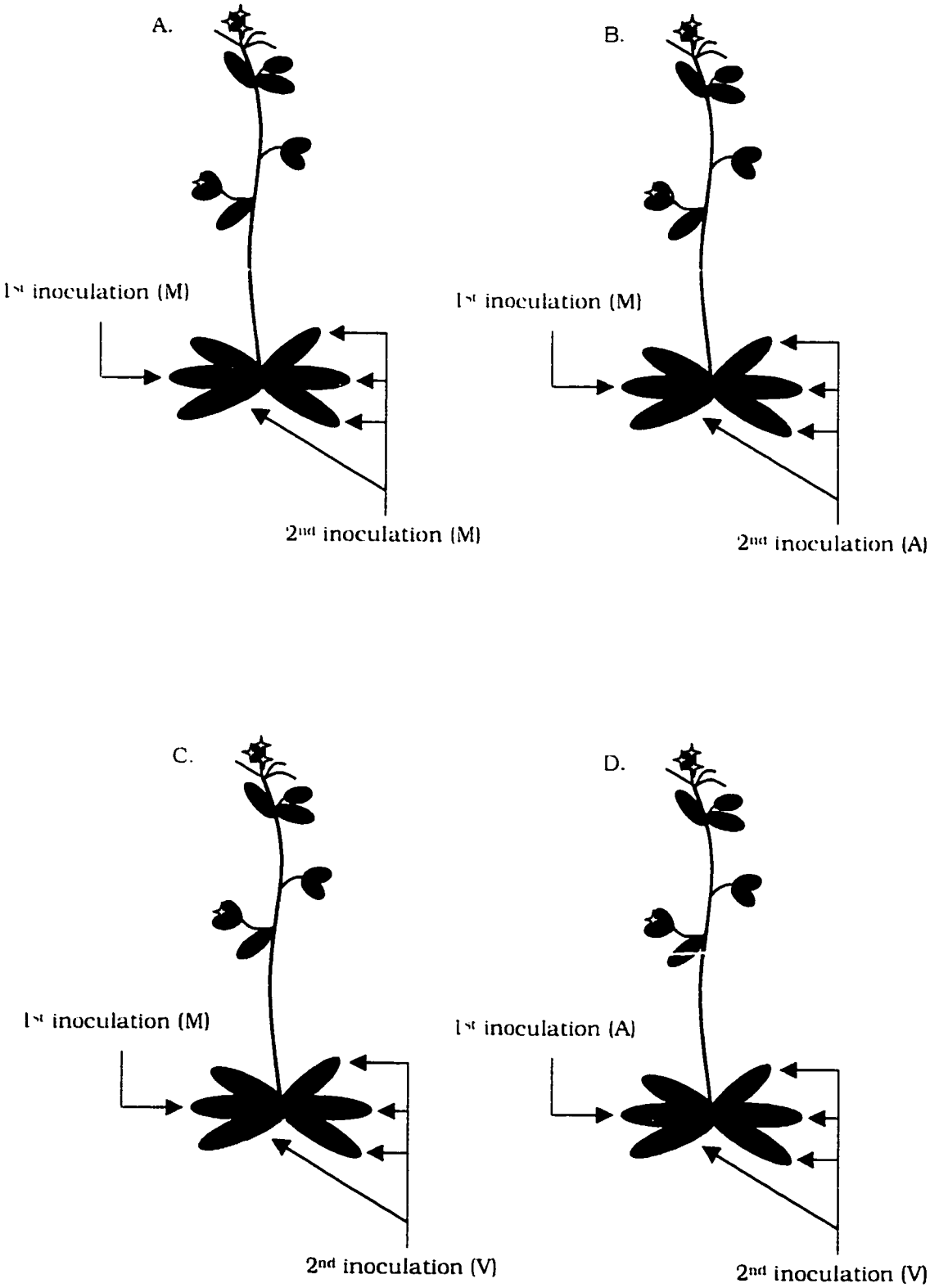
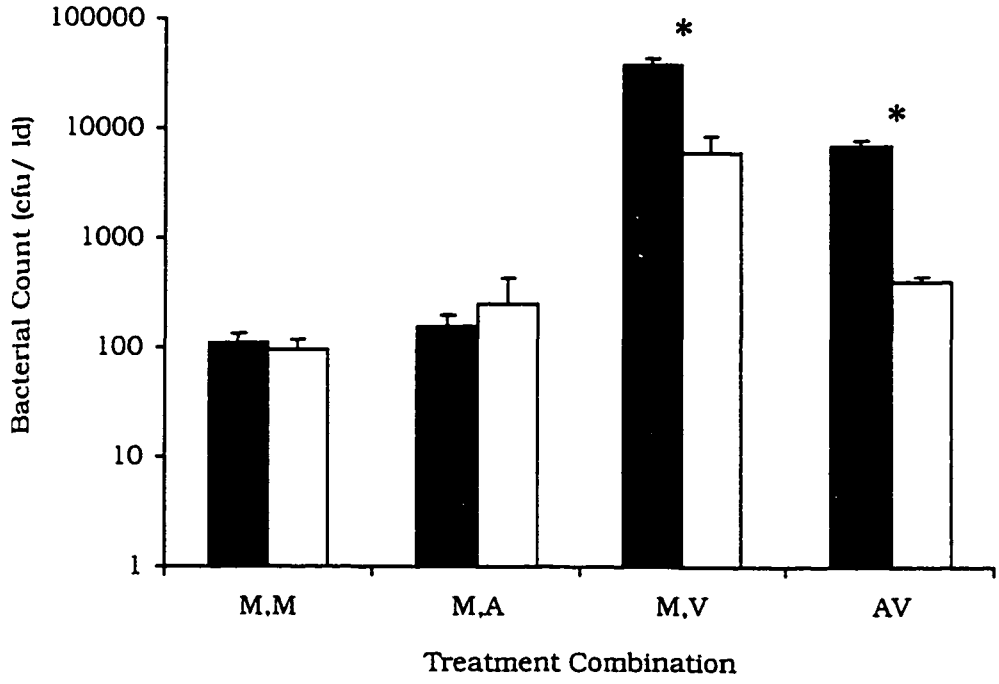

A.
1st inoculation (M)
2nd inoculation (M)
B.
1st inoculation (M)
2nd inoculation (A)
C.
1st inoculation (M)
2nd inoculation (V)
D.
1st inoculation (A)
2nd inoculation (V)

Figure 16. *In planta* bacterial growth in challenged leaves of wild-type (■) and transgenic (□ , line A) *Arabidopsis* plants. Bacterial numbers were determined as colony forming units per leaf disk for all four treatments, (M,M), (M,A), (M,V) and (A,V). M, mock inoculation; A, avirulent inoculation; V, virulent inoculation. Values are means ± SE for n = 8 plants. Asterisks indicate significant differences at 95% confidence limits as determined by a paired t-test.


100000
10000
1000
100
10
1
Bacterial Count (cfu/ ld)
*
*
M.M
M.A
M.V
AV
Treatment Combination

In transgenic plants, the *in planta* (M,M) and (M,A) bacterial counts were also comparable, being 95 cfu/ leaf disk and 250 cfu/leaf disk, respectively (Fig. 16). In addition, the (M,M) and (M,A) counts for transgenic plants were of comparable magnitude to the counts obtained in wild-type plants for identical treatments (Fig. 16). However, bacterial counts for (M,V) treatments were 6000 cfu/ leaf disk in transgenic plants, and therefore 6-fold lower, than the level of infection obtained in wild-type plants for the same treatment combination (Fig. 16). Such a decline in cfu/leaf disk in transgenic plants not only confirms the anti-bacterial properties of *(3Z)*-hexenal *in vivo*, but also demonstrates that up-regulation of *(3Z)*-hexenal levels results in increased *in vivo* resistance against bacterial infection.

In addition, transgenic *Arabidopsis* plants were tested for enhanced systemic acquired resistance (SAR). In the event SAR is induced, a localized inoculation with avirulent bacteria not only reduces *in planta* bacterial counts upon subsequent infection with virulent bacteria at the site of primary inoculation, but also confers systemic resistance in tissues remote from the initial site of infection (Cameron *et al.*, 1994; Whalen *et al.*, 1991). Consequently, for a full SAR response, *in planta* bacterial counts of (A,V) treatments should be comparable to counts obtained for (M,A) treatments. On the other hand, in the event of partial SAR response, (A,V) treatment counts should be lower than corresponding (M,V) counts, but higher than (M,A) counts.

Cameron *et al.* (1994) have reported induction of partial systemic acquired resistance in wild-type *Arabidospsis thaliana*. In the present study, *in planta* bacterial counts in (A,V)-treated wild-type plants, a treatment designed to quantify the level of systemic acquired resistance, decreased ~ 3-fold by comparison with (M,V) plants, but still remained 90-

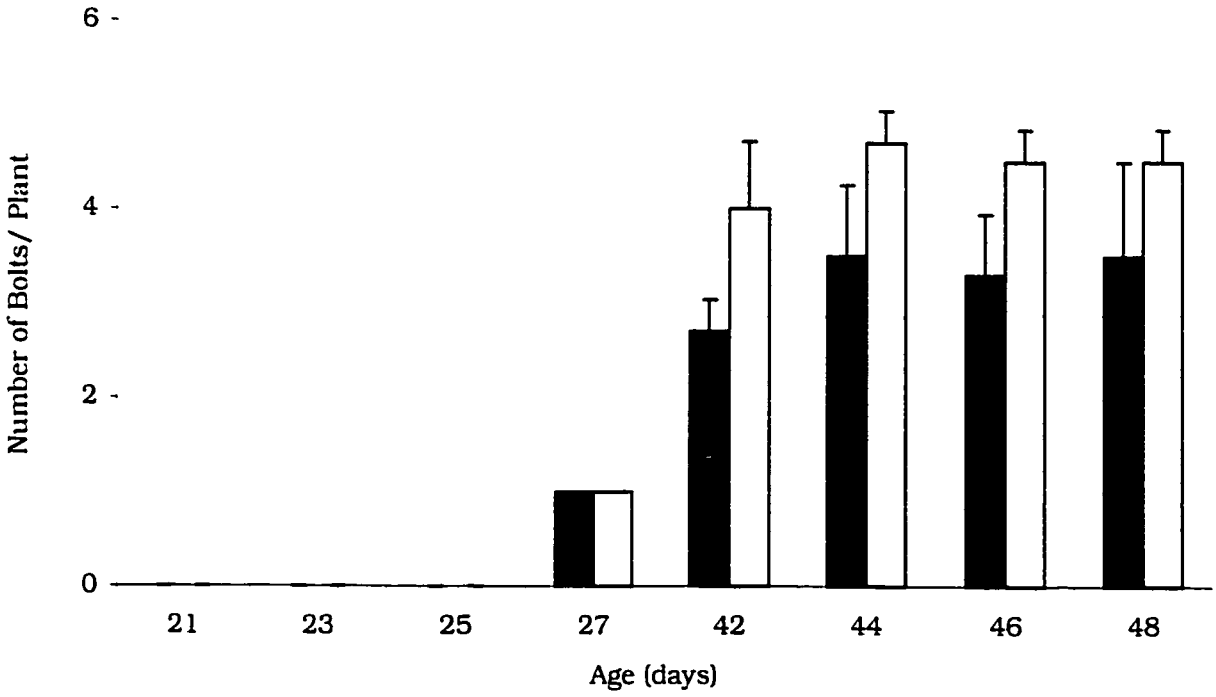
fold higher than counts obtained for (M,A)-treated wild-type plants (Fig. 16). Specifically, *in planta* bacterial counts were 38 000, 14 000 and 155 cfu/ leaf disk for (M,V)-, (A,V)- and (M,A)-treated wild-type plants, respectively (Fig. 16). This indicates the induction of partial systemic acquired resistance in the wild-type plants. On the other hand, bacterial counts in transgenic plants were comparable for (A,V) and (M,A) treatments, being 405 cfu/ leaf disk and 250 cfu/ leaf disk, respectively (Fig.16). Furthermore, (A,V) bacterial counts for transgenic plants decreased 15-fold by comparison to (M,V) treatments, being 405 cfu/ leaf disk and 6000 cfu/ leaf disk, respectively (Fig.16). Thus, transgenic plants revealed not only enhanced, but also fully induced systemic acquired resistance.

In summary, transgenic *Arabidopsis* with up-regulated *(3Z)*-hexenal levels revealed increased resistance against virulent *Pseudomonas syringae* by a factor of 6 and full systemic acquired resistance equivalent to 15-fold by comparison to wild-type plants. Consequently, an overall resistance increase of 90-fold was achieved within the transgenic plants.

4. Up-regulation of Hydroperoxide Lyase and its Impact on Stress-Induced Senescence.

In order to evaluate the effect of up-regulated hydroperoxide lyase on the response of plants to stress, anoxia leading to senescence was induced in wild-type and transgenic *Arabidopsis* plants by flooding the soil. Senescence as determined by the onset of bolting was initiated at approximately day 27 after planting for flooded wild-type and transgenic plants (Fig. 17). The number of bolts per plant increased for both wild-type

Figure 17. Changes in bolt number of over-watered wild-type (■) and transgenic (□ , line A) *Arabidopsis* plants during development and senescence. Values are means ± SE for n = 12-18 plants. Although, the transgenic plants tended to have larger numbers of bolts between days 42 and 48, these differences were not significant at 95% confidence limits as determined by a paired t-test. Age, days after planting.


6
4
2
0
Number of Bolts/ Plant
21
23
25
27
42
44
46
48
Age (days)

and transgenic plants between days 27 and 42 after planting (Fig. 17). Of particular interest, however, is the finding that, although initially there was no difference in the number of bolts between flooded wild-type and flooded transgenic plants, by days 42 through 48 the transgenic plants tended to have a larger number of bolts (Fig. 17). Bolt length also increased for both wild-type and transgenic plants between days 27 and 42 (Fig. 18). Moreover, bolt length was significantly higher for the transgenic plants at day 27, and although the differences were less pronounced, this trend continued through days 42 to 48 (Fig. 18). Leaf fresh weight also increased between days 21 and 44 after planting, and fresh weight of the aggregate of rosette leaves proved to be higher for the flooded transgenic plants as early as day 23, well before bolting (Fig. 19). This was also evident from digital pictures of wild-type and transgenic plants (Fig. 20). This difference was particularly evident at days 42 to 44 after bolt number and bolt length had reached a plateau (Figs. 17, 18 and 19). After day 44, the fresh weight of rosette leaves decreased for both transgenic and wild-type plants as the plants began to senesce (Fig. 19).

In order to elucidate whether rosette leaves of transgenic plants grow larger or growth of the wild-type plants is impaired as a consequence of flooding, leaf sizes of stressed and unstressed transgenic and wild-type plants were compared. In the absence of flooding stress, the leaves of wild-type plants and transgenic plants at 29-days of age were of similar size (Figs. 21A and B). However, for stressed plants at 29-days of age leaves of wild-type plants were smaller than those of transgenic plants (Figs. 22A and B). Moreover, the transgenic plants were also at a more advanced stage of development as indicated by more abundant and longer bolts (Figs. 22A and B). In fact, the transgenic stressed plants and the transgenic control (non-

Figure 18. Changes in bolt length of over-watered wild-type (■) and transgenic (□ , line A) *Arabidopsis* plants during development and senescence. Values are means ± SE for n = 12-18 plants. Asterisk indicates significant differences at 95% confidence limits as determined by a paired t-test. Age, days after planting.

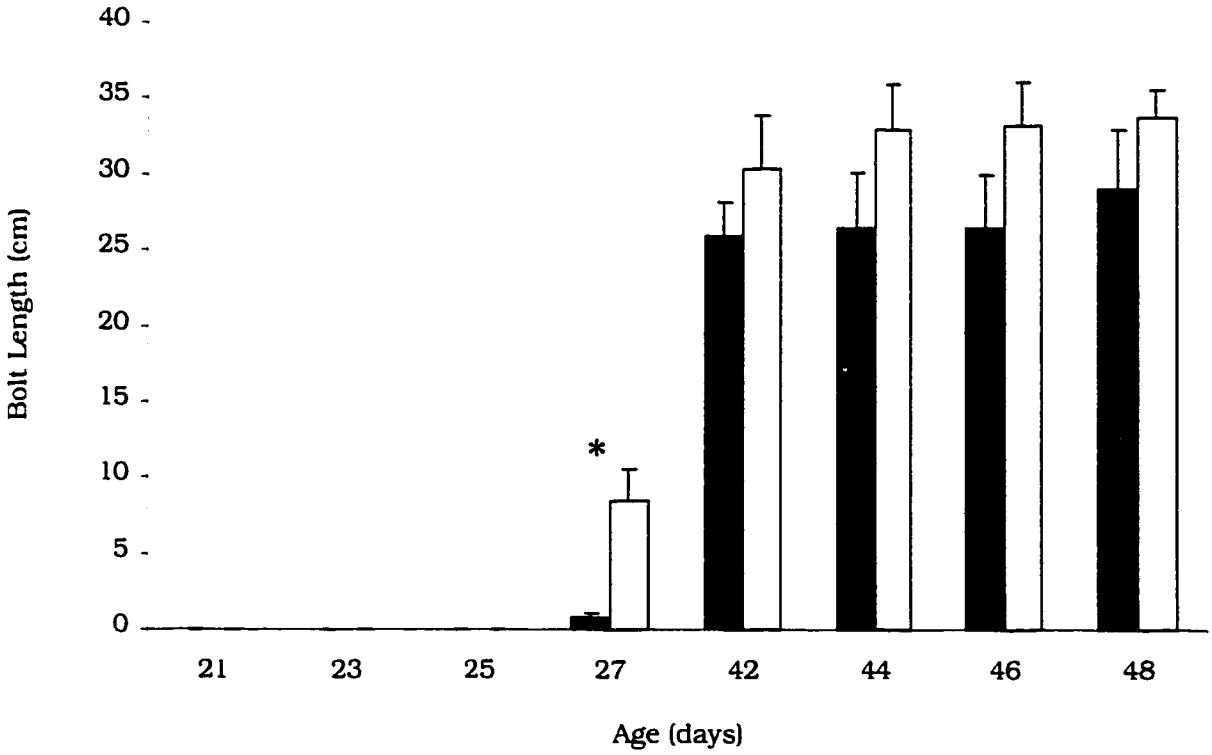

40
35
30
25
20
15
10
5
0
Bolt Length (cm)
*
21
23
25
27
42
44
46
48
Age (days)

Figure 19. Changes in fresh weight of the rosette leaf aggregate for over-watered wild-type (■) and transgenic (□ , line A) *Arabidopsis* plants during development and senescence. Values are means ± SE for n = 12-18 plants. Asterisk indicates significant differences at 95% confidence limits as determined by a paired t-test. Age, days after planting.

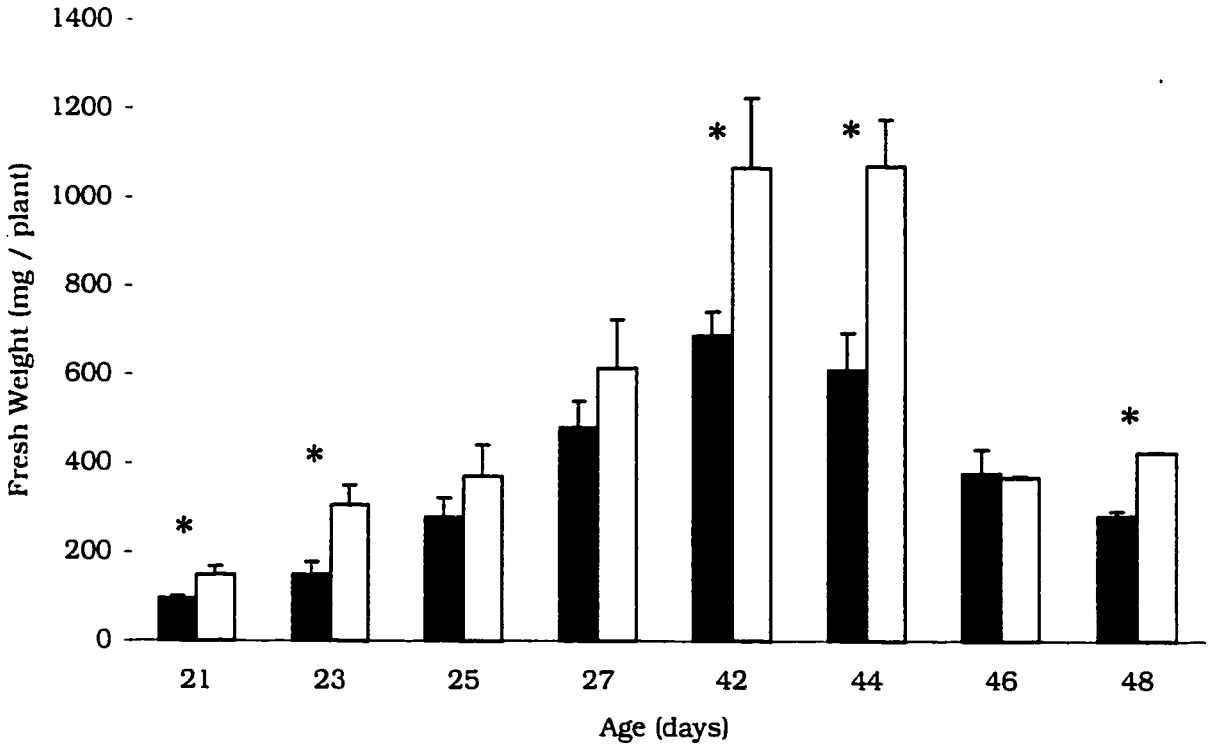
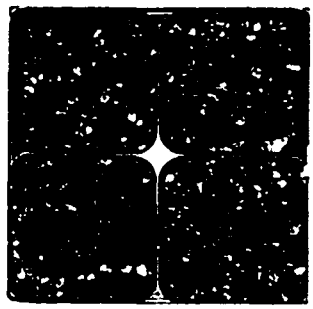
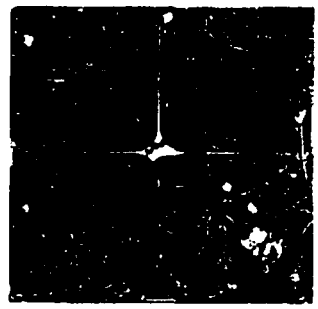

1400
1200
1000
800
600
400
200
0
Fresh Weight (mg / plant)
*
*
*
*
*
21
23
25
27
42
44
46
48
Age (days)

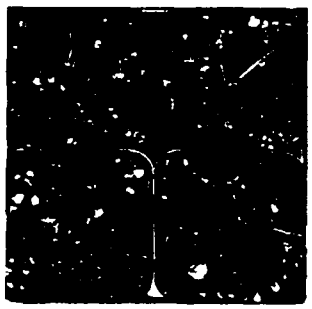
Figure 20. Digital pictures of over-watered *Arabidopsis* plants. (A) wild-type, 23 days after planting; (B) transgenic line A, 23 days after planting; (C) wild-type, 25 days after planting; (D) transgenic line A, 25 days after planting. Bar = 6 cm.



A.



C.

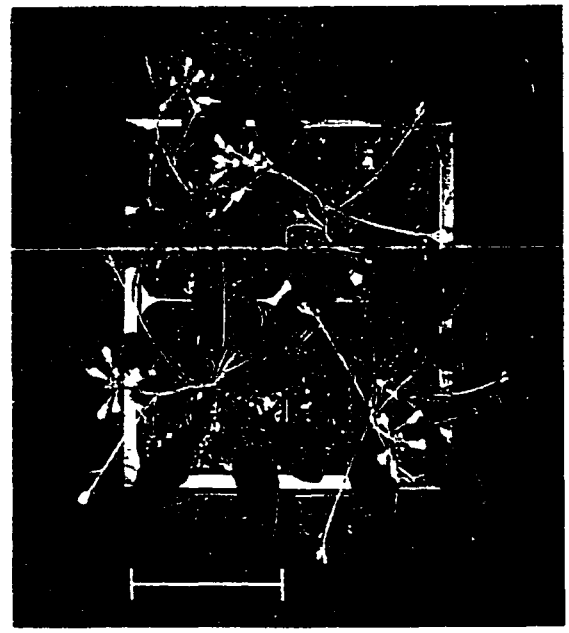


B.

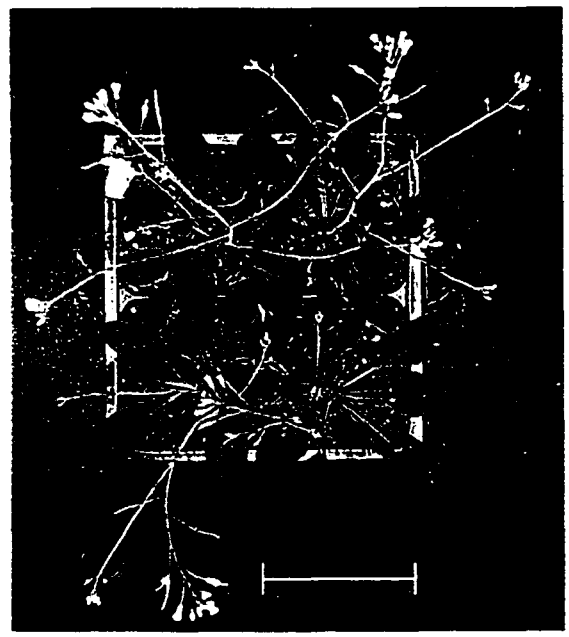


D.

Figure 21. Digital pictures of control (normal watering) *Arabidopsis* plants. (A) wild-type, 29 days after planting; (B) transgenic line A, 29 days after planting. Bar = 6 cm.

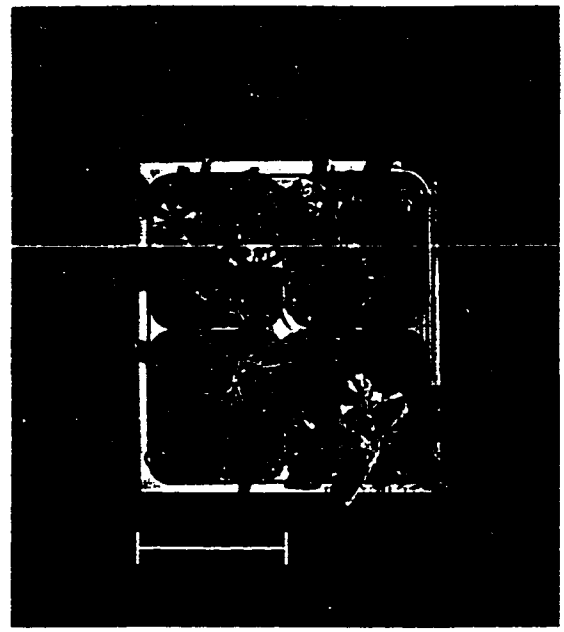


A.

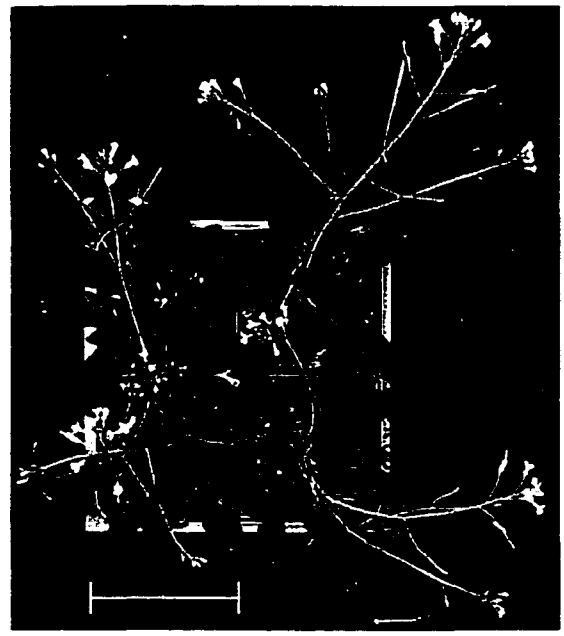


B.

Figure 22. Digital pictures of over-watered *Arabidopsis* plants. (A) wild-type, 29 days after planting; (B) transgenic line A, 29 days after planting. Bar = 6 cm.



A.



B.

stressed) plants had achieved similar stages of development by 29 days, and their leaves were of comparable size (Figs. 21B and 22B). It is apparent, therefore, that growth of the wild-type plants is impaired as a consequence of flooding-induced stress. The data in Figure 23 provide a more quantitative illustration of this finding. In these experiments, the aggregate leaf dry weights of flooded wild-type and transgenic plants were compared. Leaf biomass continues to increase during development of the plants to days 42 and 44 after planting (Fig. 23). At this stage of development the leaf biomass of transgenic plants is 1.7-fold higher than that for control plants (Fig.23).

Loss of leaf chlorophyll is an accepted index of leaf senescence (Thompson *et al.*, 1998; Thompson *et al.*, 1997). Chlorophyll levels began to decline for flooded wild-type *Arabidopsis* plants and flooded transgenic plants between days 23 and 25 after planting (Fig. 24). This decline continued through day 48 at which point levels of chlorophyll had been reduced by 31-fold in comparison with values at day 23 after planting (Fig. 24). Between days 42 and 48, the decline in chlorophyll levels tended to be more rapid for stressed wild-type plants than for stressed transgenic plants (Fig. 24), suggesting that the presence of the transgene delayed the progression of senescence. When the decline in chlorophyll is expressed per unit dry weight, the changes as a function of senescence are closely similar to those indicated in Figure 24. That senescence is somewhat delayed in the transgenic plants by comparison with the wild-type plants at day 46 is also evident from the digital pictures illustrated in Figure 25.

The possibility that up-regulation of hydroperoxide lyase decreased the accumulation of hydroperoxides in membranes under conditions of stress was examined. Levels of peroxidized lipids in preparations of total leaf

Figure 23. Changes in dry weight of the aggregate of rosette leaves of over-watered wild-type (■) and transgenic (□ , line A) *Arabidopsis* during development and senescence. Values are means ± SE for n = 12-18 plants. Asterisk indicates significant differences at 95% confidence limits as determined by a paired t-test. Age, days after planting.

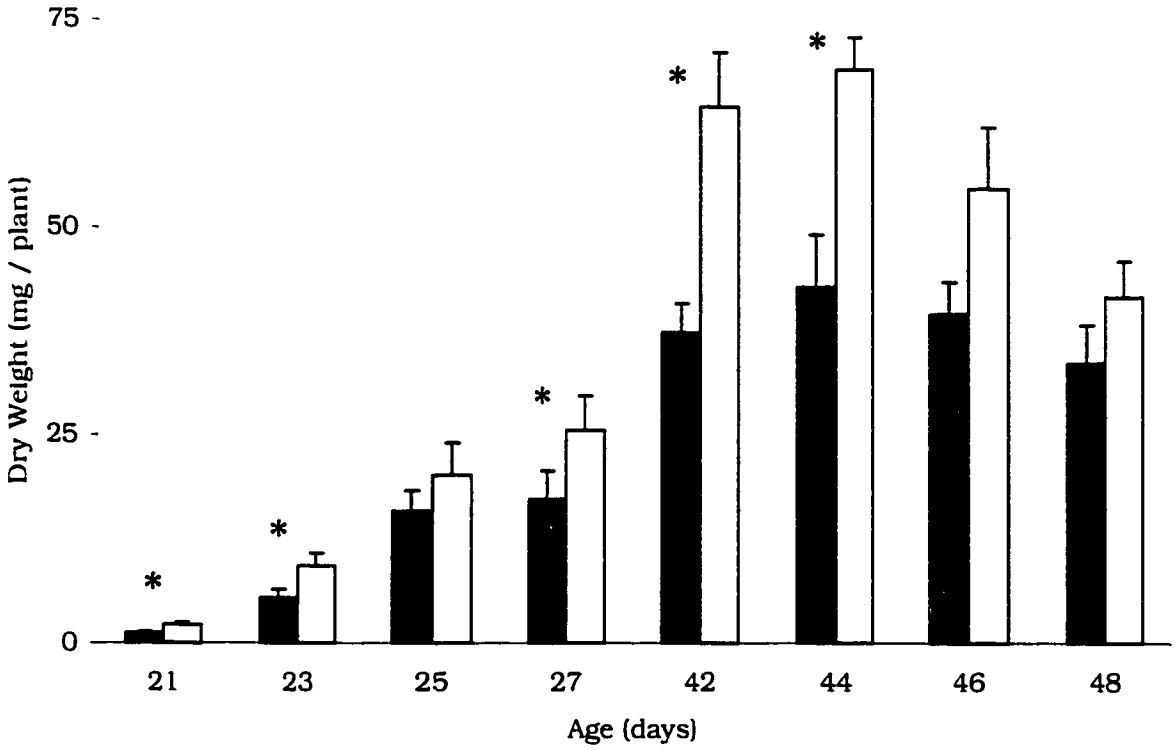

75
50
25
0
Dry Weight (mg / plant)
*
*
*
*
*
21
23
25
27
42
44
46
48
Age (days)

Figure 24. Changes in leaf chlorophyll levels of over-watered wild-type (■) and transgenic (□ , line A) *Arabidopsis* plants. Values are means ± SE for n = 12-18 plants measurements. Values for wild-type and transgenic plants are not significantly different at 95% confidence limits for any stage of senescence as determined by a paired t-test. Age, days after planting.

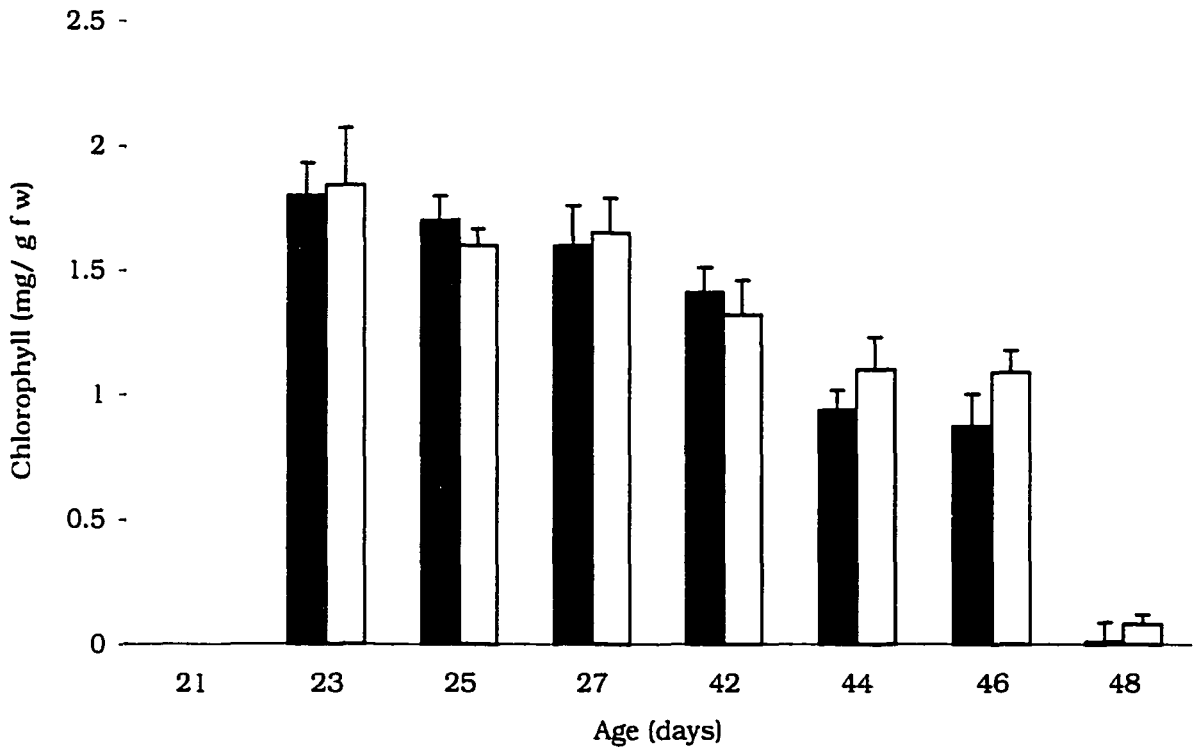

2.5
2
1.5
1
0.5
0
Chlorophyll (mg/ g f w)
21
23
25
27
42
44
46
48
Age (days)

Figure 25. Digital pictures of over-watered *Arabidopsis* plants. (A) wild-type, 46 days after planting; (B) transgenic line A, 46 days after planting. Bar = 6 cm.



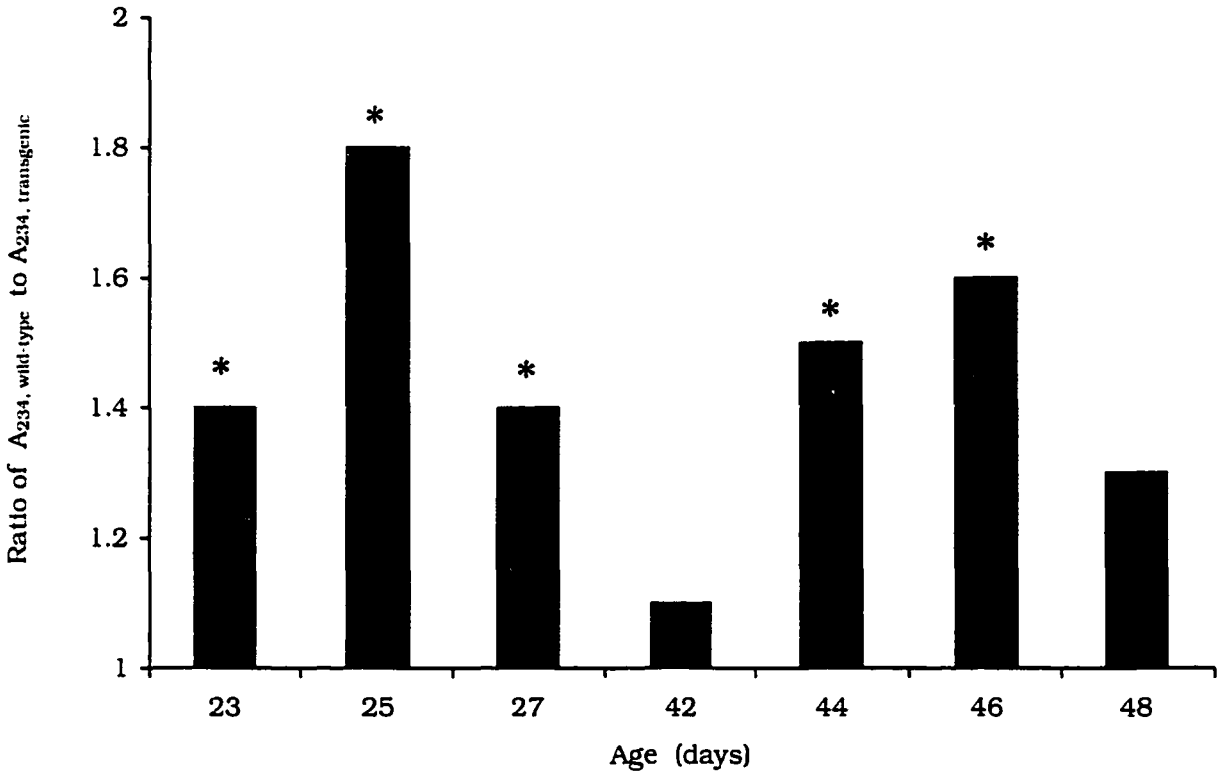
A.



B.

membrane were measured for stressed wild-type plants and stressed transgenic plants at selected stages of development from days 23 to day 48 after planting. At all stages of development, the membrane peroxide levels were higher in wild-type plants than in control plants (Fig. 26), indicating that up-regulation of hydroperoxide lyase does indeed reduce the titre of membrane peroxides. That this occurs beginning at the early stages of development indicates that it is correlated with the higher biomass of the transgenic plants and not just senescence.

Figure 26. Changes in levels of peroxidized lipids in total membrane preparations from leaves of over-watered wild-type and transgenic (line A) *Arabidopsis* plants. Differences are expressed as the ratio $A_{234,\text{wild-type}}$ to $A_{234,\text{transgenic}}$ for membrane fractions from identical fresh weights of tissue. Values are means ± SE for n = 12-18 plants. Asterisk indicates significant differences at 95% confidence limits as determined by a paired t-test. Age, days after planting.


2
1.8
1.6
1.4
1.2
1
Ratio of $A_{234,\ wild\text{-}type}$ to $A_{234,\ transgenic}$
*
*
*
*
*
23
25
27
42
44
46
48
Age (days)

Discussion

The green-note volatiles, hexanal and *(3Z)*-hexenal, are important flavour and fragrance additives. Both are produced industrially by chemical synthesis or extraction from specific plant sources in which they are abundant. Naturally derived hexanal and *(3Z)*-hexenal find especially widespread consumer acceptance, and industries are intensifying their efforts to find ways to produce these volatiles naturally (Rouhi, 1999; Bate *et al.*, 1998; Ohloff, 1994). In the present dissertation, two novel strategies, which have not been employed by industry, are presented for obtaining higher levels of green-note volatiles. A packed-bed bioreactor with immobilized enzymes has been used for the continuous production of hexanal, and transgenic plants in which hydroperoxide lyase is up-regulated have been shown to contain higher steady-state levels of *(3Z)*-hexenal than corresponding wild-type plants. In both cases the recovery of the volatiles is significantly increased. Hexanal production in the bioreactor, using a tomato membrane biocatalyst over a 30 min time period, proved to be 112-fold higher than steady-state levels of the volatile in an equivalent amount of fresh tissue. *(3Z)*-Hexenal levels were enhanced 29-fold in transgenic *Arabidopsis* plants when compared to wild-type plants.

Several tissues naturally enriched in hexanal were tested in the bioreactor, and of these, the maximum yield of hexanal was obtained from the membrane fraction isolated from tomato leaves. The observation that membranes are the source of the enzymes responsible for hexanal production is not surprising, as several lines of evidence support this (Perez *et al.*, 1999; Hudak and Thompson, 1997; Kausch and Handa, 1997; Matsui

et al., 1997; Blée and Joyard, 1996). Specifically, hydroperoxide lyase has been shown to be associated with plastid envelope membranes in leaves (Blée and Joyard, 1996), and the enzyme is also associated with microsomal membrane preparations from ripening strawberry (Perez *et al.*, 1999), which would contain vesicles of chloroplast envelope membrane. Subcellular fractionation studies with carnation flower petals have indicated that green-note volatiles also originate from membranes within this tissue (Hudak and Thompson, 1997). As well, Kausch and Handa (1997) reported that a lipoxygenase isoform associated with membranes of tomato fruit is capable of forming C_6-aldehydes.

Interestingly, product-inhibition appears to be an important consideration in bioreactor-based hexanal production. This observation is supported by several results. First, in a series of earlier experiments Schade (1998) noted that the steady-state level of hexanal in carnation petals remained constant after homogenization, which could mean that further formation of the volatile in the disrupted cell suspension is inhibited by the presence of endogenous hexanal. In addition, a batch shaker-flask experiment using immobilized biocatalyst and operating conditions similar to those used for the bioreactor demonstrated that hexanal levels increased only 4.5-fold (Schade, 1998), whereas hexanal levels increased 23-fold using the continuously operated bioreactor. This difference in hexanal generation is not attributable to enzyme stabilization by entrapment and surfactant addition (Suurmeijer *et al.*, 2000), nor to removal of the cytosolic fraction, for it this were the case yields of the batch and continuously operated reactors would be comparable. Rather, the difference appears to be due to removal of hexanal generated during the process. This contention is supported by the work of Suurmeijer *et al.* (2000), who observed that

enzyme activity of purified hydroperoxide lyase is inactivated by low concentrations of C_6-aldehydes. Thus, it appears that continuous hexanal removal by the on-line separation unit lowers the hexanal concentration in the reactor below the threshold for enzyme inhibition, allowing a many-fold increase in hexanal generation when compared to the batch-operated shaker-flask.

The concentration of substrate used in the bioreactor is critical. A minimum substrate concentration of 6.7 mM linoleic acid, in the form of mixed linoleic acid - Tween 20 micelles, was required to generate hexanal, and a concentration of 10.7 mM linoleic acid was found to be optimum. These results demonstrated that hexanal levels in the permeate did not simply reflect endogenous volatile released from the biocatalyst, and that hexanal production did indeed occur in the reactor. A substrate preparation of mixed linoleic acid and Tween 20 micelles was necessary because of the low solubility of linoleic acid. Solubilization required the addition of the surfactant, Tween 20. Indeed, upon addition of the surfactant the linoleic acid suspension cleared. In addition, the membrane selected for the ultrafiltration unit, which has a molecular weight cut-off of 100 kDa, retained 100% of the substrate. Thus, it seems reasonable to propose that linoleic acid and Tween 20 formed mixed micelles with an average molecular weight exceeding 10^5 g/mol.

In an earlier report, Tanaka *et al.* (1984) hypothesised that particles with a molecular weight exceeding 10^5 g/mol adsorb to the bead surfaces rather than diffuse into the calcium-alginate matrix. However, diffusion of the linoleic acid-Tween 20 micelles (MW > 10^5 g/mol) into the beads was confirmed in the present study. The 2^2-factorial design revealed that an increase in catalyst loading by a factor of 3, which does not affect permeate

flux across the ultrafiltration unit, decreased hexanal production regardless of the initial substrate concentration. This supports the notion that increased catalyst loading reduces diffusivity of the linoleic acid-Tween 20 micelles in the beads because of a corresponding decrease in free space within the pores. Consequently, substrate must diffuse into the beads.

Diffusional limitations might have been further minimized by reducing bead diameter to less than 2.5 mm, thereby shortening the pore length (Perry, 1999). However, smaller beads would have increased the pressure drop (Δp) across the packed-bed of the reactor (Perry, 1999). In light of this, a reduction in bead diameter was not feasible, as even the 2.5 mm diameter beads showed slight signs of pressure-induced deformation, which can result in clogging of the packed-bed. This deformation was a consequence of the reactor design. Specifically, having the ultrafiltration unit, which operates at elevated pressure (transmembrane pressure = 5 psi), immediately succeeding the packed bioreactor core resulted in elevated pressure on the beads in the packed-bed, and this pressure was apparently high enough to cause deformation. Enhancing the mechanical strength of the beads by increasing the alginate concentration above 3% was not technically feasible because of the greatly increased viscosity of the alginate-membrane suspension at higher alginate concentrations. Higher alginate concentrations would also decrease pore diameter (Martinsen *et al.* 1992), and decreased pore diameter would have further reduced diffusivity of the linoleic acid–Tween 20 micelles.

The 2^2-factorial design proved to be sufficient to describe the complexity of the bioreactor design. Indeed, several observations support the validity of the regression model. First, statistical analysis revealed a squared regression coefficient of $R^2 = 0.986$. Second, the residuals *(ε)* of the

model displayed low scattering without any statistical patterns, and third, testing the response of the model at its centre point demonstrated that the experimental value fitted the calculated value. In addition, the model showed that a decline in bioreactor-based hexanal production was not only attributable to diffusion limitations within the beads, but also to extensive fouling of the separation unit. This latter effect is evident from the finding that permeate flux decreased independently of catalyst loading when substrate concentration was increased from low to high levels.

pH was also critical for optimizing hexanal generation in the bioreactor. The membrane-bound isoforms of hydroperoxide lyase and lipoxygenase have both been reported to be most active within a pH range of 6 to 8 (Suurmeijer *et al.*, 2000; Kausch and Handa, 1997; Blée and Joyard, 1996; Riley *et al.*, 1996; Rouet-Mayer *et al.*, 1992). Also, calcium-alginate beads are thought to be stable over this pH range (Martinsen *et al.*, 1992). The effects of pH 6 and 7.4 (physiological pH) upon bioreactor-based hexanal production were tested, and it was found that hexanal yield doubled at pH 6 in comparison to pH 7.4. However, the beads started to dissolve after 15 min of reactor operation at pH 6, and after two hours at this pH 50% of the beads had completely dissolved, clogging the reactor. Interestingly, this appears to contradict the reported stability of alginate-beads at pH 6 (Martinsen *et al.*, 1992). Clarification of this apparent contradiction was obtained by Baer (unpublished data) who demonstrated that beads alone at pH 6 or pH 7.4 do not dissolve. However, the addition of Tween 20 at pH 6 caused the beads to dissolve. Thus, it would appear that, at pH 6, Tween 20 preferentially dissolves Ca^{2+} required for the alginate matrix formation, whereas, at pH 7.4, Tween 20 preferentially forms aggregates with the substrate, linoleic acid, instead of reacting with Ca^{2+}.

Therefore, for long-term operation pH 7.4 appears more suitable than pH 6. Nevertheless, the possibility that calcium is slowly leached from the beads at pH 7.4 should be further studied.

Temperature also played a critical role in the function of the bioreactor. Bioreactor-based hexanal generation peaked at 35°C in experiments in which hexanal production as a function of temperature was analysed. A time-course of hexanal production as a function of reactor temperature revealed that an initial increase in yield at higher temperatures was likely caused by increased permeate flux and accelerated reaction rate attributable to the increase in temperature. However, over time this increase in yield was dampened by thermal enzyme denaturation. That the Arrhenius dependence breaks down at high temperatures for enzyme reactions is well established and has been attributed to thermal inactivation of proteins (Sizer, 1944). Moreover, Bailey and Ollis (1986) have reported that most proteins denature at temperatures of 45°C and higher. In the present study, there was a significant decrease in hexanal yield when the reactor temperature was increased from 35°C to 45°C.

Bioreactor-based generation and recovery of *(3Z)*-hexenal from linolenic acid (18:3) failed. This may be attributable to product inhibition, but more likely reflects the high reactivity of *(3Z)*-hexenal (Suurmeijer *et al.*, 2000; Ohloff, 1994). Indeed, *(3Z)*-hexenal is thermally and chemically unstable, and is readily isomerized to *(2E)*-hexenal. In addition, it is prone to react in an aldol-like condensation with sugars present in the homogenate and in the reactor buffer, especially at elevated temperatures (Ege, 1986; Ohloff, 1994). This thermal instability has industrial relevance as a means of obtaining *(2E)*-hexenal from *(3Z)*-hexenal once a stable system with increased *(3Z)*-hexenal levels has been attained. In order to produce

high levels of *(3Z)*-hexenal, an alternative approach was developed. Hydroperoxide lyase-overexpressing plants were successfully obtained by transforming *Arabidopsis thaliana* with full-length cDNA encoding an exogenous plant hydroperoxide lyase. The exogenous hydroperoxide lyase was expressed in the sense orientation under the regulation of a constitutive promoter. This resulted in increased endogenous *(3Z)*-hexenal levels of up to 29-fold compared to wild-type plants. Thus, the transformed plants appear to be suitable bioreactors for *(3Z)*-hexenal production.

Of particular interest is the finding that levels of hexanal, another product of hydroperoxide lyase, remained unaltered for all tested transgenic lines. This confirms the existence of at least two isoforms of hydroperoxide lyase within the aldehyde pathway, one acting on linolenic acid hydroperoxide and the other on linoleic acid hydroperoxide, thereby yielding *(3Z)*-hexenal and hexanal, respectively. The fact that levels of *(3Z)*-hexenal increased and levels of hexanal did not indicates that the hydroperoxide lyase cDNA used for transforming *Arabidopsis thaliana* encodes the isoform of the enzyme acting on linolenic acid hydroperoxide. The presence of two hydroperoxide lyase isoforms has been reported for other tissues (Matsui *et al.*, 1996; Gardner, 1995; Matsui *et al.*, 1989). Another conclusion which can be drawn from the increased *(3Z)*-hexenal levels is that hydroperoxide lyase catalyses the rate-limiting step in the pathway for *(3Z)*-hexenal production.

Northern-blot analysis of transgenic *Arabidopsis thaliana* revealed that hydroperoxide lyase mRNA levels for all transgenic lines were higher than hydroperoxide lyase mRNA levels of wild-type plants. However, it is interesting to note that mRNA band intensity and measured levels of *(3Z)*-hexenal were not correlated. The reason for this is not clear, but it may

reflect different rates of *(3Z)*-hexenal metabolism among the transgenic lines.

The physiological role of C_6-aldehydes within plants has not been clearly established (Matsui *et al.*, 1999; Creelman and Mullet, 1997), but there is increasing evidence that they are directly or indirectly involved in plant-pathogen defense (Farmer *et al.*, 1998; Gardner, 1995; Croft *et al.*, 1993; Vick and Zimmerman, 1987a; Vick and Zimmerman, 1987b; Vick and Zimmerman, 1984). Farmer *et al.* (1998) and Croft *et al.* (1993) reported that hexanal and *(2E)*-hexenal have anti-microbial properties, and demonstrated that high concentrations of unsaturated C_6-aldehydes cause necrosis and that their production increases during the hypersensitive resistance response. Indeed, several lines of evidence support the notion of involvement of the lipoxygenase pathway in plant-pathogen interactions (Rogers *et al.*, 1988, Vick and Zimmerman, 1987a; Vick and Zimmerman, 1987b; Vick and Zimmerman, 1984). For example, Vick and Zimmerman (1987a, 1987b, 1984) demonstrated that various lipid-breakdown products, including C_6-aldehydes, are formed by the lipoxygenase pathway during pathogen ingression or other forms of biotic or abiotic stresses, and Rogers *et al.* (1988) showed that lipid peroxidation is induced by elicitors.

Of particular interest is the finding in the present study that during the bioreactor-based production of hexanal, there was no evident microbial contamination of the reactor, which is normally a major concern during the operation of bioreactors. Indeed, the present study is the first report demonstrating anti-microbial properties of *(3Z)*-hexenal *in vivo* and that increased *in situ* levels of *(3Z)*-hexenal provide enhanced resistance against bacterial infection. When transgenic *Arabidopsis thaliana* was challenged with *Pseudomonas syringae*, *in planta* bacterial counts of transgenic plants

revealed increased resistance to infection by a factor of 6 compared to wild-type plants. The mechanisms by which C_6-aldehydes exert their anti-microbial properties have not been fully elucidated, but it is assumed that the toxicity of the unsaturated C_6-aldehydes arises from their high reactivity, specifically their ability to cross-link proteins and to modify sulfhydryl and amino groups (Zidek *et al.*, 1997 - in Matsui *et al.*, 1999; Schauenstein *et al.* 1977). It is possible that unsaturated C_6-aldehydes facilitate cell death during the hypersensitive response to infection through such reactions (Farmer *et al.*, 1998).

Bate and Rothstein (1998) suggested that C_6-aldehydes might be involved in signaling. Thus, an attempt was made to elucidate the putative involvement of *(3Z)*-hexenal in long-distance signaling during plant-pathogen defense, specifically in respect of systemic acquired resistance. In general, the induction of defense genes requires the generation of endogenous signal molecules by the challenged cells in the infection site. These signal molecules in turn set in motion signal transduction cascades in receiving cells, leading to the activation of defense genes. Thus, these signals serve to amplify and spread the response of the host after initial recognition of the pathogen (Penninckx *et al.*, 1998). Several signal molecules whose synthesis is increased in response to elicitor recognition and that are involved in the activation of defense genes have been identified. Among the long-distance signals, salicylic acid is the most prominent, and the role of salicylic acid in systemic acquired resistance has been extensively studied (Sticher *et al.*, 1997).

The exploration of systemic acquired resistance is of particular commercial interest, as it is expressed against a spectrum of organisms which differ from the inducing organism/agent. Thus, it confers quantitative

protection against a broad spectrum of diseases, which can last over weeks (Sticher *et al.*, 1997). It has been postulated that salicylic acid is the only primary endogenous signal responsible for inducing systemic resistance (Sticher *et al.*, 1997). However, grafting and leaf-detachment experiments have clearly demonstrated that, although salicylic acid is necessary for the induction of systemic acquired resistance, at least one additional signal may also be involved (Pallas *et al.*, 1996; Vernooij *et al.*, 1994; Rasmussen *et al.*, 1991). The involvement of signals other than salicylic acid in systemic acquired resistance is supported by other investigations as well. For example, Penninckx *et al.* (1998) demonstrated that ethylene and jasmonic acid are both required to trigger activation of the defensin gene, *PDF 1.2*, in *Arabidopsis* upon pathogen infection, and expression of this gene normally accompanies the development of systemic acquired resistance. In addition, Epple *et al.* (1995) have shown that certain defense genes, including those induced in the event of systemic acquired resistance, were inducible by *Fusarium* infection and methyl jasmonate, but not by salicylic acid. It has also been demonstrated that transgenic tobacco plants unable to accumulate salicylic acid synthesize pathogenesis-related proteins (PR proteins) and develop systemic acquired resistance upon infection with *Erwinia carotovora* (Vidal *et al.*, 1997).

Several lines of evidence indicate that hitherto unidentified signal(s) for systemic acquired resistance may originate from the lipoxygenase pathway. First, lipoxygenase activity has been found to increase following ingression by a number of pathogens. For example, Kessmann *et al.* (1994) and Melan *et al.* (1993) have demonstrated that a local infection with tobacco mosaic virus or *Pseudomonas syringae* pv. syringae systemically induces lipoxygenase activity, and Wen *et al.* (1991) have reported that

inhibition of lipoxygenase not only reduces levels of peroxidized fatty acids, but also inhibits the formation of phytoalexins during the development of systemic acquired resistance. Second, synthetic inducers of systemic acquired resistance, like 2,6-dichloroisonicotinic acid, enhance lipoxygenase activity (Sticher *et al.*, 1997). Third, Cohen *et al.* (1991) have reported that linoleic and linolenic acids induce systemic acquired resistance against *P. infestans* in potato, and Namei *et al.* (1993) have shown that linolenic acid accumulates in infected leaves during the development of systemic acquired resistance. Jasmonates, molecules derived through the lipoxygenase pathway and especially involved in signaling during wounding, appear not to be a primary signal for the induction of systemic acquired resistance (Sticher *et al.*, 1997).

When transgenic *Arabidopsis thaliana* plants with up-regulated hydroperoxide lyase and increased *(3Z)*-hexenal levels were challenged with *Pseudomonas syringae* in the present study, *in planta* bacterial counts revealed that systemic acquired resistance was enhanced 15-fold in comparison to wild-type plants. Therefore, it seems reasonable to propose that the formation of *(3Z)*-hexenal mediated by hydroperoxide lyase represents a key step in signal transduction during systemic acquired resistance. Whether or not *(3Z)*-hexenal and/or one of its derivatives represent the unknown primary signal(s) cannot be evaluated from the present data. However, *(3Z)*-hexenal possesses the general characteristics of a signal molecule, in that it is volatile and of low molecular mass. The contention that *(3Z)*-hexenal might be a signal molecule is further supported by the fact that treatment of *Arabidopsis thaliana* with C_6-aldehydes results not only in up-regulation of the genes encoding enzymes of the lipoxygenase pathway, but also in the induction of a subset of defense genes (Bate and

Rothstein, 1998). Of particular interest is the observation that an accumulation of C_6-aldehydes occurs before formation of phytoalexins when bean is infected with *Pseudomonas syringae* pv. phaseolicola (Croft *et al.*, 1993). It is also noteworthy that lipoxygenase and especially hydroperoxide lyase activities increase during germination, a stage of development which is particularly vulnerable to infection by pathogens (Vick and Zimmerman 1987a).

The hydroperoxide lyase transgene introduced into *Arabidopsis* in the present study encodes the isoform of the enzyme that metabolizes linolenic acid hydroperoxide. This raises the possibility that fatty acid hydroperoxide accumulation in response to stress and at the onset of senescence may be reduced in the transgenic plants. This was investigated through experiments in which transgenic plants and corresponding wild-type plants were exposed to anoxic stress by root-flooding.

One of the earliest physiological changes marking the onset of senescence is loss of chlorophyll (Noodén and Leopold, 1988). Accordingly, changes in leaf chlorophyll levels were used to identify the onset of senescence and mark its progress during development of wild-type and transgenic *Arabidopsis* plants. Leaf chlorophyll levels of wild-type and transgenic plants exposed to flooding stress during development declined in parallel during the early stages of senescence. This indicates that the presence of the hydroperoxide lyase transgene had no effect on the timing of senescence initiation in response to anoxic stress. However, during the late stages of flooding-induced senescence (days 44 to 48 after planting) the decline in leaf chlorophyll tended to be more rapid for wild-type plants than for transgenic plants, suggesting that the presence of the transgene reduces the rate at which senescence intensifies at the end of the life-span of the

leaves. Moreover, this reduction in rate of chlorophyll loss in stressed transgenic plants correlated temporally with decreased levels of lipid hydroperoxides in leaf membrane preparations by comparison with wild-type plants. The titre of lipid hydroperoxides in leaf membranes of flooding-stressed transgenic plants proved to be ~ 1/3 lower than levels in corresponding membrane preparations from flooding-stressed wild-type plants at this later stage of senescence. These observations are consistent with the view that a reduction in membranous peroxidized lipids in flooded transgenic plants reduces the rate at which chlorophyll loss intensifies during the latter stages of senescence. It is noteworthy in this context that chlorophyll is associated with chloroplast thylakoids and hydroperoxide lyase with the chloroplast envelope (Lodish *et al.*, 1995, Blée and Joyard, 1996). However thylakoids break down during senescence before the chloroplast envelope (Woolhouse, 1984).

Of particular interest is the finding that the presence of the transgene encoding hydroperoxide lyase resulted in lower levels of membrane lipid hydroperoxides in the leaves of flooding-stressed transgenic *Arabidopsis* plants during earlier stages of development as well. For example, at days 23 to 27 after planting coincident with the initiation of bolting membrane hydroperoxide levels were 1.4 times to 1.8 times higher in the leaves of flooding-stressed wild-type plants than in leaves of flooding-stressed transgenic plants. Moreover, flooding resulted in impaired leaf growth for the wild-type plants, but had no effect on the growth of leaves of the transgenic plants. There was also a reduction in bolt-length and bolt number for flooding-stressed wild-type plants in comparison with flooding-stressed transgenic plants. These observations collectively suggest that hydroperoxide lyase may play an important role in membrane turnover by

metabolizing lipids that have been damaged by peroxidation. The enzyme converts peroxidized fatty acids, which destabilize the structure of membrane bilayers, into green-note volatiles which presumably easily diffuse out of the membrane into the cytosol.

Several lines of evidence indicate that the lipoxygenase pathway is activated during senescence. This activation is initially manifested as deesterification of membrane phospholipids by a lipase or lipases resulting in the release of free fatty acids, mainly linoleic and linolenic acid (Matsui *et al.*, 1999; Gardner, 1995; Thompson *et al.*, 1982). Deesterification of membrane lipids and the subsequent accumulation of free fatty acids in the membrane bilayer result in loss of membrane structural integrity, which leads to leakiness and impairment of cell function (Hong *et al.*, 2000; Thompson *et al.*, 1998). More specifically, lipid bilayers of non-senescent plant membranes are liquid-crystalline, reflecting rotational motion of the membrane fatty acids. However, the accumulation of free fatty acids in senescing membranes not only changes the chemical composition of the membrane bilayer, but also alters membrane fluidity. This arises by reason of the fact that the free fatty acids phase-separate and form domains of gel phase lipid. The gel phases laterally separate from the remaining liquid crystalline domains, and the resulting mixture of phases renders the bilayers leaky due to packing imperfections at the phase boundaries. This results in loss of essential ion gradients and impairment of cell function (Siedow, 1991; Hildebrand, 1989).

Activation of membranous lipoxygenase during senescence appears to be attributable to release of the free fatty acids, linoleic acid and linolenic acid, which are both substrates for this enzyme, from membrane phospholipids (Lynch *et al.*, 1985). This in turn results in an increased titre

of linoleic acid hydroperoxide and linolenic acid hydroperoxide, products of the action of lipoxygenase, within membrane bilayers (Lynch *et al.*, 1985). Of particular interest are the observations that membrane-bound lipoxygenase activity is increased by treatment with ethylene, and that treatment of ethylene-sensitive tissues with this hormone also induces a decline in phospholipid levels and changes in membrane lipid fluidity (Thompson *et al.*, 1998; Thompson *et al.*, 1982). Therefore, it seems probable that, at least for some tissues, increased ethylene production results in increased lipid peroxide levels. In addition, naturally senescing membranes accumulate peroxides, even though some, like 13-hydroperoxide, can be further metabolised by hydroperoxide lyase or other branches of the lipoxygenase pathway (Gardner, 1995). These peroxidation products further destabilise the membrane-bilayer. Moreover, lipid peroxidation generates activated oxygen species, like singlet oxygen ($^1O_2$) and alkoxy radicals (RO·), which are in themselves able to initiate lipid peroxidation, rendering the process autocatalytic (Gardner 1995; Kappus, 1985).

Membrane-associated proteins are also affected by these senescence-related changes in bilayer lipids. They are altered by changes in membrane-bilayer fluidity as well as by direct oxidative damage. In detail, changes in the conformation of membrane proteins occurs when they are vertically displaced towards the membrane surface as a consequence of decreasing membrane fluidity. Under these conditions they are exposed to an increasingly hydrophilic environment and, accordingly, undergo conformational changes. In addition, activated oxygen species directly attack certain amino acid residues of membrane proteins causing

conformational changes. These conformational changes in turn result in enhanced proteolysis (Duxbury *et al.*, 1991).

These observations collectively indicate that under conditions in which ethylene formation is favoured, such as senescence or following episodes of environmental stress, a cascade of events that leads to increased lipid peroxide levels in membranes is set in motion. Ethylene formation can be induced by a number of stresses including water-saturation of the soil and ensuing anoxia. Indeed, increased ethylene levels in leaves as a consequence of O_2 depletion in water-saturated soil is a well-established phenomenon (Pennel and Lamb, 1997; Nilson and Orcutt, 1996; Brailsford *et al.*, 1993; Wiedenroth, 1992). When transgenic and wild-type *Arabidopsis* plants were flooded, growth of wild-type *Arabidopsis* was impaired, whereas transgenic plants under the same conditions grew like wild-type *Arabidopsis* plants that were not flooded. Specifically, the biomass of flooded wild-type plants was reduced, and membrane peroxide levels in total leaf membrane preparations were higher when compared to flooded transgenic plants. In fact, the ratio of membrane peroxides in stressed wild-type plants to those in stressed transgenic plants remained >1 throughout development and senescence. There was, however, fluctuation in this ratio, which may reflect variations in the availability of free fatty acid substrate for lipoxygenase throughout development and senescence. This contention is supported by previous observations indicating that the timing and extent of lipoxygenase-initiated peroxidation in membranes is determined more by substrate availability than by changes in levels of lipoxygenase protein (Lynch *et al.*, 1985).

It seems clear, therefore, that up-regulation of hydroperoxide lyase partially alleviates the effects of stress induced by flooding. The transgene

presumably effects enhanced conversion of 13-hydroperoxides into *(3Z)*-hexenal. In addition, the lower levels of peroxides are likely to reduce the formation of activated oxygen species arising from autocatalysis of lipid peroxidation (Thompson *et al.*, 1997; Gardner 1995). This in turn is likely to reduce destabilization of membrane bilayers attributable to the anoxia and to minimize the deleterious effects of the stress on growth.

In this dissertation, novel, alternative processes for natural production of the green-note volatiles, hexanal and *(3Z)*-hexenal, are presented. Enzyme templates from tomato leaves were immobilized in a natural alginate matrix and used as a biocatalyst within a packed-bed bioreactor for the production of the green-note volatile, hexanal. Hexanal production was increased 112-fold in this reactor, and due to the anti-microbial properties of hexanal, reduced reactor contamination, a major concern of bioreactor design, was observed. Key parameters - namely pH, reaction temperature, and substrate and catalyst concentrations - affecting hexanal generation were identified and optimized. A 2^2-factorial design proved to be a quick and efficient way to achieve this optimization. Bioreactor-based generation and recovery of *(3Z)*-hexenal was not achieved due to the high reactivity of *(3Z)*-hexenal. However, *Arabidopsis thaliana* was genetically modified to produce high levels of *(3Z)*-hexenal by up-regulating hydroperoxide lyase. Overexpression of a hydroperoxide lyase cDNA in *Arabidopsis* resulted in increased levels of *(3Z)*-hexenal for the transgenic lines of up to 29-fold by comparison to wild-type plants, whereas hexanal levels remained unaltered. Accordingly, such transformed plants are suitable bioreactors for *(3Z)*-hexenal production in themselves.

The transgenic *Arabidopsis* plants with up-regulated *(3Z)*-hexenal levels were tested for increased resistance against bacterial infection and for

enhanced systemic acquired resistance. *In planta* bacterial counts revealed increased resistance to primary infection for the transgenic lines of 6-fold and enhancement of systemic acquired resistance by 15-fold in comparison to wild-type plants. Thus, overall resistance against bacterial infection was increased by 90-fold in the transgenic plants. Therefore, it seems reasonable to propose that the formation of *(3Z)*-hexenal mediated by hydroperoxide lyase represents a key step in signal transduction during the establishment of systemic acquired resistance. Whether or not *(3Z)*-hexenal represents a novel primary signal for the induction of systemic acquired resistance cannot be determined from the present data. Further experiments are required. However, up-regulation of hydroperoxide lyase appears to be an efficient way of increasing broad-spectrum disease resistance in plants.

The transgenic plants also proved to have increased tolerance to stress. Flooding stress resulted in impaired leaf growth in wild-type plants, whereas leaf development in the transgenic plants was unaffected. In addition, peroxidized lipid levels of total membrane preparations from the transgenic plants were significantly reduced in comparison with wild-type plants. This suggests not only that hydroperoxide lyase activity might be an important factor in the process of membrane turnover, but also that up-regulation of hydroperoxide lyase reduces membrane bilayer destabilization by converting destabilizing peroxides into green-note volatiles.

Literature Cited

Agrios, G.N. (1996). Plant Pathology. Academic Press, Toronto.

A/G Technology Corporation (1997). UF/MF Operating Guide. A/G Technology Corporation, Needham.

Amsden, B. & Turner, N. (1999). Diffusion characteristics of calcium alginate gels. Biotechnolgy and Bioengineering 65, 605-610.

Armstrong, W. (1994). Polargraphic oxygen electrodes and their use in plant aeration studies. Proceedings of the Royal Society of Edinburgh 102, 511-528.

Bailey, J.E. & Ollis, D.F. (1986). Biochemical Engineering Fundamentals. McGraw Hill, New York.

Bate, N.J., Sivasankar, S., Moxon, C., Riley, J.M.C., Thompson, J.E. & Rothstein, S.J. (1998). Molecular characterization of an *Arabidopsis* gene encoding hydroperoxide lyase, a cytochrome P-450 that is wound inducible. Plant Physiology 117, 1393-1400.

Bate, N.J. & Rothstein, S.J. (1998). C_6-volatiles derived from the lipoxygenase pathway induce a subset of defense-related genes. Plant Journal 16(5), 561-569.

Battu, S.R., Chable, H., Beneytout, J.-L. (1994). Effectiveness of talc as absorbent for purification and immobilization of plant lipoxygenases. Journal of Agricultural and Food Chemistry 43, 2115-2120.

Bechtold, N., Ellis, J. & Pelletier, G. (1998). In planta *Agrobacterium* mediated transformation of adult *Arabidopsis thaliana* plants by vacuum infiltration. Methods in Molecular Biology 82, 259-266.

Belfort, G. (1994). Membranes and bioreactors: A technical challenge in biotechnology. Biotechnology and Bioengineering 33, 1047-1066.

Blée, E. & Joyard, J. (1996). Envelope membranes from spinach chloroplasts are a site of metabolism of fatty acid hydroperoxides. Plant Physiology 110, 445-454.

Bodalo-Santoya, A., Gomez-Carrasco, J.L., Gomez-Gomes, E., Bastida-Rodriquez, J., Maximo-Martin, M.F. & Hidalgo-Montesinos, A.M. (1999). Production of optically pure L-valine in fluidized and packed bed reactors with immobilized L-aminoacyclase. Journal of Chemical Technology and Biotechnology 74, 403-408.

Brailsford, R.W., Voesenek, L.A.C.J., Blom, C.W.P.M., Smith, A.R., Hall, M.A. & Jackson, M.B. (1993). Enhanced ethylene production by primary roots of *Zea mays* L. in response to sub-ambient partial pressures of oxygen. Plant Cell & Environment 16, 1071-1080.

Bryjak, J. & Kolarz, B.N. (1997). Immobilization of trypsin on acrylic copolymers. Process Biochemistry 33(4), 409-417.

Buchanon-Wollaston, V. (1997). The molecular biology of leaf senescence. Journal of Experimental Botany 48, 181-199.

Buchholz, K. & Klein, J. (eds.) (1987). Methods in Enzymology 135. Academic Press, Toronto, 3-121.

Bunch, A.W. (1988). The uses and future potential of microbial hollow-fiber bioreactors. Journal of Microbiological Methods 8, 103-119.

Bucke, C. (1983). Immobilized cells. Philosophical Transactions. Royal Society of London. Biological Sciences 300, 369-389.

Cameron, R.K., Dixon, R.A. & Lamb, C.J. (1994). Biologically induced systemic acquired resistance in *Arabidopsis thaliana*. The Plant Journal 5, 715-725.

Cass, B.J., Schade, F., Robinson, C.W., Thompson, J.E. & Legge, R.L. (2000). Production of tomato flavor volatiles from a crude enzyme preparation using a hollow-fiber reactor. Biotechnology and Bioengineering 67, 372-377.

Chirgwin, T., Drzbyla, A., MacDonald, R. & Rutter, W. (1979). Isolation of biologically active ribonucleic acid from sources enriched in ribonucleases. Biochemistry 18, 5294-5299.

Cohen, Y., Gisi, U., Mösinger, E. (1991). Systemic resistance of potato plants against *Phytophthora infestans* induced by unsaturated fatty acids. Physiological and Molecular Plant Pathology 38, 255-263.

Creelman, R.A. & Mullet, J.E. (1997). Biosynthesis and action of jasmonates in plants. Annual Review of Plant Physiology and Plant Molecular Biology 48, 355-381.

Croft, K.P.C., Juettner, F. & Slusarenko, A.J. (1993). Volatile products of the lipoxygenase pathway evolved from *Phaseolus vulgaris* (L.) leaves inoculated with *Pseudomonas syringae* pv. phaeseolicola. Plant Physiology 101, 13-24.

Cuperus, F.P., Kramer, G.F.H., Derksen, J.T.P. & Bouwer, S.T. (1995). Activity of immobilized lipoxygenase used for the formation of perhydroxyacids. Catalysis Today 25, 441-445.

Dainty, A.L., Goulding, K.H., Robinson, P.K., Simpkins, I. & Trevan, M.D. (1986). Stability of alginate-immobilized algal cells. Biotechnology and Bioengineering 28, 210-216.

Devore, J. & Peck, R. (1992). Statistics – The Exploration and Analysis of Data. Duxbury Press, California.

Dong, X. (1998). SA, JA, ethylene, and disease resistance in plants. Current Opinion in Plant Biology 1(4), 316-323.

Dong, X., Mindrinos, M., Davis, K.R. & Ausubel, F.M. (1991). Induction of defense genes by virulent and avirulent *Pseudomonas syringae* strains and by a cloned avirulence gene. The Plant Cell 3, 61-72.

Drew, M.C. (1992). Soil aeration and plant root metabolism. Soil Science 154(4), 259-268.

Droillard, M.-J., Rouet-Mayer, M.-A., Bureau, J.-M. & Lauriere, C. (1993). Membrane-associated and soluble lipoxygenase isoforms in tomato pericap. Plant Physiology 103, 1211-1219.

Duxbury, C.L., Legge, R.L., Paliyath, G., Barber, R.F. & Thompson, J.E. (1991). Alterations in membrane protein conformation in response to senescence-related changes. Phytochemistry 30, 63-68.

Edelman, M., Hallick, R.B. & Chua, N.-H. (eds.) (1982). Methods in Chloroplast Molecular Biology. Elsevier Biomedical Press, New York.

Ergun, M. & Mutlu, S.F. (2000). Application of a statistical technique to the production of ethanol from sugar beet molasses by *Saccharomyces cerevisiae*. Biosource Technology 73, 251-255.

Epple, P., Apel, K. & Bohlmann, H. (1995). An *Arabidopsis thaliana* thionin gene is inducible via a signal transduction pathway different from that for pathogen-related proteins. Plant Physiology 109, 813-820.

Ege, S. (1986). Organic Chemistry. D.C. Heath Company, Toronto.

Farmer, E.E., Weber, H. & Vollenweider, S. (1998). Fatty acid signaling in *Arabidopsis*. Planta 206, 167-174.

Feinberg, A.P. & Vogelstein, B. (1983). A technique for radiolabelling DNA restriction endonuclease fragments to high specific activity. Analytical Biochemistry 132, 6-13.

Gardner, H.W. (1995). Biological roles and biochemistry of the lipoxygenase pathway. Hort Science 30 (2), 197-205.

Goodman, R.N. & Novacky, A.J. (1994). The hypersensitive reaction in plants to pathogens. APS Press, St. Paul.

Gray, J.C. (1982). Use of proteolytic inhibitors during isolation of plastid proteins. In Edelman, M. (ed.), Methods in Chloroplast Molecular Biology. Elsevier Biomedical Press, North-Holland, 1093-1101.

Grechkin, A. (1998). Recent developments in biochemistry of the plant lipoxygenase pathway. Progress in Lipid Research 37(5), 317-352.

Groep, M.E., Gregory, M.E., Kershenbaum, L.S. & Bogle, D.E. (2000). Performance modeling and simulation of biochemical process sequences with interacting unit operations. Biotechnology and Bioengineering 67, 300-311.

Grund, G., Robinson, C.W. & Glick, B.R. (1992). Protein type effects on steady-state crossflow membrane ultrafiltration fluxes and protein transmission. Journal of Membrane Science 70, 177-192.

Gutteridge, J.M.C. & Halliwell, B. (1990). The measurement and mechanism of lipid peroxidation in biological systems. Trends in Biochemical Sciences 15, 129-135.

Hammerschmidt, R. (1999). Induced disease resistance: how do induced plants stop pathogens? Physiological and Molecular Plant Pathology 55, 77-84.

Hammerschmidt, R. & Kuc, J. (1995). Induced Resistance to Disease in Plants. Dodrecht, Kluwer.

Haumont, M., Magdalou, J., Ziegler, J.-C., Bidault, R., Siest, J.-P. & Siest, G. (1991). Immobilization of microsomes into alginate beads is a convenient method for producing glucuronides from drugs. Applied Microbiology and Biotechnology 35, 440-446.

Hildebrand, D.F. (1989). Lipoxygenases. Physiologia Plantarum 76, 249-253.

Hong, Y., Wang, T.-W., Hudak, K.A., Schade, F., Froese, C.D. & Thompson, J.E. (2000). An ethylene-induced cDNA encoding a lipase (lipolytic acyl hydrolase) expressed at the onset of senescence. Proceedings of the National Academy of Sciences of the United States of America 97(15), 8717-8722.

Horitsu, H., Yahashi, Y., Takamizawa, K., Kawai, T.S. & Watanabe, N. (1992). Production of xylitol from D-xylose by *Candida tropicalis*: optimization of production rate. Biotechnology and Bioengineering 40, 1085-1091.

Hsu, A., Foglia, T.A. & Piazza, G.J. (1997). Immobilization of lipoxygenase in an alginate-silicate solgel matrix: formation of fatty acid hydroperoxides. Biotechnology Letters 19, 71-74.

Hudak, K.A. & Thompson, J.E. (1997). Subcellular localization of secondary lipid metabolites including fragrance volatiles in carnation petals. Plant Physiology 114, 705-713.

Hudak, K.A. (1995). Characterization of lipid-protein particles and their role in membrane turnover in carnation petals. Dissertation, University of Waterloo, Waterloo, Ontario.

ICN (1997). ICN Protease Inhibitors. ICN, Costa Mesa.

Itoh, A. & Vick, B.A. (1999). The purification and characterization of hydroperoxide lyase in sunflower. Biochimica et Biophysica Acta 1436, 531-540.

Kappus, H. (1985). Oxidative Stress. Academic Press, New York, 273-309.

Kausch, K.D. & Handa, A.K. (1997). Molecular cloning of ripening-specific lipoxygenase and its expression during wild-type and mutant tomato fruit development. Plant Physiology 113, 1041-1044.

Kessmann, H., Staub, T., Hofmann, C., Maetzke, T. & Herzog J. (1994). Induction of systemic acquired resistance in plants by chemicals. Annual Review of Phytopathology 32, 439-59.

Kierstan, M. & Bucke, C. (1977). The immobilization of microbial cells, subcellular organelles, and enzymes in calcium alginate gels. Biotechnology and Bioengineering 19, 387-397.

Klein, J., Stock, J. & Vorlop, K.-D. (1983). Pore size and properties of spherical Ca-alginate biocatalysts. European Journal of Applied Microbiology and Biotechnology 18, 86-91.

Knoester, M., van Loon, L.C., van den Heuvel, J., Hennig, J., Bol, J.F. & Linthorst, H.J.M. (1998). Ethylene-insensitive tobacco lacks nonhost resistance against soil-borne fungi. Proceedings of the National Academy of Sciences of the United States of America 95, 1933-1937.

Knudsen, J.T., Tollsten, L. & Bergström, L.G. (1993). Floral scents – A checklist of volatile compounds isolated by head-space techniques. Phytochemistry 33 (2), 253-280.

Kondo, Y., Hashidoko, Y. & Mizutani, J. (1995). An enzymatic formation of 13-oxo-trideca-9,11-dienoic acid from 13-hydroperoxylinolenic acid by a homolytic hydroperoxide lyase in elicitor-treated soybean cotyledons. Biochimica et Biophysica Acta 1255, 9-15.

Kuc, J. (1982). Induced immunity to plant disease. Bioscience 32, 845-856.

Leshem, Y.Y., Sridhara, S. & Thompson, J.E. (1984). Involvement of calcium and calmodulin in membrane deterioration during senescence of pea foliage. Plant Physiology 75, 329-335.

Levenspiel, O. (1989). The Chemical Reaction Omnibook. Self-published, Chicago.

Lichtenberg, D. (1985). Characterization of the solubilization of lipid bilayers by surfactants. Biochimica et Biophysica Acta 821, 470-478.

Lichtenberg, D., Robson, R.J. & Dennis E.A. (1983). Solubilization of phospholipids by detergents. Structural and kinetic aspects. Biochimica et Biophysica Acta 737, 285-304.

Lodish, H., Baltimore, D., Berk, A., Zipursky, S.L., Matsudaira, P. & Darnell, G. (1995). Molecular Cell Biology. Scientific American Books, New York.

Luther, H., Hirsch, S., Schuster, E. & Weber E. (1992). Hollow fibre modules as membrane reactor in biocatalysis. Acta Biotechnologica 12, 133-142.

Lynch, D.V., Sridhara, S. & Thompson, J.E. (1985). Lipoxygenase-generated hydroperoxides account for the nonphysiological features of ethylene formation from 1-aminocyclopropane-1-carboxylic acid by microsomal membranes of carnations. Planta 164, 121-125.

Lynch, D.V. & Thompson, J.E. (1984). Lipoxygenase-mediated production of superoxide anion during plant senescence. FEBS Letters 173, 251-254.

Maleck, K. and Lawton, K. (1998). Plant strategies for resistance to pathogens. Current Opinion in Biotechnology 9, 208-213.

Mauch-Mani, B. & Métraux, J.-P. (1998). Salicylic acid and systemic acquired resistance to pathogen attack. Annals of Botany 82, 535-540.

Martinsen, A., Storroe, I. & Skjak-Braek, G. (1992). Alginate as immobilization material: III. Diffusional properties. Biotechnology and Bioengineering 39, 185-194.

Matsui, K., Wilkinson, J., Hiatt, B., Knauf, V. & Kajiwara, T. (1999). Molecular cloning and expression of *Arabidopsis* fatty acid hydroperoxide lyase. Plant Cell Physiology 40(5), 477-481.

Matsui, K., Shibata, Y., Tateba, H., Hatanaka, A. & Kajiwara, T. (1997). Changes of lipoxygenase and fatty acid hydroperoxide lyase activities in bell pepper fruits during maturation. Bioscience, Biotechnology, Biochemistry 61(1), 199-201.

Matsui, K., Shibutani, M., Hase, T. & Kajiwara, T. (1996). Bell pepper fruit fatty acid hydroperoxide lyase is a cytochrome P450 (CYP74B). FEBS Letters 394 (1), 21-24.

Matsui, K., Shibata, Y., Kajiwara, T. & Hatanaka, A. (1989). Separation of 13- and 9-hydroperoxide lyase activities in cotyledons of cucumber seedlings. Zeitschrift zur Naturforschung 44(c), 883-885.

Mattiason, B.M. (1983). In Mattiason, B.M. (ed.), Immobilized Cells and Organelles. Vol. I & II. CRC Press, Boca Raton.

Melan, M.A., Dong, X., Endara, M.E., Davis, K.R., Ausubel, F.M. & Peterman, T.K. (1993). An *Arabidopsis thaliana* lipoxygenase gene can be induced by pathogens, abscisic acid, and methyl jasmonate. Plant Physiology 101, 441-450.

Meyers, R.H. & Montgomery, D.C. (1995). Response Surface Methodology. John Wiley & Sons, New York.

Namai, T., Kato, T., Yamaguchi, Y. & Hirukuwa, T. (1993). Anti-rice blast activity and resistance induction of C-18 oxygenated fatty acids. Bioscience, Biotechnology, Biochemistry 57, 611-613.

Nillson, K. & Mosbach, K. (1980). Preparation of immobilized animal cells. FEBS Letters 188, 145-150.

Nilson, E.T. & Orcutt, D.M. (1996). The Physiology of Plants under Stress. John Wiley & Sons, New York.

Nilsson, J.L. (1990). Protein fouling of UF-membranes: causes and consequences. Journal of Membrane Science 52, 121-142.

Nitrampemba, G., Langlois, B.E., Archbold, D.D., Hamilton-Kemp, T.R. & Barth, M.M. (1998). Microbial populations of *Botrytis cinerea*-inoculated strawberry fruit exposed to four volatile compounds. Journal of Food Protection 61(10), 1352-1357.

Noodén, L.D. & Leopold, A.C. (eds.) (1988). Senescence and Aging in Plants. Academic Press Inc., San Diego.

Noordermeer, M.A., Veldink, G.A. & Vliegenhart, F.G. (1999). Alfalfa contains substantial 9-hydroperoxide lyase activity and *3Z:2E*-enal isomerase. FEBS Letters 443, 201-204.

Nunez, A., St.Armand, G., Foglia, T.A. & Piazza, G.J. (1997). Immobilization of hydroperoxide lyase from *Chlorella*. Biotechnology and Applied Biochemistry 25, 75-80.

Ohan, N.W. & Heikkila, J.J. (1995). Involvement of differential gene expression and mRNA stability in the developmental regulation of the hsp30 gene family in heat shocked *Xenopus laevis* embryos. Developmental Genetics 17, 176-184.

Ohloff, G. (1994). Scent and Fragrances. Springer Verlag, New York.

Pallas, J.A., Paiva, N.L., Lamb, C. & Dixon R.A. (1996). Tobacco plants epigenetically suppressed in phenylalanine ammonia-lyase expression do not develop systemic acquired resistance in response to infection by tobacco mosaic virus. Plant Journal 10, 281-293.

Platt-Aloia, K.A. & Thomson, W.W. (1985). Freeze-fracture evidence of gel-phase lipid in membranes of senescing cowpea cotelydons. Planta 163, 360-369.

Pennel, R.I & Lamb, C. (1997). Programmed cell death in plants. The Plant Cell 9, 1157-1168.

Penninckx, I.A.M.A., Thomma, B.P.H.J., Buchala, A., Métraux, J.-P. & Broekaert, W.F. (1998). Concomitant activation of jasmonate and ethylene response pathways is required for induction of a plant defensin gene in *Arabidopsis*. The Plant Cell 10, 2103-2113.

Perez, A.G., Olias, R. & Olias, J.M. (1999). Lipoxygenase and hydroperoxide lyase activities in ripening strawberry fruits. Journal of Agricultural and Food Chemistry 47(1), 249-253.

Perry, R.H. (1999). Perry's Chemical Engineers' Handbook. McGraw Hill, New York.

Pinto, M.C. & Macias, P. (1996). Synthesis of linoleic acid hydroperoxide using immobilized lipoxygenase in polyacrylamide gel. Applied Biochemistry and Biotechnology 59, 309-318.

Raskin, I. & Kende, H. (1984). Regulation of growth in stem sections of deep-water rice. Planta 160, 66-72.

Rasmussen, J.B., Hammerschmidt, R. & Zook, M.N. (1991). Systemic induction of salicylic acid accumulation in cucumber after inoculation with *Pseudomonas syringae* pv. syringae. Plant Physiology 97, 1342-1347.

Rehm, H.-J. (1995). Biotechnologie 2. Auflage. VCH, Weinheim.

Reymond, P. & Farmer, E.E. (1998). Jasmonate and salicylate as global signals for defense gene expression. Current Opinion in Plant Biology 1, 404-411.

Riley, J.C.M., Willemont, C. & Thompson, J.E. (1996). Lipoxygenase and hydroperoxidase lyase activities in ripening tomato fruit. Postharvest Biology and Technology 7, 97-107.

Robinson, C.W., Siegel, M.H., Condemine, A., Fee, C., Fahidy, T.Z. & Glick, B.R. (1993). Pulsed-electric-field crossflow ultrafiltration of bovine serum albumin. Journal of Membrane Science 80, 209-220.

Rogers, K.R., Albert, F. & Anderson, A.J. (1988). Lipid peroxidation is a consequence of elicitor activity. Plant Physiology 86, 547-553.

Ross, A.F. (1966). Systemic effects of local lesion formation. In Beemster, A.B.R. & Dijkstra, J. (eds.), Viruses of Plants. Amsterdam, 127-150.

Rouet-Mayer, M.-A., Bureau, J.-M. & Lauriere, C. (1992). Identification and characterization of lipoxygenase isoforms in senescing carnation petals. Plant Physiology 98, 971-978.

Rouhi, M. (1999). Perfumes: a whiff of chemistry. Chemical & Engineering News 77, 38-46.

Schade, F., Legge, R.L., Thompson, J.E. (2000). Fragrance volatiles of developing and senescing carnation flowers. Phytochemistry, submitted.

Schade, F. (1998). Bioreactor-based production of fragrance volatiles from membranes of carnation petals. Diplomarbeit, Universität Paderborn, Paderborn, Nordrhein-Westfalen.

Schardl, C.L., Byrd, A.D., Benzio, G., Altschuler, M.A., Hildebrand, D.F. & Hunt, A.G. (1987). Design and construction of a versatile system for the expression of foreign genes in plants. Gene 61, 1-11.

Schauenstein, E., Esterbauer, H. & Zollner, H. (1977). α, β-unsaturated aldehydes. In Lagnado, J.R. (ed.), Aldehydes in Biological Systems: Their Natural Occurence and Biological Activities. Pion, London, 25-102.

Senaratra, T., McKersie, B.D. & Borochov, A. (1987). Desiccation and free radical mediated changes in plant membranes. Journal of Experimental Botany 38, 2005-2014.

Shah, S., Li, J., Moffatt, B.A. & Glick, B.R. (1998). Isolation and characterization of ACC deaminase genes from two different plant growth-promoting rhizobacteria. Canadian Journal of Microbiology 44, 833-843.

Shinitzky, M. (1984). Physiology of Membrane Fluidity. Vol. I. CRC Press, Boca Raton, 1-52.

Siedow, J.N. (1991). Plant lipoxygenase: structure and function. Annual Review of Plant Physiology and Plant Molecular Biology 42, 145-188.

Sizer, I.W. (1944). Temperature activation and inactivation of the crystalline catalase-hydrogen peroxide system. Journal of Biological Chemistry 154, 461-466.

Skjak-Braek, G., Grasdalen, H. & Smidsroed, O. (1989). Inhomogeneous polysaccharide ionic gels. Carbohydrate Polymers 10(1), 31-54.

Smidsroed, O. & Skjak-Braek, G. (1990). Alginate as immobilization matrix for cells. Trends in Biotechnology 8, 71-78.

Sticher, L., Mauch-Mani, B. & Métraux, J.P. (1997). Systemic acquired resistance. Annual Review of Phytopathology 35, 235-270.

Suurmeijer, C.N.S.P., Perez-Gilabert, M., van Unen, D.-J., van der Hijden, H.T.W.M., Veldink, G.A. & Vliegenhart, J.F.G. (2000). Purification, stabilization and characterization of tomato fatty acid hydroperoxide lyase. Phytochemistry 53, 177-185.

Takamizawa, K., Nakashima, S., Yahashi, Y., Kubata, K.B., Suzuki, T., Kawai, K. & Horitsu, H. (1996). Optimization of kojic acid production rate using the Box-Wilson method. Journal of Fermentation and Bioengineering 82(4), 414-416.

Tanaka, H., Matsumura, M. & Veliky, I.A. (1984). Diffusion characteristics of substrates in Ca-alginate gel beads. Biotechnology and Bioengineering 16, 53-58.

Thompson, J.E., Froese, C.D., Madey, E., Smith, M.D. & Hong, Y. (1998). Lipid metabolism during plant senescence. Progress in Lipid Research 37 (2), 119-141.

Thompson, J.E., Froese, C.D., Hong, Y., Hudak, K.A. & Smith, M.D. (1997). Membrane deterioration during senescence. Canadian Journal of Botany 75(6), 867-879.

Thompson, J.E., Mayak, S., Shinitzky, M. & Havely, A.H. (1982). Acceleration of membrane senescence in cut carnation flowers by treatment with ethylene. Plant Physiology 69, 859-863.

Todd, J.F., Paliyath, G. & Thompson, J.E. (1990). Characteristics of a membrane-associated lipoxygenase in tomato fruit. Plant Physiology 94, 1225-1232.

Uknes, S., Mauch-Mani, B., Moyer, M., Potter, S. & Williams, S. (1992). Acquired resistance in *Arabidopsis*. The Plant Cell 4, 645-656.

Vick, B.A. & Zimmermann, D.C. (1987). Oxidative systems for modification of fatty acids: the lipoxygenase pathway. In Stumpf, P.K. (ed.), Lipids: structure and function. The Biochemistry of Plants. Vol. 9. Academic Press, New York, 53-90.

Vick, B.A. & Zimmermann, D.C. (1987). Pathways of fatty acid hydroperoxide metabolism in spinach leaf chloroplasts. Plant Physiology 85, 1073-1078.

Vick, B.A. & Zimmermann, D.C. (1984). Biosynthesis of jasmonic acid in plants. Plant Physiology 75, 458-461.

Vidal, S., de Leon, I.P., Denecke, J. & Palva, E.T. (1997). Salicylic acid and the plant pathogen *Erwinia carotovora* induce defense genes via antagonistic pathways. Plant Journal 11, 115-123.

Vernooij, B., Friedrich, L., Morse, A., Reist, R. & Kolditz Jahwar, R. (1994). Salicylic acid is not the translocated signal responsible for inducing systemic acquired resistance but is required in signal transduction. The Plant Cell 6, 959-965.

Wang, N.S. (1996). Enzyme immobilization by gel entrapment. http://132.187.96.115/pub/PROJEKTE/INTERNA/FORSCH/biot?PROTOCOL/immo-ex2.htm.

Webb, C., Black, G.M. & Atkinson, B. (1986). Process engineering aspects of immobilsed cell systems. Institution of Chemical Engineers. Pergamon Press, Toronto.

Wen, X.L, Kodama, O. & Akatsuka, T. (1991). The role of oxygenated fatty acids in rice phytoalexin production. Agricultural and Biological Chemistry 55, 1041-1047.

Whalen, M.C., Innes, R.W., Bent, A.F. & Staskawicz, B.J. (1991). Identification of *Pseudomonas syringae* pathogens of *Arabidopsis* and a bacterial locus determining avirulence on both *Arabidopsis* and soybean. The Plant Cell 3, 49-59.

Wiedenroth, E.-M. (1992). Response of roots to hypoxia: their structural and energy relations with the whole plant. Environmental and Experimental Botany 33(1), 41-51.

Woolhouse, H.W. (1984). The biochemistry and regulation of senescence in chloroplasts. Canadian Journal of Botany 62, 2934-2942.

Zarambinski, T.I. & Theologis, A. (1993). Ethylene biosynthesis and action: a case of conservation. Plant Molecular Biology 26, 1579-1597.

Zhang, J. & Davis, W.J. (1987). ABA in roots and leaves of flooded pea plants. Journal of Experimental Botany 38, 649-659.